DAF-16/FOXO and PQM-1/GATA factors up-regulate ferritin to promote cold survival upon ETS-4/SPDEF depletion

Inauguraldissertation

zur

Erlangung der Würde eines Doktors der Philosophie

vorgelegt der

Philosophisch-Naturwissenschaftlichen Fakultät

der Universität Basel von

Tina Pekeč

aus Kroatien

Basel, 2019

Genehmigt von der Philosophisch-Naturwissenschaftlichen Fakultät auf Antrag von:

Prof. Dr. Susan Gasser

Prof. Dr. Rafal Ciosk

Prof. Dr. Dominique Glauser

Basel, 21st May 2019

Prof. Dr. Martin Spiess
The Dean of Faculty of Science, University of Basel

TABLE OF CONTENTS

SUMMARY

Animal hibernation is one of great examples of physiological plasticity where by animals enter a hypometabolic state for extended periods of time (Storey and Storey, 2004). This state allows prolonged exposure to cold temperatures without tissue damage. In humans, clinically induced hypothermia has shown protective effects in brain and heart, prolonging damage free survival with low oxygen supply and allowing longer operative time for these patients (Palmers et al., 2015). Although used in the clinic, how hypothermia provides protection in humans is not clear.

Here we use *Ceanorhabditis elegans* as a genetically tractable model to study cold adaptation. Insulin signaling inhibition and FOXO activation in cold provides protection in both hibernating animals as well as in *C. elegans* (Savory et al., 2011; Wu and Storey, 2014). We know from previous studies that a conserved ribonuclease REGE-1 is essential for cold survival because it inhibits a transcription factor ETS-4 by degrading mRNA (Habacher et al., 2016). Upon ETS-4 depletion animals subjected to cold adaptation will survive cold temperature longer, by upregulating both DAF-16/FOXO and PQM-1/GATA factors, both known for their role in lifespan extension (Tepper et al., 2013). We show that these two transcription factors converge together to upregulate FTN-1, which sequesters iron from the cell. Iron has a profound role in the cell, besides being a co-factor of many enzymes and essential redox buffer in mitochondria, it is known that it can induce damage by generating reactive oxygen species in the cell (Joppe et al., 2019). In hibernating animals, the oxidative stress response plays a crucial role in preservation of animal tissues and is needed to ensure survival (Yin et al., 2016). Therefore, understanding iron metabolism and its underlying molecular regulation contributes to our understanding of cold adaptation.

We also used *C. elegans* to uncouple cold adaptation from fat content. This indicates that there are multiple pathways involved in cold adaptation that function independent of body fat.

CHAPTER 1: INTRODUCTION

HIBERNATION – HYPOMETABOLIC STATE UPON COLD

Hibernation, a reversible metabolic depression in mammals, is one of the more extreme examples of phenotypic plasticity. In hibernation, animals undergo profound physiological, morphological and behavioral changes upon seasonal or daily temperature changes when there is a high energy demand coupled with reduced energy availability (Carey et al., 2003). This strategy allows the animal to mitigate exposure to unfavorable environmental conditions and then resume activity once the temperature rises and food is readily available. The phenomenon of hibernation occurs in eight groups of mammals: monotremes, marsupials, rodents, shrews, bats, insectivores, carnivores and even primates, as observed in the fat tailed dwarf lemur (Ruf and Geiser, 2015). In order to survive hibernation, it is crucial for animals to suppress ATP expensive processes such as transcription and translation, to conserve fuel and energy by switching from carbohydrate to lipid metabolism, and to preserve macromolecules from damage by upregulating for example, oxidative stress response (Storey, 2010). Many hibernators are even able to enter torpor independently from external cues, providing evidence that the ability to hibernate is driven by molecular and/or genetic mechanisms, (Carey et al., 2003; Storey, 2015).

Repression of energy consuming processes

During early autumn, seasonal hibernators accumulate fat in white adipose tissue to prepare energy stores for winter (Arnold et al., 2011; Carey et al., 2003; Dark, 2005). To achieve proper hibernation, they start with so called “test drops “, where they gradually decrease the body temperature in which they will stay in torpor in short periods of time, eventually being able to reduce it to minimal required for a longer hibernation or up to months (Wu and Storey, 2016). Some hibernators, like 13-lined ground squirrel, are able to reduce their basal metabolic rate to just 2-4% of normal, with concomitant reductions in heart rate, respiration and renal function (Barnes, 1989; Carey et al., 2003; Zatzman, 1984). Although these processes are suppressed, they continue functioning during torpor, demonstrating their importance in maintaining organismal viability (Carey et al., 2003). To

achieve the hibernating phenotype, an organism modulates gene expression on multiple levels, including mRNA transcription, translation and posttranslational modifications of proteins (Frerichs et al., 1998; Lee et al., 2007; Osborne et al., 2004).

Hibernation is associated with a strong global transcriptional repression, although some genes remain preferentially expressed during torpor (Storey, 2010). RNA polymerase II (Pol II) activity decreases in the muscle tissue of hibernating ground squirrels compared to non-hibernating animals, suggesting direct Pol II contribution to the global transcription repression during torpor (Morin and Storey, 2006) (Figure 1A). RNA binding proteins have been implicated in hibernation as well. mRNA chaperones such as T-cell intracellular antigen 1 (TIA-1), TIA-1 -related (TIAR) and poly A-binding protein (PABP-1) will inhibit transcription, mRNA splicing and stability of mRNA (Suswam et al., 2005; Tessier et al., 2014). These factors have been found stored in the cells of the hibernating animals in nuclear bodies that disappear upon arousal, suggesting that transcripts are stably stored during torpor (Tessier et al., 2014).

One strong characteristic of hibernation is a global and reversible repression of protein translation (Knight et al., 2000). It was shown that a hibernating arctic ground squirrel loses polyribosomes associated with active mRNA translation upon torpor entry, and most of the mRNA becomes associated with one ribosome, unable to be translated efficiently Similarly, several ribosomal subunits, like translation initiation factor eIF2α and the translation elongation factor eEF2, will be directly repressed by reversible protein phosphorylation, blocking translation progression (Frerichs et al., 1998). Despite a dramatic global downregulation of transcription during hibernation, some genes essential for survival and stress resistance will be preferentially transcribed and translated into protein (Grabek et al., 2015a). For example, in brown adipose tissue (BAT) certain mRNAs of genes involved in mitochondrial stability as well as fatty acid metabolism, will be stabilized and polyadenylated. These transcripts are then translated since polyribosomes seem to remain intact and protein synthesis will continue during torpor in BAT (Grabek et al., 2015a; Grabek et al., 2015b).

Posttranslational modifications (PTM) are an important contributor to the gene regulation in hibernating animals, as mentioned above, protein phosphorylation plays a major role in fast, reversible changes upon exit and re-entry in torpor (Herinckx et al., 2017;

Storey, 2015). Phosphorylation has been shown to regulate enzymes involved in carbohydrate catabolism such as glycogen phosphorylase, hexokinase and pyruvate dehydrogenase. Additionally, Na^+/K^+ - ATP pumps and Ca^{2+} - ATPases decrease activity upon phosphorylation which reduces the heat produced by ATP hydrolysis and allows proper reduction of core body temperature (Storey and Storey, 2004, 2007). Another characteristic PTM in hibernating animals is SUMOylation (Storey, 2010). Small ubiquitin-related modifier (SUMO) -conjugated proteins have been found elevated in brain, liver and kidney during torpor and is protective to cells entering hypothermia (Lee et al., 2007). All together allow a multilayered gene repression upon hibernation, promoting regulated entry into torpor.

Fat metabolism regulation during torpor

A hallmark of many hibernators is a profound metabolic switch from carbohydrate to fatty acid metabolism (Rigano et al., 2017). Animals preparing to hibernate undergo a massive increase in their body fat, stored mainly as triglycerides in white adipose tissue (WAT) (Andrews, 2004; Wu and Storey, 2016). Active reduction in carbohydrate metabolism is achieved through phosphorylation and inhibition of several key enzymes as described above. This allows lipids to become a sole energy source in torpor. Hibernators are also able to use glycerol generated from triacylglycerols to generate glucose through gluconeogenesis in liver and kidney (Carey et al., 2003).

This switch to fatty acid metabolism is regulated transcriptionally (Andrews, 2004). Pyruvate dehydrogenase kinase isoenzyme 4 (PDK4) and pancreatic triacylglycerol lipase (PTL) are upregulated on the level of mRNA and protein, in hibernating ground squirrel. In addition, a hormone sensitive lipase (HSL), which is necessary for the release of fatty acids from WAT is upregulated in hibernating marmots and ground squirrels (Carey et al., 2003). PDK4 is a kinase that will phosphorylate pyruvate dehydrogenase and directly inhibit pyruvate production and subsequent citric acid cycle (Figure 1B). On the other hand, PTL will hydrolyze triacyclglycerols to liberate fatty acids that are used in β-oxidation.

The metabolic switch is accompanied by reversible insulin resistance during torpor entry (Rigano et al., 2017). For example, in preparation for hibernation, ground squirrel elevates serum insulin levels by 4-fold (Wu et al., 2013). Insulin is a key metabolic hormone

that promotes glucose uptake and glycogen synthesis (Figure 2B). It also inhibits HSL, preventing lipolysis. In an insulin resistant hibernating animal, HSL will be upregulated and allow the free fatty acids to be processed by PTL and enter fatty acid oxidation (Rigano et al., 2017). The levels of pancreatic insulin continue to rise during hibernation and they peak just before the final arousal from torpor (Andrews, 2004). This provides a large pool of insulin that will be released upon arousal and stimulate glucose metabolism once the animal starts feeding again. Hibernators are known of naturally occurring model for type 2 diabetes mellitus (T2DM) (Wu et al., 2013). T2DM is associated with insulin resistance in skeletal muscle, increased glucose production in the liver and progressive decline in insulin production in the pancreas (Guevara-Aguirre and Rosenbloom, 2015).

Antioxidant response

As animals enter torpor, many ATP consuming processes are repressed, including tissue repair, leading to damage accumulation generated by reactive oxygen species (ROS). In torpor, brown adipose tissue (BAT) remains active and massively increases non-shivering thermogenesis in mitochondria through uncoupling of oxidative phosphorylation and promoting proton leak through uncoupling proteins, allowing animals to maintain their body temperature in the appropriate range (Hindle and Martin, 2014) (Figure 1C). Additionally, many tissues reduce blood perfusion and reduce delivery of oxygen to cells during torpor which, when reversed upon arousal, can lead to a large burst of mitochondrial oxidation, exceeding the limits of antioxidant defenses, leading to oxidative damage (Vucetic et al., 2013; Wu and Storey, 2016). All of these processes require a well-controlled antioxidant response to protect the tissue from damage during hibernation.

Mitochondrial respiration is one of the sources of ROS, mainly through production of superoxide anion $O_2^{\bullet -}$ radical (Majima et al., 1998). Although not highly reactive on its own, it is able to oxidase iron – sulfur clusters, that are essential part of the electron transport chain in mitochondria, leading to release of iron Fe^{2+} ions. They then enter a Fenton reaction with hydrogen peroxide (H_2O_2) generating hydroxyl radical $HO^{\bullet}$. In contrast to superoxide, hydroxyl radical is highly reactive and creates damage of molecules in its vicinity (Winterbourn, 1995). It can also lead to lipid peroxidation and subsequent impairment of membrane function (Yin et al., 2016).

Several studies have shown that the upregulation of antioxidant defense genes is tissue specific and not a global phenomenon in hibernating animals (Page et al., 2009; Wei et al., 2018). Two main transcription factors participate in oxidative stress response in hibernating animals: FoxO3a and Nrf-2 (Wu and Storey, 2016) (Figure 1C). Nrf-2 is upregulated during hibernation in several tissues including heart, BAT, liver and skeletal muscle (Morin et al., 2008). It promotes cytoprotection through expression of detoxification genes like heme oxygenase 1 (HO1) that catalyzes the first step in heme degradation, leading to production of bilirubin and biliverdin, molecules with antioxidative capacities (Ni and Storey, 2010). In hibernating squirrels, the transcription factor FoxO3a will be upregulated to induce expression of oxidative stress response genes such as *MnSOD*, catalase and *Prdx3* of which all participate in ROS inactivation (Wu and Storey, 2014). For example, superoxide dismutase (SOD) converts a superoxide radical into oxygen and hydrogen peroxide. Similarly, catalase reduces hydrogen peroxide into oxygen and water. Both are upregulated in brown adipose tissue and muscle, but not in liver and white adipose tissue, in the hibernating ground squirrel (Vucetic et al., 2013). The antioxidative properties of FOXO3a-controlled transcription is conserved in humans (Kops et al., 2002).

To cope with redox imbalance from oxidative stress, hibernating animals express genes that help restore and preserve functional proteins. For example, ubiquitin is a small polypeptide that labels damaged or undesirable proteins for proteasomal degradation (van Breukelen and Carey, 2002). During torpor, proteins conjugated to ubiquitin are highly increased, suggesting an increase in protein turnover. Cellular stress and redox imbalance induce stress responsive factors such as HSP70 and HSP90 in brown adipose tissue and HSP60 in liver (Wu et al., 2015). GRP75 is a constitutively expressed mitochondrial chaperone protein that is upregulated in the arousal from torpor when there is a sudden high oxygen consumption generating ROS (Lee et al., 2002).

All of these processes collectively allow the hibernating animal to survive prolonged inactivity in the hypometabolic state and result in remarkable phenomena such as the prevention of muscle wasting during extended torpor (Miyazaki et al., 2019).

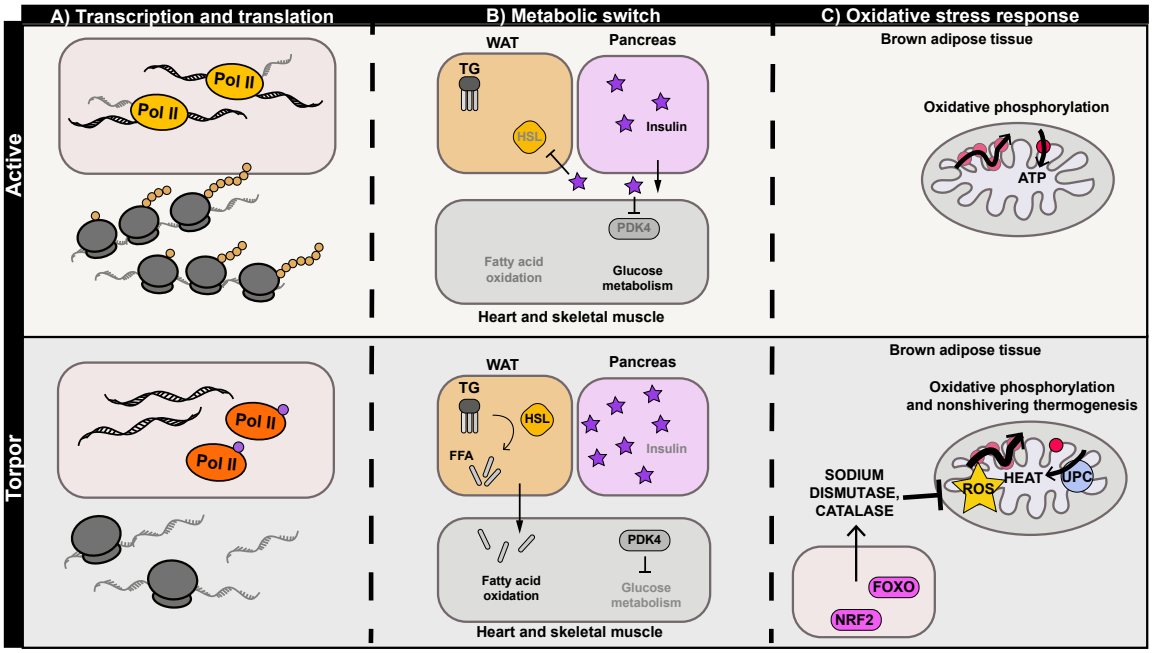

Figure 1. **Molecular changes upon cold induced torpor.** A) Characteristic of cold induced torpor is Pol II inactivation by phosphorylation and a shift from polysomes to monosomes, repressing global mRNA translation. B) Pyruvate dehydrogenase kinase isoenzyme 4 (PDK4) is a well described enzyme facilitating the metabolic switch from glucose metabolism to fatty acid oxidation. Hormone sensitive lipase (HSL) is like PDK4 repressed by insulin and will hydrolase triglycerides (TG) into free fatty acids (FFA). Adapted from (Andrews, 2004) C) In Brown adipose tissue, mitochondria will enhance oxidative phosphorylation and engage into non-shivering thermogenesis via. Uncoupling proteins (UCP) shuttling protons through the membrane without ATP production. Upon excess generation of reactive oxygen species (ROS), FOXO3 and NRF2 upregulate oxidative stress responsive genes.

Human hibernation and therapeutic use

While hibernating animals are able to actively modulate their core body temperature and remain in the hypometabolic state for prolonged periods of time, humans do not hibernate and will not be able to willingly enter torpor (van Breukelen and Martin, 2015). However, therapeutic hypothermia gained attention in 1950, when it was used in combination with general anesthesia to protect the brain and heart in newborn children that

were not breathing (Benedetti and Silverstein, 2018; Westin et al., 1959). In the 1960s, hypothermia was used in post cardiac arrest to prevent neuronal damage. However, longer and deeper hypothermia caused bleeding and sepsis, leading to a complete halt in its use for the following 20 years (Perman et al., 2014). Only after a randomized trial showing beneficial effects of hypothermia on post-cardiac arrest in the 2000's, was it re-introduced into the clinic (Bernard et al., 2002).

Now we know that therapeutic hypothermia is neuroprotective and is therefore used in treatment of traumatic brain injury (Yokobori and Yokota, 2016). It can also be used following stroke, meningitis, acute liver failure, spinal cord injury, hypoxic ischemic encephalopathy and myocardial infarction (McGinniss et al., 2015; Saigal et al., 2015). Hypothermia in humans is defined as body temperature below 36°C and in the clinic it can reach lower than 28°C, below which is considered deep hypothermia (Saigal et al., 2015). Induced hypothermia reduces cerebral metabolism by 5% for every degree of temperature reduction, but reduced metabolism is not the only protective effect of hypothermia (Erecinska et al., 2003; Nakashima et al., 1995). Therapeutic hypothermia is able to provide protection against ischemia/reperfusion injury (I/R) which is a pathology that occurs upon acute reintroduction of oxygenated blood following a period of low oxygen availability, creating ischemia. Additionally, it controls abnormal free radical production, reducing cell death and inflammatory responses (Shao et al., 2010).

Despite the potential benefits of induced hypothermia, such treatments are not without tradeoffs. One of the main issues while administering therapeutic hypothermia is the urge of the body to keep warm, and induction of shivering thermogenesis. In order to achieve lower body temperature, chemical agents are given to patients to keep shivering at bay (Choi et al., 2011; Madden et al., 2017). In addition, the current cooling, maintenance and re-warming process is not ideal and requires external cooling systems like cooling pads, that are not precise enough for tight temperature control. A better understanding of the molecular events that occur in cold stressed animals may lead to development of pharmacological interventions that provide the benefits of cooling without the need to cool the body down (Gu et al., 2015; Tupone et al., 2013).

CAENORHABDITIS ELEGANS AS A MODEL ORGANISM TO STUDY COLD ADAPTATION

Caenorhabditis elegans is a poikilothermic animal, which allows it to acquire the temperature from its surrounding. This is in contrast to endotherms that require temperature homeostasis and have elaborate mechanisms that keep the body temperature constant. Although poikilotherms, the *C. elagans* are unable to survive prolonged exposure to extreme temperatures that are above 25°C and below 15°C, making it a suitable model organism to study effects of temperature and ways to overcome the negative effects extreme temperature exposure can cause.

Cold acclimation

How sub-physiological temperatures affect diverse organisms has been extensively studied in many species. *C. elegans* has been a promising tool to study low temperature adaptation. For example, decreasing cultivation temperature from 20°C to 15°C extends lifespan (Klass, 1977), but extreme temperature exposure (0 – 4 °C) causes injury and death (Habacher et al., 2016; Ohta et al., 2014; Robinson and Powell, 2016). The lethality of cold shock can be circumvented by exposing the animals to a lower physiological temperature prior to the extreme one, improving their survival dramatically (Habacher et al., 2016; Murray et al., 2007; Ohta et al., 2014), suggesting that the animals are able to change their metabolic program and physiology to accommodate a low temperature environment. The existence of such programs is consistent with the ability of *C. elegans* populations to tolerate broad temperature ranges experienced in their natural habitat (Frezal and Felix, 2015; Okahata et al., 2016).

Adaptation to low temperatures was long time considered a passive process that is a result of lowered rate of chemical reactions, but recent studies showed that adapting to both moderately low temperatures, as well as extremely low temperatures and subsequent rewarming are highly regulated processes (Jiang et al., 2018; Ohta et al., 2014; Xiao et al., 2013). Adaptation to 15 °C is mediated through a highly conserved thermosensitive TRP channel that is expressed both in PVD neurons and in the intestine (Figure 2 – left panel). *C. elegans* intestine is a fat storing tissue and can be compared to mammalian fat cells that are

able to sense and respond to temperature changes (McGhee, 2007; Ye et al., 2013). Interestingly, overexpression of either neuronal or intestinal TRPA-1 was sufficient to extend survival, arguing the intestine as the novel temperature sensing organ (Xiao et al., 2013). Upon cold exposure, intestinal TRPA-1 releases calcium that in turn activates a calcium sensitive protein kinase (PKC-2). The subsequent signaling cascade activates the Serum and Glucocorticoid-inducible Kinase-1 (SGK-1) to activate a well conserved transcription factor DAF-16/FOXO (Xiao et al., 2013) (Mizunuma et al., 2014).

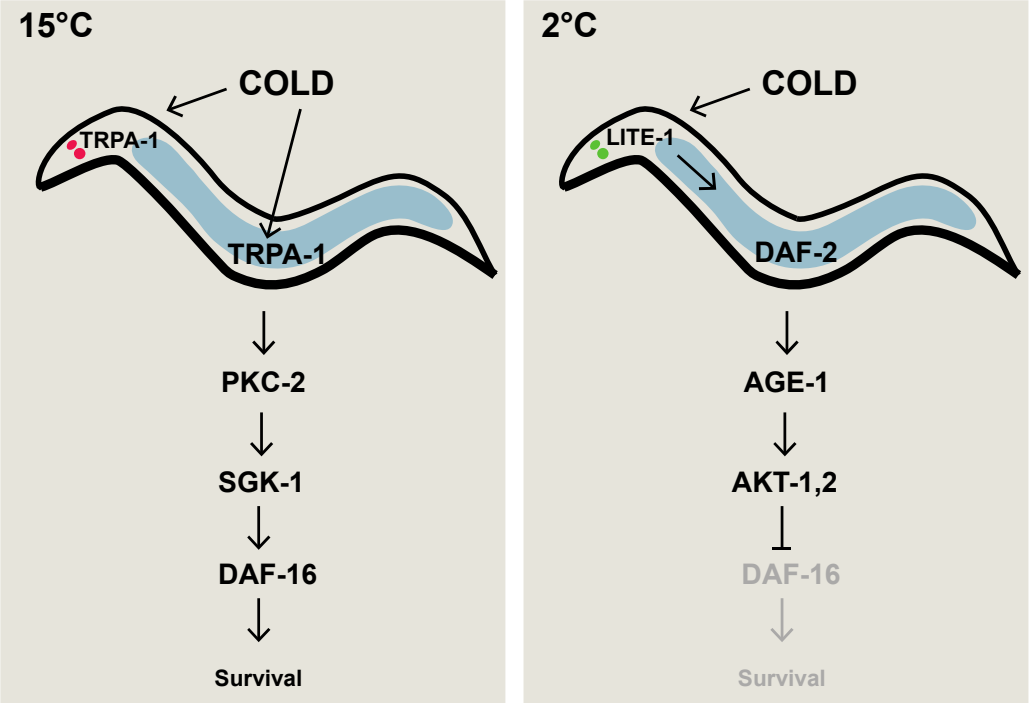

Figure 2. Different response to mild and extreme cold. On the left-hand side, schematic representation of animals exposed to 15°C will sense cold through PVD neurons (pink) and through the intestine via the TRPA-1 channel. This will induce a kinase cascade through PKC-2 and SGK-1 ultimately phosphorylating DAF-16 promoting nuclear localization and activation. Adapted from (Xiao et al., 2013). On the right-hand side, schematic representation of animals exposed to very low temperatures, such as 2°C, will sense the cold through LITE-1 located in ASJ neurons (green) and will signal to the intestine to inhibit DAF-16 by activating the insulin signaling pathway. Adapted from (Ohta et al., 2014).

In contrast to adaptation to 15°C, exposure to below physiological temperatures do not seem to rely on TRPA-1. When the animals are exposed directly to 2°C, they respond through the ASJ neuron and engage a signaling cascade through cGMP signaling (Figure 2 – right panel). Two insulin like peptides, DAF-28 and INS-6 were shown to act downstream of ASJ signaling. They will activate insulin signaling and inhibit DAF-16 in the intestine, suggesting ASJ signaling acts a negative regulator of cold survival, unlike TRPA-1 in the PVD neurons (Ohta et al., 2014). Another G protein coupled receptor, FSHR-1, was linked to cold-shock survival (Robinson and Powell, 2016). It was shown to be required for survival of endogenous oxidative stress, failing to activate ROS detoxification. Interestingly, *fshr-1* mutant animals were able to survive cold shock better, suggesting that oxidative stress might play an important role in signaling to upregulate additional ROS defense genes and provide protection. Taken together, these findings indicate that cold response is a highly regulated process, without which animal viability is at risk, as demonstrated by the recently described Cold-Warming response (CW), a phenomenon where animals exiting cold upregulate transcriptional programs that induce cell death (Jiang et al., 2018).

One of the most studied changes during cold exposure in *C. elegans* is homeoviscous adaptation, that is defined by changing lipid unsaturation to increase membrane fluidity upon cold exposure (Murray et al., 2007; Sinensky, 1974). This then allows the membranes to adapt to cold, remain functional, and to facilitate survival of the cold exposed animal. Exposure to low temperature is accompanied with a gradual loss of body fat, which is essential for survival as animals utilize the fat stores for energy (Habacher et al., 2016; Liu et al., 2017; Svensk et al., 2013). cAMP-PKA pathway has been shown to be required for cold survival where PKA allows the gradual fat loss upon cold (Liu, Xiao et al. 2017). Fatty acid unsaturation is also critical to maintain membrane fluidity in cold to preserve cellular function and was proposed to be the main enzyme promoting homeoviscous adaptation (Lee et al., 2018; Svensk et al., 2013). Interestingly, even if the lipid profile changes in the cold, it does not seem to benefit survival on its own (Murray et al., 2007), leaving open the potential for novel pathways that are unrelated to fat metabolism. The role of fat in cold survival will be revisited in Chapter 3.

ROLE OF TRANSCRIPTION FACTORS IN STRESS RESPONSES

Insulin like signaling has a profound role in ageing where its inhibition leads to prolonged lifespan through activation of its downstream target, the transcription factor FOXO and this feature is conserved across species (Mathew et al., 2017). FOXO plays a major protective role in hibernating animals, where it is upregulated to facilitate protection against oxidative stress, while an upstream kinase called AKT is repressed during torpor (Eddy and Storey, 2003; Wu and Storey, 2014; Yin et al., 2016). We have also seen that the inhibition of insulin signaling protects *C. elegans* from extreme cold, suggesting a universal role of insulin signaling and FOXO activation in cold tolerance.

Insulin and insulin-like growth factor signaling

In mammals, the insulin and IGF signaling (IIS) pathway serves as a food sensing system. Insulin peptide hormones are produced in pancreas and secreted into the bloodstream in response to increasing blood glucose levels (Leto and Saltiel, 2012). Insulin then binds certain receptor tyrosine kinases, activating a signaling cascade leading to translocation of the glucose transporter GLUT4 to the cellular membrane to internalize glucose and facilitate glucose metabolism (Leto and Saltiel, 2012). Modulation of insulin signaling allows regulated energy metabolism and if disrupted it can lead to severe disease states such as obesity and type 2 diabetes mellitus (Guevara-Aguirre and Rosenbloom, 2015; Yaribeygi et al., 2019). Interestingly, hibernating mammals emerged as an interesting model to study insulin resistance since they are able to enter an obesity-like state in a reversible manner (Wu et al., 2013).

When dysregulated, insulin signaling in mammals leads to either insulin resistance or diabetes, while decreased overall IIS activity promotes increased longevity across species, even in humans (Giannakou et al., 2004; Kappeler et al., 2008; Suh et al., 2008). In *C. elegans* mutations in either the insulin receptor homolog *daf-2* or downstream kinases are able to dramatically extend lifespan (Kenyon et al., 1993; Kenyon, 2010). Besides extending lifespan, animals have decreased brood size, slower rate of development, increased fat content and increased resistance to a broad array of stresses. Insulin signaling is characterized by a cascade starting from secreted insulins that bind to an insulin-like growth factor -1 receptor

DAF-2/IGF-1R (Figure 3). This activates a kinase cascade: phosphoinositide 3 kinase PI3K/AGE-1, that will phosphorylate phosphatidylinositol bisphosphate (PIP2) into a phosphatidylinositol trisphosphate (PIP3) recruiting protein kinase D, PDK/AKT (Dorman et al., 1995; Kenyon, 2010; Murphy and Hu, 2013). AKT will eventually phosphorylate the FOXO transcription factor, DAF-16, and retain it in the cytoplasm, inhibiting its function (Lin et al., 2001). However, upon insulin signaling inhibition, DAF-16 will enter the nucleus and transcribe genes that will extend the lifespan. There are 40 insulin like peptides in *C. elegans* out of which some will stimulate insulin signaling while other will act inhibitory, giving another layer to insulin signaling regulation (Zheng et al., 2018). Additionally, DAF-18, phosphoinositide 3-phosphatase (PTEN) will inhibit insulin signaling by antagonizing AGE-1 and dephosphorylating PIP3 into PIP2 (Ogg and Ruvkun, 1998).

DAF-2 inhibition can activate several downstream transcription factors in addition to DAF-16/FOXO, such as SKN-1/Nrf2 and HSF-1/HSF (Hsu et al., 2003; Samuelson et al., 2007; Tullet et al., 2008). As in hibernating animals, SKN-1/Nrf2 promotes expression of oxidative stress response genes like superoxide dismutase (SOD) (Blackwell et al., 2015; Ni and Storey, 2010). SKN-1 is shown to be required for lifespan extension in *daf-2* mutant animals only at lower temperatures, which is in agreement with its contribution to hibernating animals (Ewald et al., 2015).

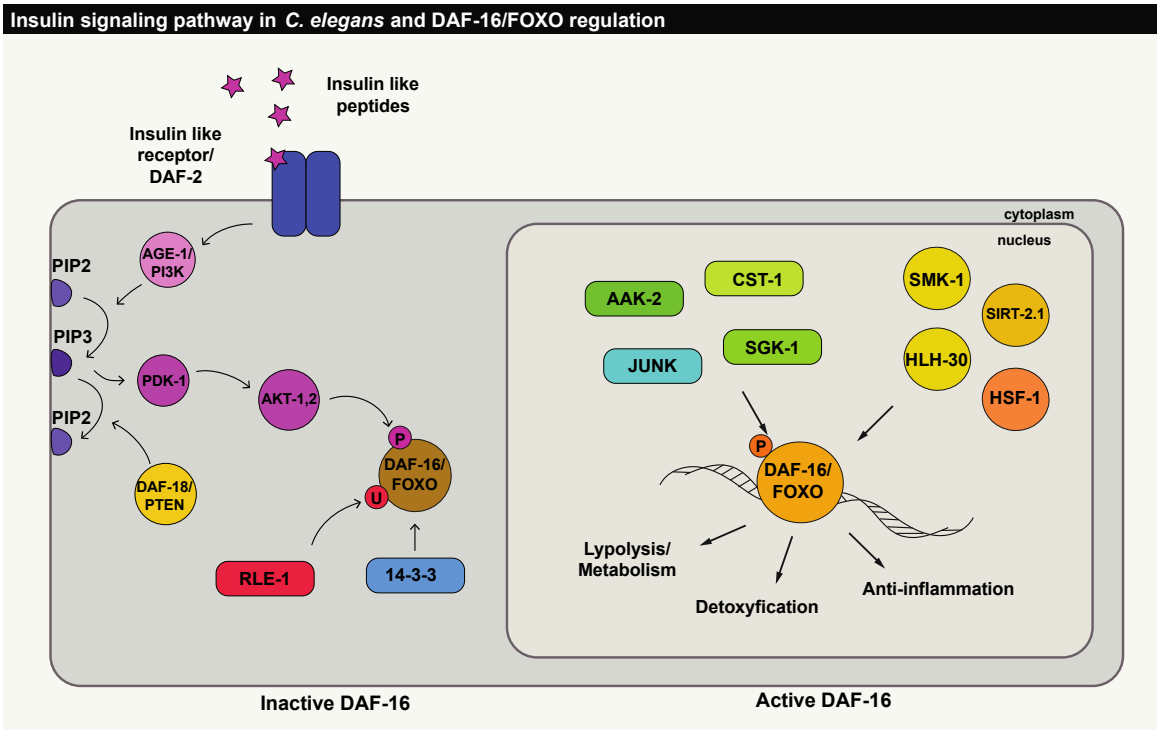

Figure 3. Insulin signaling pathway and DAF-16/FOXO regulation. Insulin signaling cascade starts with insulins binding to the Insulin receptor (DAF-2). This will facilitate a kinase cascade where AGE-1/PI3K will phosphorylate PIP2 into PIP3. PIP3 will recruit PDK-1 that will activate AKT-1,-2. AKT -1,-2 will phosphorylate (P) DAF-16/FOXO and sequester it in the cytoplasm. DAF-16 can be additionally inhibited by E3 ubiquitin ligase that will ubiquitylate (U) DAF-16 and signal for proteasomal degradation. 14-3-3 adaptor protein will directly bind and inhibit DAF-16. Kinases JUNK, AAK-2, CST-1 and SGK-1 will phosphorylate DAF-16 and activate it. SMK-1, HLH-30, HSF-1 are known binding partners and will enhance DAF-16 transcriptional activity. SIRT-2.1 is a deacetylase that will as well promote DAF-16 activity.

FOXO transcription factors promote stress resistance and longevity

FOXO is a conserved transcription factor that belongs to a class O of Forkhead transcription factors with a Forkhead box (FOX) or "winged helix" DNA binding domain (Sun et al., 2017). Mammals have four closely related FOXO proteins – FOXO1, 3 and 4, and a less

well conserved protein, FOXO6 (Lee and Dong, 2017). Although sharing some targets and having overlapping expression pattern, they function in distinct ways. FOXO1 is required for angiogenesis and results in lethality if deleted in mice, whereas *foxo3* mutants are viable but females progressively loose fertility, and *foxo4* has no obvious phenotype (Wang et al., 2014). They have been shown to function as redundant tumor suppressors. Interestingly, FOXO3 is upregulated in hibernating animals where it provides protection against oxidative stress (Wu and Storey, 2014). FOXO3a mutations have also been found in human centenarians showing a conserved role in aging across species (Suh et al., 2008). *foxo6* mutation was found to be beneficial in glucose intolerance and insulin resistance in mice by attenuating gluconeogenesis and reducing inflammatory response (Calabuig-Navarro et al., 2015). Interestingly, unlike other FOXO proteins, FOXO6 is constitutively nuclear and is not be sequestered in the cytoplasm by Akt/PKB phosphorylation, but rather leads to target genes transcription upon inhibition of insulin signaling (Lee and Dong, 2017).

In *C. elegans* the homolog of FOXO transcription factors is DAF-16. Most of the described transcriptional changes seen in stress-resistant *daf-2* mutants are DAF-16 dependent (Murphy, 2006). Genes upregulated in *daf-2* mutants are involved in stress response, xenobiotic detoxification or encode for molecular chaperones (Hsu et al., 2003; Li and Zhang, 2016). Collectively, these genes are referred to as class 1 genes. On the other hand, downregulated genes are involved in ubiquitin mediated protein degradation, lipid binding and ribosomal proteins and are grouped together as class II genes (Murphy, 2006; Tepper et al., 2013). Several genome wide experiments led to finding of two distinct DNA motifs associated with DAF-16 in the promoters of changing genes. The DAF-16 binding element (DBE) (GTAAACA or TGTTTAC) seems to be preferentially bound by DAF-16, while the DAF-16 associated element (DAE) (TGATAAG or CTTATCA) is a GATA-like binding site and is preferentially bound and regulated by the GATA transcription factor PQM-1 (Kenyon and Murphy, 2006; Tepper et al., 2013).

As in *C. elegans,* where DAF-16 upregulates manganese superoxide dismutase SOD-3, in *daf-2* mutant background, human FOXO3a is activated upon the depletion of insulin signaling, in order to provide protection from oxidative stress in quiescent cells (Honda and Honda, 1999). It will do so by increasing MnSOD, the homolog of SOD-3, an enzyme able to scavenge superoxide radicals and prevent apoptosis (Kops et al., 2002). Interestingly, SOD

genes were shown to be required for survival at low temperatures in *C. elegans* (Yen et al., 2009). Part of the DAF-16 protective response to oxidative stress is as well upregulation of the ferritin gene (Ackerman and Gems, 2012). Ferritin is a large iron binding molecule that will sequester iron from the cell, preventing production of ROS and subsequent cellular damage. Interestingly sequestration of iron has been shown to provide protection in mammalian cells incubated at low temperatures (Pizanis et al., 2011).

Modulation of DAF-16/FOXO activity

Unlike mammals, *C. elegans* contain a single DAF-16/FOXO genetic locus, but multiple promoters drive transcription of several different isoforms, and each isoform has a different contribution to the lifespan phenotype of *daf-2* (Bansal et al., 2014; Kwon et al., 2010). *daf-16a1* and *daf-16a2* are controlled by the same promoter and the protein differs in only two amino acids. *daf-16b* encodes a short isoform expressed from a different promoter. *daf-16d/f* is transcribed from a different promoter located some 10kb upstream of the *daf-16a1/2* promoter (Bansal et al., 2014). Only *daf-16a1/2* and *daf-16d/f* have been implicated in lifespan regulation. *daf-16a* and *daf-16d/f* transcription has been shown to be regulated by GATA factors ELT-2 and ELT-4, which are required both for normal intestinal development and DAF-16 mediated longevity (Bansal et al., 2014; Fukushige et al., 1998). SWI/SNF complex, that is known to regulate nucleosome positioning and allows DNA access for specific transcription factors, promotes longevity specifically through *daf-16d/f* (Bansal et al., 2014; Barisic et al., 2019). Additionally, each isoform regulates slightly different gene sets, suggesting a multilayered regulation of the stress response (Chen et al., 2015).

It is known that overexpression of DAF-16 will lead to only minor extension of lifespan in wild-type animals, suggesting DAF-16 may require partners or post-translational modifications to co-regulate the beneficial genes (Henderson and Johnson, 2001; Landis and Murphy, 2010) (Figure 3). This is not surprising given that each stress type is slightly different and it might require a different set of genes. Known regulation of DAF-16 spans from phosphorylation, regulation of transcription initiation and to regulation upon shift in redox balance (Landis and Murphy, 2010). DAF-16 can be regulated by diverse set of kinases. Some act inhibitory, like AKT-1/-2 whose phosphorylation will promote DAF-16 sequestration to the cytoplasm, while on the other hand SGK-1, Jun-N-terminal kinase (JUNK), and

AMPK/AAK-2, a nutrient sensing kinase, will positively regulate DAF-16 transcriptional activity (Dorman et al., 1995; Hertweck et al., 2004; Ogg and Ruvkun, 1998; Oh et al., 2005; Tullet et al., 2014; Xiao et al., 2013). JUNK will act in parallel to insulin signaling to promote oxidative stress resistance through DAF-16 activation.

14-3-3 adaptor proteins can also inhibit DAF-16 binding to co-factors such as NAD-dependent deacetylases, known as sirtuins that are NAD+-dependent deacetylases whose overexpression increases longevity (Berdichevsky et al., 2006; Rizki et al., 2011). DAF-16 also interacts with serine/threonine-protein phosphatase-4 regulatory subunit, SMK-1 that is required for DAF-16 mediated innate immune response, UV and oxidative stress response, but not thermotolerance (Wolff et al., 2006). MATH-33, a deubiquitylase, was shown to physically interact with DAF-16, removing ubiquitin placed by RLE-1, E3 ubiquitin ligase, and finally stabilizing DAF-16 in the nucleus (Heimbucher et al., 2015). Even some transcription factors will directly influence DAF-16 output through direct binding, like in the case of HLH-30, that was recently described as a novel DAF-16 binding partner that promotes stress resistance and longevity (Lin et al., 2018).

Interestingly, an emerging transcription factor PQM-1 has been shown to co-regulate lifespan extension with DAF-16 in many cases and could potentially be a novel binding partner in longevity.

PQM-1/GATA a novel DAF-16 partner in lifespan regulation

PQM-1/GATA a zinc-finger transcription factor was recently described as a DAF-16 partner promoting longevity as it is also required for *daf-2* mutant lifespan extension, albeit to a different extent (Tepper et al., 2013). In *pqm-1* mutant animals, both Class I and Class II groups of genes are downregulated through PQM-1 binding the DAE (Tepper et al., 2013). It also decreases *daf-2* thermotolerance and dauer recovery, suggesting that PQM-1 plays a role in several observed *daf-2* phenotypes. In lifespan studies, PQM-1 was found to be required for the long life of *daf-2*, *eat-2*, *glp-1* and several long-lived mitochondrial mutants like *isp-1*, *clk-1* and *nuo-6* (Senchuk et al., 2018). Although upon deletion *pqm-1* will not exhibit a lifespan phenotype, PQM-1 seems to contribute to lifespan extension in multiple genetic contexts. It seems to contribute strongest in mitochondrial mutant models of longevity, suggesting a role

in oxidative stress resistance. Consistently, PQM-1 was discovered and named for being an oxidative stress responsive gene upon treatment with a ROS inducing agent paraquat (Tawe et al., 1998). PQM-1 is also able to induce a set of molecular chaperones that provide protection against chronic stress such as dietary restriction (Shpigel et al., 2019). In addition, overexpression of HSP-90 is able to upregulate PQM-1 cell-nonautonomously from both neurons and intestine (O'Brien et al., 2018). Loss of *pqm-1* will in turn increase protein aggregates and enhances heat stress sensitivity as compared to wild type.

PQM-1 is found to interact with other proteins to facilitate gene expression. CEH-60 was identified as a binding partner of PQM-1 that associates with it through DAE at promoters, regulating gene expression (Dowen, 2019). CEH-60 is a conserved transcription factor, whose loss leads to lifespan extension, for which PQM-1 is required. Although PQM-1 does not dramatically influence genes regulated by CEH-60, it is interesting that PQM-1 is able to associate with other factors and bind and potentially enhance repression of these factors (Dowen, 2019). PQM-1 nuclear stabilization was shown to be affected by DAF-18/PTEN, HSF-1 and SGK-1, but conversely it can be excluded from the nucleus in heat response and upon *daf-2* inactivation (Tepper et al., 2013). While this nuclear localization does not correlate with PQM-1 requirements in both heat stress survival and *daf-2* longevity, how and under what conditions PQM-1 becomes relevant requires further examination (Dowen et al., 2016; Tepper et al., 2013).

ETS transcription factors in stress and lifespan

Another transcription factor that regulates *C. elegans* ageing is E-twenty-six 4 (ETS-4). ETS is a large family of transcription factors based on a conserved DNA binding domain that forms in a helix-turn-helix structure (Wei et al., 2010). The first ETS factor was identified in chicken leukemia cells due to its homology to the E26 virus oncogene, (Leprince et al., 1983). There are 29 family members divided in 4 functional groups based on their binding specificity that slightly differs around a consensus 5'-GGA(A/T)-3' binding site (Hollenhorst et al., 2004). A subset of ETS factors contains a pointed (PNT) domain that can be regulated by phosphorylation by the MAPK pathway altering downstream gene regulation (Mackereth et al., 2004; Seidel and Graves, 2002). Another domain associated with the SPDEF subset of ETS factors is the sterile alpha motif (SAM) domain.

ETS transcription factors are expressed in many cell types, however their functions are best described in epithelial cells (Hollenhorst et al., 2004; Luk et al., 2018). They are required in hematopoiesis in what cells where they activate cell lineage specificity genes and enhance vascular endothelial growth factor (VEGF) expression (Craig and Sumanas, 2016; Sumanas and Choi, 2016). SPDEF proteins have been found to promote mucus secretion in lung endothelium but are also implicated as oncogenic in different cancers, especially prostate cancer, (Korfhagen et al., 2012; Luk et al., 2018; Pal et al., 2013). In addition, SPDEF has been found to function in mouse intestinal cells where it is required for proper intestinal development but can also contribute to cancer (Gregorieff et al., 2009; Noah et al., 2010; Noah et al., 2013). Interestingly, ETS1 was also shown to play a role in ROS regulation by upregulating the iron-uptaking transferrin receptor in erythrocytes, increasing iron levels in the cell (Marziali et al., 2002).

In *C. elegans* there are 10 orthologs in the ETS transcription factor family and they function in different tissues and pathways. The homologue of ETV1, AST-1, regulates dopaminergic neuron differentiation as well as axon guidance (Schmid et al., 2006). The best characterized of them is LIN-1/ELK1, found to regulate cell fate decisions in vulva development (Beitel et al., 1995). LIN-1 functions downstream of the Ras/MAP kinase pathway as a transcriptional repressor when SUMOylated and as a transcriptional activator when phosphorylated (Jacobs et al., 1998; Leight et al., 2005; Leight et al., 2015). In addition, it was shown to be inhibited by the increased ROS in the cell, causing inhibition of vulva development (Shibata et al., 2003). ETS-5, that is an ortholog of mammalian FEV, was found to regulate carbon-dioxide sensing and in addition to participating in a complex network to regulate food-regulated behavioral state switching (Guillermin et al., 2011; Juozaityte et al., 2017). *ets-5* mutant animals enter quiescence on a diluted food and accumulate fat (Juozaityte et al., 2017). Upon inhibition of fatty acid synthesis both of the phenotypes are restored.

Another well described ETS factor in *C. elegans* is ETS-4, an ortholog of mammalian SPDEF. ETS-4 was originally described as a transcription factor that will extend lifespan upon deletion (Thyagarajan et al., 2010). It functions in the intestine, where it promotes transcription of mostly DAF-16 target genes. Additionally, the extended lifespan of *ets-4* mutants is completely abolished upon additional *daf-16* deletion, suggesting that these targets may contribute to the lifespan phenotype. However, it has additive effect on lifespan

with mutations that reduce insulin signaling suggesting it acts in parallel to DAF-16 (Thyagarajan et al., 2010). ETS-4 was also found to be required for axonal regeneration upon injury (Li et al., 2015). The coregulation of ETS and FOXO factors is also evident at the promoters of mammalian FOXO targets where there is an enriched occurrence of ETS binding motifs suggesting a possible co-factor relationship between FOXO and ETS factors (De Val et al., 2008; Webb et al., 2016). While ETS binding elements are not enriched in targets of *C. elegans* FOXO, DAF-16 (De Val et al., 2008), in *Drosophila,* two ETS transcription factors, pointed (Pnt) and anterior open (Aop) function as transcriptional activator and repressor respectively, to regulate lifespan (Duncan et al., 2018). Interestingly, Aop functions with FOXO downstream of insulin signaling to promote extended survival and neuronal health by aiding mitochondrial function (Duncan et al., 2018; Slack et al., 2015; Vivekanand, 2018). Nevertheless, how ETS and FOXO transcription factors interact remains unclear.

ets-4 mRNA is a main target of a very well conserved ribonuclease REGE-1/MCPIP1. In the wild-type situation, REGE-1 cleaves *ets-4* mRNA on a in its 3'UTR leading to its degradation (Habacher et al., 2016). In the absence of REGE-1, *ets-4* mRNA is translated and ETS-4 is stably present in intestinal nuclei. Subsequently, this ETS-4 overexpression leads to several phenotypes including developmental delay, severe fat loss, and cold sensitivity. ETS-4 was found to regulate genes involved in innate immunity but also fat catabolism, explaining in part the phenotypes observed (Habacher et al., 2016). How ETS-4 undermines cold survival will be examined in detail in chapter 2.

IRON METABOLISM: POSSIBLE TARGET IN HYPOTHERMIA

Iron is an essential metal in mammals it is essential part of hemoglobin, that contributes to oxygenation of the tissues (Muckenthaler et al., 2017). As a part of iron-sulfur clusters it becomes an essential electron donor in mitochondria. There it participates in oxidative phosphorylation that is the main source of reactive oxygen species (ROS) in the cell, but also the in the hibernating animals. Therefore, it is crucial to understand how regulating iron levels can prevent oxidative damage in the cell and aid cold adaptation.

Cellular iron balance in mammalian systems

Iron is taken up from the environment via transferrin (Tf) which has two high affinity binding sites for Fe (III) (Ponka et al., 1998). Diferric transferrin will then bind a high affinity transferrin receptor (TFR1) and enter into the cell by endocytosis. The acidic environment of the early endosome facilitates the release of iron which is then reduced to Fe (II) (Ohgami et al., 2005). Reduced iron is transported into the cytoplasm by divalent metal transporter 1 (DMT1), while Tf and TFR1 are recycled and brought back to the cell surface (Muckenthaler et al., 2017). Iron taken up into the cell becomes part of the so-called "labile iron pool" where iron is sorted for either storage or utilization largely in the mitochondria where it binds as a co-factor in heme and iron- sulphur (Fe-S) clusters (Hamdi et al., 2016). Iron enters mitochondria through a mitoferrin (MFRN) where it is bound to porphyrin IX to form heme which will be then exported to the cytoplasm (Chiabrando et al., 2013). Iron that is not used from the labile iron pool is stored in the cytosolic heteropolymer ferritin, made out of heavy (FTH1) and light subunits (FTL) (Macara et al., 1972). FTH1 acts as an enzyme ferroxidase that will facilitate the formation of the ferritin nanocage with up to 4500 atoms of iron (Lawson et al., 1991; Montemiglio et al., 2019). Ferritin is expressed ubiquitously and loss of *Fth1* in mice is lethal because free iron is highly toxic and will induce premature apoptosis (Ferreira et al., 2001) (Eid et al., 2017).

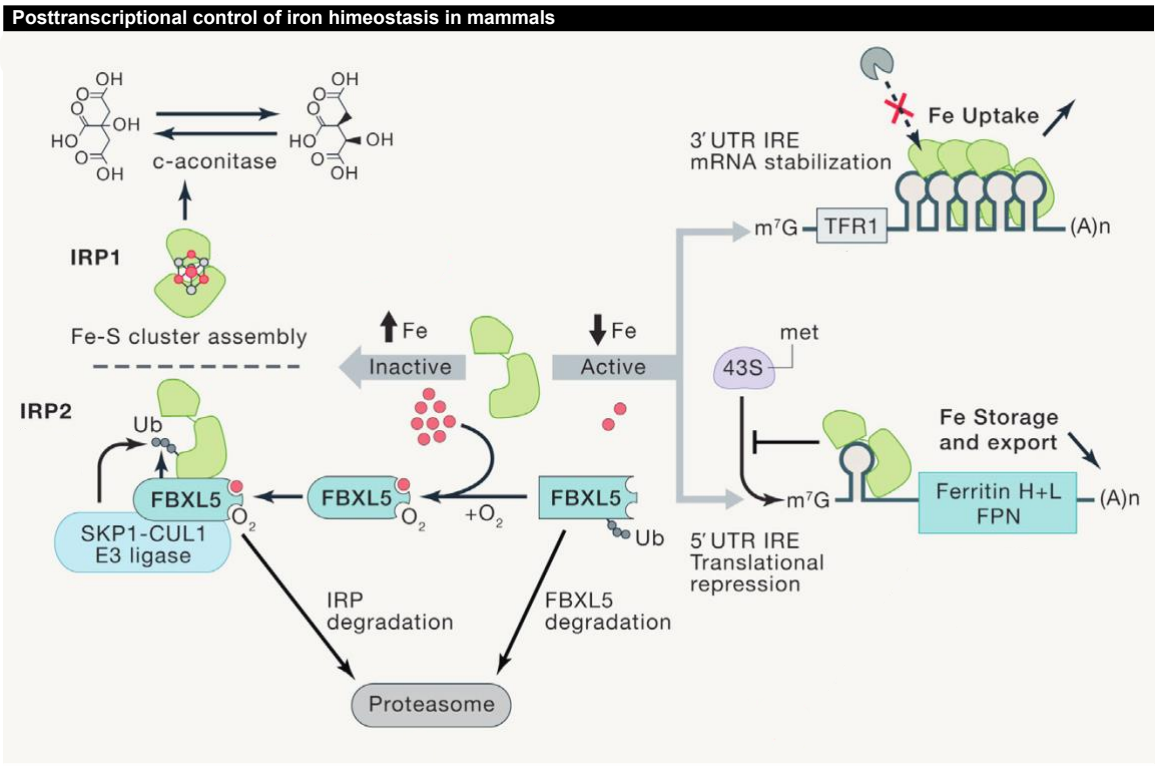

Figure 4. Posttranscriptional control of iron homeostasis in mammalian systems. FBXL5 is an intracellular iron and oxygen sensor. Upon binding iron and oxygen, it will bind an iron responsive protein IRP1 or IRP2, and facilitate proteasomal degradation. In turn, transcripts baring iron responsive hairpin (IRE) in the 5'UTR will be translated. This includes the iron storage protein, ferritin and iron export protein ferroportin (FPN). Additionally, IRPs can bind iron directly in form of iron-sulfur clusters and transfer it to enzymes such as c-aconitase. If iron levels are low, FBXL5 will be degraded and IRPs will bind the IRE at 5'UTRs to inhibit translation and IREs at the 3'UTR to stabilize the transcripts and promote translation. In this case mRNA of iron uptake proteins like transferrin (TFR1) will be translated. Adapted from (Muckenthaler et al., 2017).

As iron is of great importance to the cell, it will be kept in a narrow range through a complex posttranscriptional regulatory system. Genes encoding for proteins that facilitate iron sequestration like FTH1 and FTL have an hairpin structure named iron responsive element (IRE) located in the 5'UTR, while genes coding for proteins required for iron intake, like TFR1 will have it in the 3'UTR (Jaffrey et al., 1993). A set of iron responsive RNA binding

proteins IRP1 and IRP2 will bind these IRE and regulate the genes in response to iron levels in the cell (Kim and Ponka, 1999; Ponka et al., 1998). When bound at the IRE located at the 5'UTR, IRPs inhibit translation while if the IRE is in the 3'UTR, it will stabilize the mRNA and promote translation (Theil, 2000). Proteins that facilitate iron sequestration like FTH1 and FTL have an IRE located in the 5'UTR and therefore won't be translated upon high iron levels in the cell, while proteins required for iron intake, like TFR1 will have it in the 3'UTR will be stabilized if the iron level is too low in the cell.

The IRPs are not direct sensors of cellular iron but in turn they interact with F-box and leucine rich repeat protein 5 (FBXL5) that has an iron binding domain at its N-terminus (Thompson et al., 2012). When not bound to iron, FBXL5 will recruit an E3 ubiquitin ligase complex and promote its own proteasomal degradation (Salahudeen et al., 2009). If the iron is abundant, FBXL5 will bind iron and IRPs which will all together be degraded by the proteasome (Thompson and Bruick, 2012). To facilitate IRP degradation, FBXL5 also requires oxygen, which means that the IRPs will be stabilized upon hypoxia as well (Chollangi et al., 2012). Hypoxia response is tightly coupled with iron levels (Salahudeen and Bruick, 2009). In hypoxic situations, the body will increase erythropoiesis for which iron is essential. Therefore, it is not surprising that hypoxia inducible factor alpha has an IRE where IRPs can bind and titrate its translation rate.

Iron metabolism in *C. elegans*

Given the importance of iron homeostasis, many components of iron metabolism are conserved across species. In *C. elegans* we find orthologs of DMT1 transporter (SMF-3) ferritin (FTN-1, FTN-2) as well as ferroportin that will export iron from the cell (FPN-1.1, FPN-1.2, FPN-1.3) (Anderson and Leibold, 2014). SMF-3 is expressed in the intestinal lumen where it uptakes iron from the diet. Loss of SMF-3 leads to iron deficiency rendering animals hypersensitive to oxidative stress (Romney et al., 2011). Ferritin genes are homologous to human ferritin heavy subunit more than to the light chain subunit. They contain a ferroxidase active site, suggesting that they are able to oxidize iron from ferrous form into the inactive ferric form in order to sequester it in the ferritin nanocage (Gourley et al., 2003).

Both *ftn-1* and *ftn-2* were shown to be expressed in the intestine, by promoter fused GFP transcriptional reporters, while *ftn-2* showed more global expression pattern including pharynx, body-wall muscle and hypodermis (Gourley et al., 2003; Romney et al., 2008). Using *in vivo* x-ray fluorescent imaging it was found that FTN-2 is the main iron storage in the adult animal, and, if depleted, it will dramatically reduce total iron content in the animal (James et al., 2015). *smf-3*, *ftn-1*, and *ftn-2* are able to respond to changes in iron levels (Gourley et al., 2003; Kim et al., 2004). Interestingly, it was shown that *ftn-1* responds better to both iron supplementation or iron chelation, compared to *ftn-2* (Romney et al., 2008) Detailed dissection of both *ftn-1* and *ftn-2* promoters revealed a 63bp iron dependent element (IDE) that contains three direct repeats separated by two GATA sites bound by transcription factor ELT-2 (Romney et al., 2008). Later on, the direct repeats were found to be bound by hypoxia inducible factor 1 (HIF-1) and have been termed hypoxia responsive elements (HRE) (Romney et al., 2011). Similar to the mammalian system, HIF-1 inhibits both *smf-3* and both ferritins through HREs located in their promoter. It is able to repress transcription of ferritins, but activate transcription of *smf-3* facilitating iron uptake upon iron shortage (Romney et al., 2011). *ftn-1* is additionally regulated by the insulin signaling pathway in parallel to HIF-1. It was shown that in *daf-2* mutant animals, *ftn-1* is highly upregulated in a DAF-16 dependent manner (Ackerman and Gems, 2012). Consistently, a DBE is located outside of the *ftn-1* IDE, and *ftn-1* was scored as a highly responsive DAF-16 class I target (Tepper et al., 2013). *daf-2* mutants are able to maintain low levels of iron throughout their post-developmental life, compared to the wild-type animals that increase total iron levels over time (James et al., 2015).

Iron has many roles in regulating cellular function. Animals supplemented with high doses of iron accumulated lipids in the intestine in a SGK-1 dependent manner (Wang et al., 2016). Additionally, iron supplementation upregulates SOD genes to battle reactive oxygen species (Valentini et al., 2012; Wang et al., 2016). On the other hand, iron supplementation can increase protein insolubility forming aggregates leading to reduced lifespan (Klang et al., 2014). Such negative effects of iron overload can even be transferred to the progeny (Hu et al., 2008). Both *ftn-1* and *ftn-2* are required for normal lifespan (James et al., 2015; Valentini et al., 2012). Iron sequestration due to overexpression of FTN-1 is able to provide protection against oxidative stress by sequestering iron and preventing it from participating in further

ROS generation (Valentini et al., 2012). Additionally, iron deprivation can induce mitophagy that will eventually lead to extended lifespan (Schiavi et al., 2015). Since iron regulation is conserved and regulates many aspects of animal life, it is essential to further understand how and when is it regulated.

Iron in cold

Iron has been shown relevant in thermogenesis in humans, as people with iron deficiency had a reduced ability to maintain normal body temperature upon cold exposure (Agarwal, 2007). It was also shown that iron is released upon cold exposure, creating damage and inducing apoptosis (Huang and Salahudeen, 2002; Pizanis et al., 2011; Rauen et al., 2000). Sequestering free iron from cold exposed cells, by iron chelators, was able to successfully repress apoptosis and increase survival upon cold exposure, suggesting that with pharmacological interventions, we may be able to reduce the damage caused by excess iron and modulate core body temperature. In the following chapter we will examine one way of regulating free iron and enhancing cold survival in *C. elegans.*

CHAPTER 2: RESULTS

Interrogating *C. elegans* hibernation unveils iron sequestration as a key mechanism for surviving hypothermia

Tina Pekec [1, 2], Jaroslaw Lewandowski [3], Yanwu Guo [4], Karolina Świtońska [3], Maciej Figiel [3], and Rafal Ciosk [3, 4]*

[1] Friedrich Miescher Institute for Biomedical Research, Maulbeerstrasse 66, 4058 Basel, Switzerland

[2] University of Basel, Faculty of Natural Sciences, Klingelbergstrasse 70, 3026 Basel, Switzerland

[3] Institute of Bioorganic Chemistry, Polish Academy of Sciences, Noskowskiego 12/14, 61-704 Poznan, Poland

[4] University of Oslo, Department of Biosciences, Kristine Bonnevies hus, Blindernveien 31, Oslo, Norway

* Correspondence: rafal.ciosk@ibv.uio.no; rafal.ciosk@ibch.poznan.pl

SUMMARY

How animals rewire cellular programs to survive cold is a fascinating problem with potential biomedical implications, ranging from emergency medicine to space travel. Studying a hibernation-like response in the free-living nematode *Caenorhabditis elegans*, we uncovered a regulatory axis, involving DAF-16/FoxO and PQM-1 transcription factors, which enhances cold survival via up-regulation of iron-trapping molecule, ferritin. By sequestering free iron, ferritin protects cells against the damage induced by reactive oxidative species (ROS), which arise upon iron overload. Mimicking the molecular function of ferritin with a drug, we show that iron sequestration also protects mammalian neurons, a cell type particularly sensitive to hypothermia, from cold-induced degeneration. Our findings substantiate hypotheses proposing the upregulation of ferritin as a hallmark of hibernation, and suggest an avenue for improvements of hypothermia treatments.

Keywords:

DAF-16, FoxO, PQM-1, ETS-4, iron, ROS, FTN-1, ferritin, neuroprotection, cold, hibernation

INTRODUCTION

Torpor is a state of decreased physiological activity in an animal, characterized by profound reduction of non-essential body functions, to survive environmental hazards. Hibernation (multiday torpor), with the characteristic reduction of physical activity and metabolism, is deployed to survive spells of cold (Andrews, 2019; Geiser, 2013; Melvin and Andrews, 2009; Wu and Storey, 2016). Although humans do not hibernate, some primates do (Blanco et al., 2018), hinting at the possibility that a hibernation-like response may, one day, be induced also in humans, with important medical implications (Cerri, 2017). For example, stroke or trauma patients are subjected to cooling to facilitate survival, primarily by preserving brain functions (Kutcher et al., 2016; Yenari and Han, 2012), so inducing a hibernation-like response could facilitate their recovery. Moreover, hibernation-related mechanisms are of interest for longevity research, as both poikilotherms (animals with fluctuating body temperature, like flies and fish) and homeotherms (like mice) live longer at lower temperatures (Conti et al., 2006; Loeb and Northrop, 1916). Finally, there has been much excitement about the possibility of inducing torpor in relation to space travel (Nordeen and Martin, 2019). Therefore, understanding the molecular mechanisms underlying physiological benefits of cold, and learning how to manipulate them, has the potential to transform several areas of medicine.

The free-living nematode *C. elegans* is a powerful model for studying torpor. Thus far, most studies have focused on the effects of nutrient or oxygen deprivation (Fielenbach and Antebi, 2008; Padilla and Ladage, 2012). By contrast, the effects of cold remain poorly understood. In the wild, *C. elegans* populates temperate climates (Frezal and Felix, 2015), indicating that these worms are capable of surviving cold. The standard laboratory cultivation temperatures are between 20-25ºC, and a moderate decrease in the temperature, often to 15°C, slows down but does not arrest worms (Klass, 1977; Xiao et al., 2013). A more drastic reduction of temperature, to 0-4ºC, is less well understood, but the emerging view is that a rapid cooling from 20-25ºC to 4ºC (cold shock) kills worms, while a slower cooling, which can be simulated by a transient "cold acclimatization/adaptation" step at an intermittent temperature of 10-15ºC, allows for a full recovery upon returning to standard temperatures (Habacher et al., 2016; Ohta et al., 2014). The cold-adapted worms survive near-freezing temperatures for many days (Habacher et al., 2016; Murray et al., 2007; Ohta et al., 2014;

Savory et al., 2011), and, remarkably, stop ageing while in the cold (Habacher et al., 2016), suggesting that they enter a hibernation-like state (Fig.1a).

Among the factors essential for surviving near-freezing temperatures, we have recently identified a conserved ribonuclease, REGE-1, homologous to the human Regnase-1/MCPIP1 (Habacher and Ciosk, 2017; Habacher et al., 2016). In addition to ensuring cold resistance, REGE-1 has been shown to promote the accumulation of body fat, which depends on the degradation of mRNA encoding a conserved transcription factor, ETS-4 (Habacher et al., 2016). Interestingly, other studies have shown that the loss of ETS-4 partly compromises insulin signaling (Thyagarajan et al., 2010), and that inhibiting the insulin pathway dramatically enhances cold survival following cold-shock/cold-adaptation (Ohta et al., 2014; Savory et al., 2011). Combined, these observations suggested that the cold survival-promoting function of REGE-1 could be related to the inhibition of ETS-4/insulin signaling axis.

Here, we show that inhibiting ETS-4 is indeed beneficial for cold survial. The ultimate effector of reduced insulin signaling is the transcription factor DAF-16/FoxO, and, expectedly, the enhanced cold survival of *ets-4(-)* mutants depends on DAF-16. DAF-16 mediates up-regulation of the so-called class I genes (involved in stress response) and down-regulation of class II gens (related to growth and development) (Murphy et al., 2003; Tepper et al., 2013). While class I genes are directly induced by DAF-16 (through a DAF-16 binding element, DBE), class II genes are induced (via a DAF-16 associated element, DAE) by another transcription factor, PQM-1, originally described as an oxidative stress-responsive transcription factor (Tawe et al., 1998). Because DAF-16 and PQM-1 also display mutually exclusive nuclear localization patterns, they have been proposed to play antagonistic roles, with DAF-16 promoting stress response, and PQM-1 promoting growth and development (Tepper et al., 2013). Surprisingly, we found that DAF-16 and PQM-1 are co-expressed in the nuclei in the cold, and are both crucial for the enhanced cold survival. Using functional genomics, we identified a critical transcriptional target of DAF-16 and PQM-1 promoting cold survival, encoding the iron-scavenging protein FTN-1/ferritin (Gourley et al., 2003).

Ferritin consists of multiple heavy and light subunits (FTH and FTL), which, by creating a large cage-like structure can sequester thousands of iron atoms (Theil, 2013); the

worm ferritins (FTN-1 and -2) are more similar to FTH (Gourley et al., 2003). Iron is an essential element whose cellular levels are tightly regulated by various molecular mechanisms that are largely conserved between worms and humans (Anderson and Leibold, 2014; Muckenthaler et al., 2017). Both iron deficiency and overload have severe consequences for human health. Excess of free iron (also referred to as labile or redox-free) is harmful to the cell, because, in the Fenton reaction, free iron catalyzes the formation of reactive oxygen species (ROS) (Dixon and Stockwell, 2014). Thus, we hypothesize that, by sequestering free iron, FTN-1 curbs the production of ROS and the ensuing cellular damage, and thereby enhancing cold survival. Testing the general applicability of this strategy, we examined murine neurons (i.e. neurons of a non-hibernating species). We observed that treating neurons with an iron-chelating drug resulted in the reduction of ROS and enhanced cold survival, reminiscent of the cold-resitance displayed by neurons from a hibernating mammal (Ou et al., 2018). Supported by observations from hibernating primates, we propose that the ferritin-mediated iron sequestration could be a conserved mechanism facilitating survival under hypothermia.

RESULTS

Inhibiting ETS-4 dramatically improves survival in the cold

Our initial study on *C. elegans* "hibernation" identified REGE-1 as a factor required for wild-type cold survival (Habacher et al., 2016). Studying REGE-1 in a different physiological context, the regulation of body fat, we found that its key target is the conserved transcription factor ETS-4 (Habacher et al., 2016). Thus, we asked whether overexpression of ETS-4, occurring in *rege-1(-)* mutants, is also responsible for the cold sensitivity; measured here at 4ºC and simply referred to as the "cold" (Fig. 1B). Indeed, we found that *rege-1(-); ets-4(-)* double mutants survived cold much better than *rege-1(-)* single mutants (Fig. 1C). In fact, the double mutants were much more resistant to cold than wild type (Fig. 1C). Intrigued, we additionally examined the *ets-4(-)* single mutants and found that they survived cold as well as the double mutants. Thus, inhibiting ETS-4 is beneficial for cold survival irrespective of REGE-1. This was somewhat surprising as, in wild type, REGE-1 inhibits ETS-4 by degrading its mRNA. However, we observed that, in wild type, *ets-4* mRNA was more abundant in the cold (Fig. S1). Thus, an incomplete/inefficient degradation of *ets-4* mRNA in the cold could explain the enhanced cold survival of *ets-4(-)* mutants.

Because many hibernators burn fat to fuel survival in the cold, the ETS-4-mediated fat loss (observed in *rege-1(-)* mutants; Habacher et al., 2016) and cold sensitivity could be connected. However, inhibiting ETS-4 restores body fat of *rege-1(-)* mutants to only wild-type levels (Habacher et al., 2016), and yet the *rege-1(-); ets-4(-)* double mutants were more resistant to cold than wild type (Fig. 1C). We additionally examined the fat content of *ets-4(-)* single mutants and found that it was indistinguishable from wild-type (Fig. 1D). Thus, ETS-4 appears to impact body fat and cold resistance via separate mechanisms (Fig. 1E).

The enhanced cold survival requires both DAF-16 and PQM-1

ETS-4 has been described to synergize with the insulin signaling pathway in limiting the worm lifespan (Thyagarajan et al., 2010). In *ets-4(-)* mutants, the lifespan is thus extended, which, as is the case with many insulin pathway mutants, depends on the transcription factor DAF-16/FOXO (Murphy and Hu, 2013; Thyagarajan et al., 2010). This and additional reports,

that insulin pathway mutants display cold resistance depending on DAF-16 (Ohta et al., 2014; Savory et al., 2011), suggested that the enhanced cold resistance of *ets-4(-)* mutants may also depend on DAF-16. First, using the *age-1(hx546)* allele (carrying a point mutation reducing the activity of AGE-1/PI3 kinase; Ayyadevara et al., 2008), we confirmed that these mutants survive cold far better than wild type, and that this depends on DAF-16 (Fig. S2A). Second, we examined the epistatic relationship between *age-1(hx546)* and *ets-4(-)* mutants. While the *age-1(hx546)* single mutants survived cold, expectedly, much better than wild type (Fig. 2A), we observed no additional benefit of combining *age-1(hx546)* and *ets-4(-)* mutations (Fig. 2A). These observations suggest that AGE-1 and ETS-4 might act in the same pathway, or alternatively converge on the same downstream effector(s). Thus, we examined whether the enhanced cold survival of *ets-4(-)* mutants depends on DAF-16. We found that, indeed, removing DAF-16 completely suppressed the enhanced cold survival of *ets-4(-)* mutants, reverting it to wild-type values (Fig. 2B).

Another transcription factor, PQM-1, has been more recently shown to complement DAF-16 in promoting lifespan in DAF-2 deficient animals (Tepper et al., 2013). In the intestinal cells of *C. elegans*, PQM-1 and DAF-16 nuclear occupancy has been shown to be mutually exclusive, and they appear to regulate separate sets of target genes (Tepper et al., 2013). On the other hand, they bind a shared subset of genes and both are required for the lifespan extension of *daf-2* loss-of-function mutants (Tepper et al., 2013), suggesting that, in certain conditions, DAF-16 and PQM-1 may function together. Therefore, we tested whether the loss of PQM-1 had a similar effect on the cold survival of *ets-4(-)* mutants as the loss of DAF-16, and, indeed, observed just that (Fig. 2C).

Importantly, in otherwise wild-type background, we observed no apparent effects on cold survival in either *pqm-1(-)* or *daf-16(-)* single mutants, nor in the *pqm-1(-); daf-16(-)* double mutants (Fig. S2B). Even the survival of *daf-16(-); pqm-1(-); ets-4(-)* triple mutants was indistinguishable from wild-type worms (Fig. 2C). Together, these observations argue for a specific, joint role for DAF-16 and PQM-1 transcription factors in cold survival that emerges only in the absence of ETS-4.

DAF-16 and PQM-1 are both enriched in the nucleus in the cold

DAF-16 and PQM-1 are transcription factors, and are therefore expected to facilitate survival by inducing transcription of specific genes. Under standard culture conditions, DAF-16 remains (inactive) in the cytoplasm and its cytoplasmic retention depends on insulin signaling. Upon inhibiting insulin signaling, DAF-16 enters the nucleus and activates target genes, though the nuclear enrichment is apparently not essential for DAF-16-mediated gene activation under either mild or severe hypothermia (Savory et al., 2011; Xiao et al., 2013). Based on our genetic analysis, we expected DAF-16 to be functional, and so decided to examine its nuclear localization in *ets-4(-)* mutants. To do this, we employed CRISPR/Cas9 editing, fusing a GFP-FLAG tag to the C-terminal end of the endogenous *daf-16* ORF (see methods). When examining DAF-16(GFP), we saw little GFP fluorescent nuclear signal at 20°C, possibly with a minimal increase in the absence of ETS-4. After one and three days at 4°C, however, we observed an increase in the nuclear signal of DAF-16(GFP) (Fig. 3A and C). Although the signal appeared slightly greater in *ets-4(-)* mutants at day one in the cold, this was no longer true at day 3 (Fig. 3A and C). Thus, although DAF-16 moves into the nucleus in the cold, the nuclear enrichment alone is insufficient to account for the cold survival-promoting activity of DAF-16, observed in *ets-4(-)* but not wild-type animals.

Since our genetic analysis suggested that both DAF-16 and PQM-1 are required for the enhanced cold survival, we performed the same analysis on PQM-1, fusing (by CRISPR/Cas9 editing) an mCHERRY-MYC tag to the C-terminal end of the endogenous *pqm-1* ORF (see methods). We did not detect any PQM-1(mCHERRY) signal at 20°C, in either wild-type worms or *ets-4(-)* mutants (Fig. 3B-C), agreeing with the previously reported expression patterns of PQM-1 (Tepper et al., 2013). By contrast, after one day at 4°C, we began detecting the nuclear PQM-1(mCHERRY) signal in wild-type worms, and a slightly stronger signal in the nuclei of *ets-4(-)* mutants (Fig. 3B-C). After three days at 4°C, the PQM-1(mCHERRY) nuclear signal increased much further (Fig. 3B-C) and, at this time point, *ets-4(-)* mutants displayed significantly higher signal than wild type (Fig. 3B-C). Thus, in contrast to the standard cultivation temperature, where DAF-16 and PQM-1 localize to the nucleus in a mutually exclusive manner (Tepper et al., 2013), we found that, in the cold, DAF-16 and PQM-1 co-exist in the nucleus, potentially coregulating gene expression.

We then checked the corresponding changes in *daf-16* and *pqm-1* mRNAs, and observed no significant changes depending on ETS-4, DAF-16, or PQM-1 (Fig. S3). However,

cold treatment induced a strong up-regulation of *pqm-1* but not *daf-16* mRNA (Fig. S3). Thus, the transcription of *pqm-1* seems to be highly sensitive to cold. Crucially, both DAF-16 and PQM-1 co-exist in the nuclei in the cold, arguing for a model where, in *ets-4(-)* mutants, these factors function together in promoting expression of cold survival-enhancing gene(s).

Identification of a PQM-1/DAF-16 co-regulated gene promoting cold survival

To test the above model, we examined gene expression (by RNAseq) in animals after one day at 4ºC. By comparing *ets-4(-)* mutants to wild type, we uncovered changes in gene expression dependent on ETS-4. Then, by comparing *pqm-1(-); ets-4(-)*, or *daf-16(-); ets-4(-)* double mutants to *ets-4(-)* single mutants, we determined which changes in gene expression, observed in the *ets-4(-)* mutants, depended on PQM-1 or DAF-16. To illustrate this, we prepared an integrative heat-map, using all the 4°C samples with individual replicates. When looking at changes between the strains, we could identify 3 distinct clusters (Fig. 4A). Cluster 1 (red) includes genes that are up-regulated (in the cold) in *ets-4(-)* mutants compared to wild type, and are not changing or are down-regulated in the *ets-4(-)* mutants also mutated for either *daf-16* or *pqm-1*. Cluster 2 (green) comprises genes up-regulated across all conditions. Finally, the smallest cluster 3 (blue), includes genes that are down-regulated in *ets-4(-)* but are not changing or are up-regulated upon additional mutation of either *daf-16* or *pqm-1*. With this analysis, we observed that many changes in gene expression, upon the loss of ETS-4, are reverted upon the additional loss of either DAF-16 or PQM-1, arguing for a functional relationship between DAF-16 and PQM-1.

Taking advantage of the ENCODE database, which reports genome-wide chromatin association of many transcription factors (Davis et al., 2018), we examined the potential binding of DAF-16 and PQM-1 around the transcription start sites (TSS) of genes within each cluster from the heat map. Even though the ENCODE data comes from experiments performed at standard growth conditions, we were able to observe that genes, whose expression in *ets-4(-)* mutants depends on DAF-16 or PQM-1 (i.e. genes in cluster 1 and 3), are enriched for TSS-proximal binding sites for both of these transcription factors (Fig. 4A). The same enrichment was not seen for the cluster 2 genes, whose expression is apparently unrelated to DAF-16 or PQM-1 (Fig. 4A). Combined, the data suggests that, in the cold, DAF-16 and PQM-1 may jointly

activate the expression of some genes that are normally repressed (directly or indirectly) by ETS-4.

To identify genes whose DAF-16 and PQM-1 dependent activation promotes cold survival, we undertook the following functional genomic approach. First, we selected genes up-regulated (in both biological replicates), at least two-fold, in *ets-4(-)* mutants compared to wild type, after one day at 4°C. Second, we intersected these genes with those whose promoters associate with either DAF-1 or PQM-1, according to the confident binding sites from Tepper et al. This analysis yielded seven genes, which were reproducibly up-regulated in *ets-4(-)* mutants, and whose promoters associate with both PQM-1 and DAF-16 (Figs. 4B and S4). If these genes were relevant for the enhanced cold survival, their inhibition would be expected to impede cold survival of *ets-4(-)* mutants. Testing this, we observed that RNAi-mediated depletion of one candidate, *ftn-1* (encoding a worm ferritin), reproducibly compromised cold survival of *ets-4(-)* mutants (Figs. 4C and S4; note that the RNAi construct is predicted to target also *ftn-2*, which is highly similar *to ftn-1*, see below).

FTN-1/Ferritin promotes cold survival

Ferritin in *C. elegans* is encoded by two genes, *ftn-1* and *ftn-2*. While *ftn-1* was previously shown to be up-regulated upon DAF-2 inactivation in a DAF-16 dependent manner (Ackerman and Gems, 2012), *ftn-2* is not considered a DAF-16 target. Confirming our RNA profiling data by RT-qPCR, we observed DAF-16 and PQM-1 dependent increase in the levels of *ftn-1* mRNA (but not *ftn-2*) in cold-treated *ets-4(-)* mutants (Figs. 5A and S5A). Because the RNAi construct targets both *ftn-1* and *ftn-2*, we also examined FTN-1 function using a previously characterized mutant allele (Valentini et al., 2012). Inhibiting a single effector of DAF-16 and PQM-1 is expected to phenocopy the loss of either *daf-16* or *pqm-1*. Testing this, we observed that the *ftn-1(-)* single mutants were indistinguishable from wild type (Fig. 5B), similar to *daf-16(-)* and *pqm-1(-)* single mutants (Fig. S2B). Crucially, examining FTN-1 function in the *ets-4(-)* background, we observed that *ftn-1* inactivation suppressed the extended cold survival of *ets-4(-)* worms to wild-type levels (Fig. 5B). Importantly, FTN-1 is highly inducible and mostly expressed in the intestine (Kim et al., 2004), i.e. the tissue where ETS-4, DAF-16 and PQM-1 are all expressed. Combined, these observations support FTN-1 as the main cold survival-enhancing effector of the *ets-4 loss-of-function*/PQM-1/DAF-16 axis.

If the cold survival-promoting role of FTN-1 were related to its function in iron storage, excess iron would be expected to impede cold survival. We tested this by supplementing culture plates with ferric ammonium citrate (FAC), and, indeed, observed a dose-dependent impediment of cold survival (Figs. 5C and S5B). Importantly, although higher iron levels (30 mM) reduced the survival of *ets-4(-)* mutants, their survival was still greater than of the corresponding (i.e. iron-treated) wild type. Moreover, the better survival of iron-treated *ets-4(-)* mutants still dependent on FTN-1, as the *ftn-1(-); ets-4(-)* double mutants responded to excess iron like the corresponding wild type (Fig. 5C). Combined, our data suggests that FTN-1, when expressed in cold-treated *ets-4(-)* animals, facilitates survival by sequestering cellular iron.

Iron sequestration enhances cold survival of mammalian neurons

Deep cooling is used to preserve organs for transplantation and facilitates survival of patients in the clinics. It has been hypothesized that inducing hibernation-like responses in organs/patients could further enhance the health benefits of cooling. To examine whether iron sequestration, uncovered in the worm, might be a conserved approach for enhancing cold survival, we turned to mammalian cells. Since the main goal of cooling patients is the preservation of neuronal functions (see the introduction), we focused on neurons. In short, we differentiated primary murine neuronal stem cells, collected from early embryos, into noradrenergic-like neurons (henceforth "neurons"), which function in both central and peripheral nervous system to affect numerous physiological functions, generally preparing the body for action. To examine their cold resistance, neurons (cultivated at the physiological temperature of 37ºC) were shifted to 10ºC for 4 hours and then returned to 37ºC. Their viability was examined, based on propidium iodide staining, after rewarming for 24 hours (Fig. 6A; for details see the methods).

First, we observed that cooling induced cell death in a large fraction of neurons (Fig. 6A). Interestingly, neuronal death was associated with re-warming (Fig. S6A), which is somewhat reminiscent of reperfusion injury, arguing that not the cold *per se*, but rather the burden associated with restoring cellular functions, is the critical challenge facing cold-treated neurons. Interestingly, a recent study comparing cold survival of neurons, derived from either hibernating or non-hibernating mammals, reported that treating "non-

hibernating" neurons with specific drugs facilitates their cold survival (Ou et al., 2018). These drugs, BAM15 (a mitochondrial uncoupler) and PI (a cocktail of protease inhibitors neutralizing digestive enzymes leaking from damaged lysosomes), are thought to induce a protective cellular environment that, in hibernators, is induced by intrinsic mechanisms. In agreement with that report, we found that treating murine (non-hibernating) neurons with either BAM15 or PI increased cold survival (Fig. 6B). Rewardingly, treating neurons with deferoxamine (DFO, iron-chelating drug, thus functioning similar to ferritin) protected neurons to the same extent as when treating neurons with BAM15, PI, or drug combinations (Fig. 6B).

The cold-mediated lethality of non-hibernating neurons has been associated with increased levels of mitochondria-derived ROS, and treating neurons with either BAM15 or PI reduces the ROS levels (Ou et al., 2018). Because free iron can catalyze the formation of hydroxyl radicals, we examined (using CellROX-green) the relationship between the protective effect of DFO and ROS levels. We observed that treating neurons with DFO, directly before the cold treatment, reduced the ROS levels to the same extent as when treating them with BAM15 (Fig. 6C), strongly implying the connection between the levels of free iron, ROS, and cell survival in the cold.

Sequestering iron protects neurites from cold-induced degeneration

Upon cold exposure, the non-hibernating neurons (but not hibernating neurons) display the striking pruning of neuronal processes/neurites (Ou et al., 2018). This has been linked to ROS-mediated oxidation of cytoskeletal proteins and, remarkably, treating non-hibernating neurons with BAM15 and/or PI stabilizes the neurites in the cold (Ou et al., 2018). By staining murine (i.e. non-hibernating) neurons against NEFH (neurofilament protein heavy polypeptide; a neuron-specific component of intermediate filaments), we observed that, like the other drugs, DFO had a strong stabilizing effect on the neuronal processes (Fig. 7A-B). The neurites of cold-exposed and DFO-treated neurons were similar in length to the control (37ºC) neurons (Fig. 7A-B). Moreover, this protection appeared to be long-lasting, as the neurites were still evident at 24 h after returning to 37ºC (Fig. S7).

DISCUSSION

DAF-16/FoxO transcription factors in hypothermia

There is compelling evidence that mild versus severe hypothermia can elicit distinct molecular responses. For example, while the cold-sensitive channel protein TRPA-1 facilitates worm survival under mild (15ºC) cold, it is not required for surviving severe (2ºC) hypothermia (Ohta et al., 2014; Xiao et al., 2013). Yet DAF-16 has been reported to promote survival under different cooling regimes (Ohta et al., 2014; Savory et al., 2011; Xiao et al., 2013), arguing that, irrespective of variable "upstream" signals, which may vary depending on exact cooling regime, DAF-16 plays a key role in surviving hypothermia. Although the functions of FoxO proteins in hibernating mammals remain to be tested, their cellular levels have been reported to rise during hibernation. For example, FoxO3a, alongside its target genes, is up-regulated in hibernating ground squirrels (Wu and Storey, 2014), arguing for conserved functions of FoxO transcription factors in evoking protection against cold-induced damage.

The functional relationship between DAF-16 and PQM-1

Various posttranslational modifications, including the nuclear translocation, impact the activity of DAF-16/FoxO transcription factors (Martins et al., 2016). Under the cooling regime used in this study, the mRNA levels of *daf-16* remained constant, irrespective of the cultivation temperature. By contrast, we did observe the nuclear enrichment of DAF-16 protein in the cold. Likewise, we noted the nuclear accumulation of PQM-1. The latter was unexpected as, at standard cultivation temperatures, DAF-16 and PQM-1 display mutually exclusive nuclear localization patterns (Tepper et al., 2013). Additionally, these transcription factors can play opposing roles; for example, while the formation of an alternative "dauer" larval stage (deployed to survive adverse environmental conditions) depends on DAF-16 (Murphy and Hu, 2013), PQM-1 facilitates the recovery from the dauer arrest (Tepper et al., 2013). Yet there is also some evidence supporting synergistic roles of DAF-16 and PQM-1. For example, both the class I and II genes (see the introduction) are down-regulated in *pqm-1* mutants (Tepper et al., 2013), and DAF-16 and PQM-1 both contribute to the lifespan extension of *daf-2* or mitochondrial mutants (Senchuk et al., 2018; Tepper et al., 2013). Thus,

at least in certain circumstances, DAF-16 and PQM-1 may collaborate in promoting transcription. Intriguingly, in wild type, the nucleus-enriched DAF-16 and PQM-1 are apparently insufficient for the enhanced cold survival or the induction of *ftn-1*. So what activates them in *ets-4(-)* mutants? We observed that mutating *ets-4* only mildly (and transiently) increased the nuclear levels of DAF-16. By contrast, PQM-1, which at standard cultivation temperatures is essentially absent from the nuclei, became strongly enriched in the nuclei, particularly in *ets-4(-)* mutants. Thus, one possibility is that the additional accumulation of PQM-1 is required to reach a threshold for DAF-16 activation. However, there are other possibilities. For example, the activation might involve additional factors normally inhibited by ETS-4, and future studies will help in distinguishing between these scenarios.

Iron, cold, and ROS

On the cellular level, overload of free iron can catalyze the production of potentially cytotoxic reactive oxygen species, causing a number of acute and chronic degenerative conditions (Dixon and Stockwell, 2014; Kell, 2009); increasing free iron was shown to elevate the formation of ROS also in live worms (James et al., 2015). How exactly, and why, cold triggers the accumulation of free iron remains to be fully understood. In epithelial cells, a sizeable fraction of cold-induced free iron pool was proposed to originate from the microsomal cytochrome P-450 enzymes, which require iron-containing heme as a co-factor (Huang and Salahudeen, 2002). It was also suggested that the cytosolic free iron causes mitochondrial permeabilization, resulting in apoptosis (Rauen et al., 2003). However, in neurons, the suppression of both increased ROS and cold-induced death, with a mitochondrial uncoupling drug, suggests the mitochondria as prime culprits (Ou et al., 2018), in agreement with the general view that most cellular ROS is of mitochondrial origin (Balaban et al., 2005). Irrespective of its source(s), once released, redox-active iron can catalyze the formation of ROS, damaging diverse cellular components (like lipids, proteins and nucleic acids). Not surprisingly, antioxidant defense is one of the hallmarks of hibernation, being particularly critical during the entry to and exit from hibernation, when oxygen sensitive tissues like the brain are particularly vulnerable to ischemia/reperfusion injury (Wu and Storey, 2016).

Iron sequestration as a protective mechanism against cold-induced ROS

To combat oxidative stress, cells evolved various defensive mechanisms. Among those, FoxO transcription factors are known to stimulate the expression of enzymes that combat oxidative damage, like superoxide dismutase and catalase (Kops et al., 2002; Nemoto and Finkel, 2002). However, through inducing FTN-1 and hence iron sequestration, DAF-16 appears to function at an earlier step, preventing the generation of free radicals. While FTN-2 appears to be responsible for sequestering bulk iron under unperturbed growth conditions (James et al., 2015), FTN-1 is more responsive to fluctuating iron levels and only *ftn-1(-)* mutants are sensitive to iron stress (Gourley et al., 2003; Kim et al., 2004). These observations help explain why FTN-1 (rather than -2) promotes cold survival of *ets-4(-)* mutants (where FTN-1 is induced) but not wild-type animals. Importantly, FTN-1 is, expectedly, capable of preventing protein oxidation (Valentini et al., 2012), arguing that, once overexpressed, it will protect worm cells from ROS-mediated damage.

Interestingly, the elevated expression of *FTH1* (the ferritin heavy chain, homologous to the nematode FTN-1) has been recognized as a hallmark of cold adaptation in hibernating lemurs (the only hibernating primates known so far), during either daily torpor or seasonal hibernation (Biggar et al., 2015; Faherty et al., 2018). Thus, the sequestration of free iron by ferritin up-regulation may be a conserved, cell intrinsic, mechanism facilitating cold survival. Crucially, by mimicking FTN-1 function with DFO, we showed that controlling the levels of free iron is an efficient strategy for protecting against cold-inflicted injuries in mammalian neurons, arguing that treatments limiting free iron could dramatically enhance the intrinsic cellular capacity for surviving hypothermia, potentially leading to improved therapies.

ACKNOWLEDGMENTS

We are grateful to Susan Gasser, and the Gasser lab, for supporting later stages of this research. We thank Susan Gasser, Dominique Glauser, and Collin Ewald for discussions and comments. We also thank S. Smallwood and S. Thiry for mRNA sequencing assistance, and L. Gelman and S. Bourke (all at the FMI) for imaging support. This work was sponsored by the following agencies: R.C. was supported by the National Science Centre grant 2015/19/B/NZ3/02412, an EMBO Installation Grant, the Foundation for Polish Science grant TEAM/2016-2/11, co-financed by the European Union Regional Development Fund within the framework of the Operational Program Innovative Economy, and the Research Council of Norway grant FRIMEDBIO-286499. M.F. was supported by the National Science Centre grant 2013/10/E/NZ4/00621. Some of the strains were provided by the Caenorhabditis Genetics Center (CGC) funded by the NIH. The Friedrich Miescher Institute is supported by the Novartis Research Foundation.

AUTHOR CONTRIBUTIONS

TP designed, performed and analyzed most experiments. YG analyzed the genomic data. JL and KS performed and analyzed the cell culture experiments, under the guidance of MF. RC conceived and supervised the project. RC and TP wrote the paper.

DECLARATION OF INTERESTS

The authors declare no competing interests.

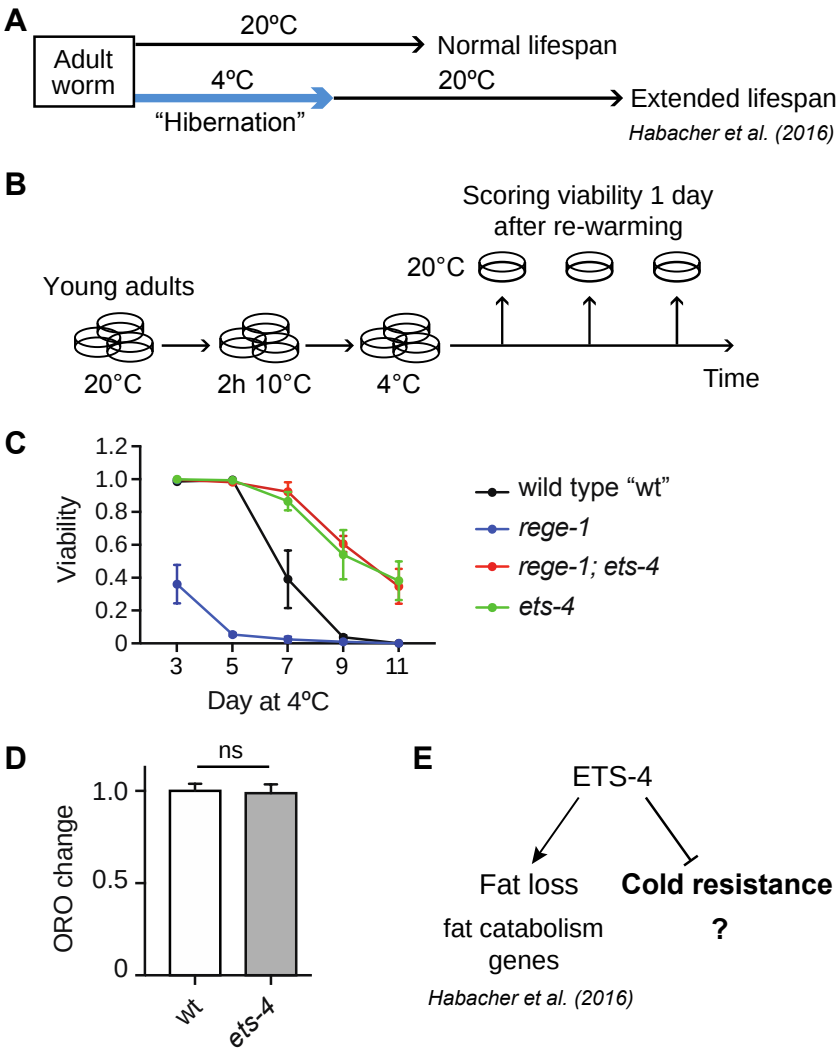

Figure 1. Enhanced cold survival in the absence of ETS-4

A. Schematic illustrating torpor/suspended animation induced by cold. Adult worms, i.e. post development, "hibernate" when incubated at 4ºC. Their lifespan, measured upon returning to standard growth conditions, is extended by the time spent in the cold (see Habacher et al., 2016).

B. Graphical view of a typical cold-survival experiment, described in details in the methods. Shortly, one day-old adults, pre-grown at 20ºC, are briefly cold adapted (for 2 hours at 10ºC) and then shifted to 4ºC. Every second day, some animals are returned to 20ºC and, after 1 day of recovery, scored for viability.

C. Cold survival of animals of the indicated genotypes. Mutant alleles throughout the paper are indicated in brackets and, unless specified otherwise, are loss-of-function alleles. Note that *ets-4(rrr16)* mutants, like *rege-1(rrr13); ets-4(rrr16)* double mutants, survived cold better than wild type (wt). The experiment was performed three times (n= 3); 200-350 animals were scored per time point. Error bars represent standard error of the mean (SEM).

D. Quantification of body fat, stained with the lipophilic dye oil red O (ORO), in animals of the indicated genotypes. The levels of body fat were similar between wt and *ets-4(rrr16)* mutants. n= 3; 10-15 animals were scored per replicate. Error bars represent SEM. Unpaired two-tailed t-test was used to calculate the p-value, "ns" = not significant.

E. Model proposing independent roles of ETS-4 in inducing fat loss, possibly by upregulating genes promoting fat catabolism (see Habacher et al., 2016), and impeding cold resistance by another mechanism.

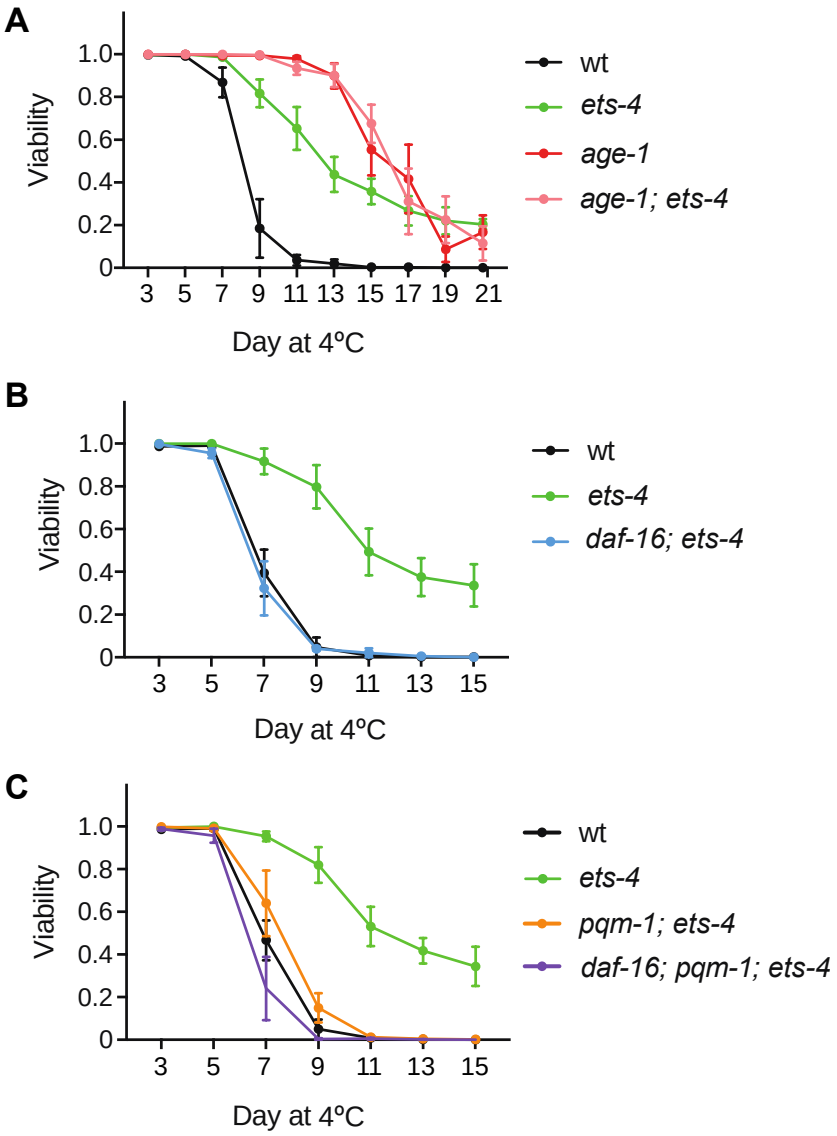

Figure 2. Enhanced cold survival of *ets-4* mutants depends on DAF-16 and PQM-1

A-C. Graphs illustrating viability of animals, of the indicated genotypes, subjected to cold, as explained in 1B. Error bars represent SEM. For statistical analysis, see Table S2.

A. The *age-1(hx546)* mutants (with inhibited insulin signaling) displayed enhanced cold resistance, and combining *age-1(hx546)* and *ets-4(rrr16)* mutations did not endow animals with additional cold resistance. n= 4; 350-500 animals were scored per time point.

B. Combining *daf-16(mu86)* and *ets-4(rrr16)* mutations abolished the enhanced cold survival of *ets-4* mutants, reverting it to wild-type values. n= 4; 350-500 animals were scored per time point.

C. Combining *pqm-1(ok485)* and *ets-4(rrr16)* mutations abolished the enhanced cold survival of *ets-4* mutants, reverting it to wild-type values. Also note that the triple *daf-16(mu86); pqm-1(ok485); ets-4(rrr16)* mutants survived cold essentially like wild type, indicating that DAF-16 and PQM-1 promote cold survival in *ets-4* but not wild-type animals. n= 4; 450-650 animals were scored per time point.

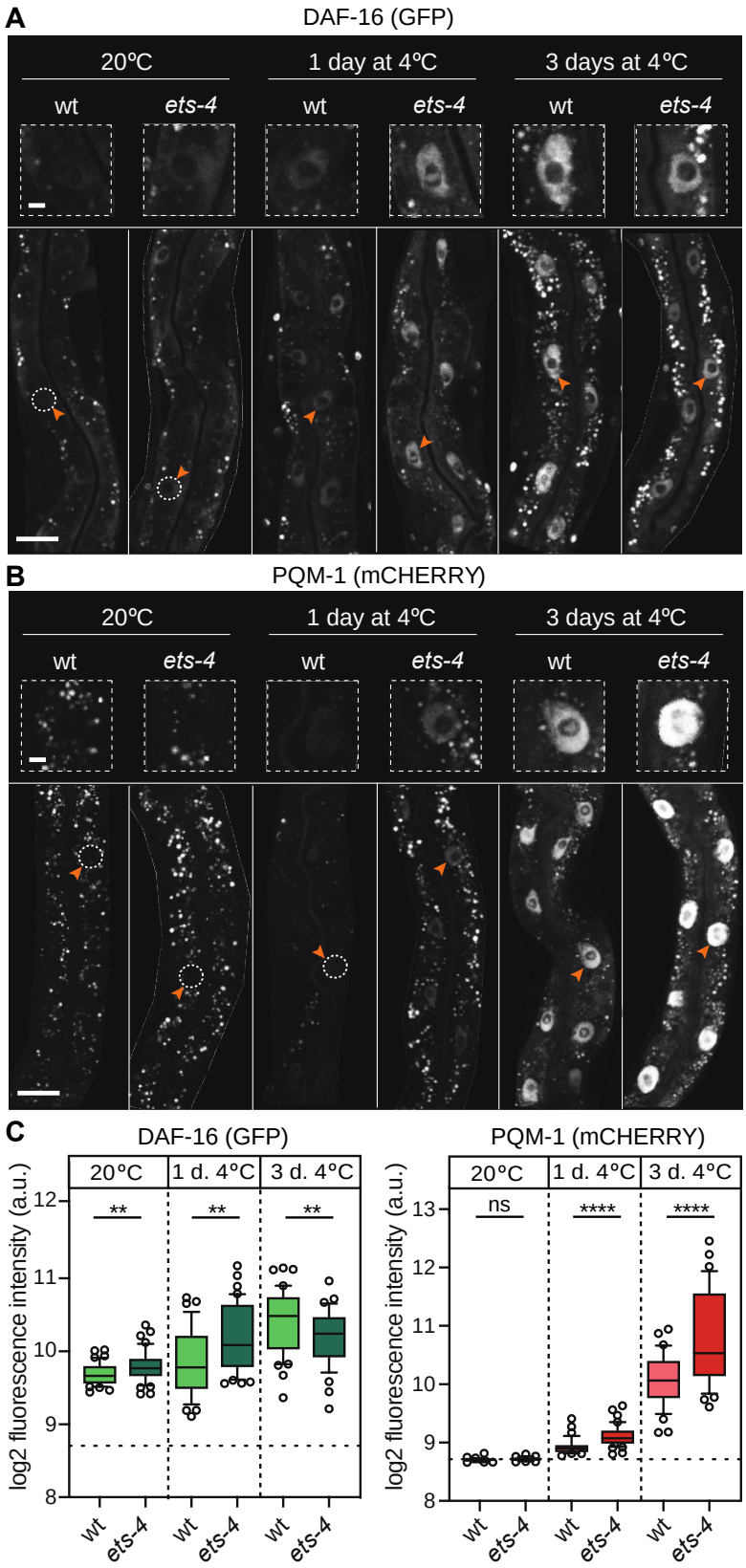
A
DAF-16 (GFP)
20ºC
1 day at 4ºC
3 days at 4ºC
wt
ets-4
B
PQM-1 (mCHERRY)
C
DAF-16 (GFP)
PQM-1 (mCHERRY)
20°C
1 d. 4°C
3 d. 4°C
log2 fluorescence intensity (a.u.)
ns
**
****

Figure 3. DAF-16 and PQM-1 are present in the gut nuclei in the cold

A. Micrographs showing representative confocal images of GFP fluorescence, reflecting the endogenously tagged DAF-16 (allele *daf-16(syb707)*), from wt or *ets-4(rrr16)* mutants. The animals were sampled at the indicated times and temperatures, according to 1B. The corresponding quantifications are shown in C. Arrowheads point to representative gut nuclei (demarcated with dashed circles when displaying little or no fluorescence), which are enlarged in the insets above. Size bars, here and in B: 5 μm (small magnification) and 25 μm (large magnification).

B. Micrographs show representative confocal images of mCherry fluorescence, reflecting the endogenously tagged PQM-1 (allele *pqm-1(syb432)*), from wt or *ets-4(rrr16)* mutants. The animals were sampled at the indicated times and temperatures as above. The corresponding quantifications are shown in C. Arrowheads point to representative gut nuclei, enlarged in the insets above.

C. Quantifications of the nuclear fluorescence, corresponding to A (left) and B (right). Each data point represents $\log_2$ transformed mean nuclear intensity per animal. Dotted line represents the average background within each experiment. Left: n= 3; 10 to 15 animals were scored per replicate. Error bars represent 10^{th} to 90^{th} percentile. Unpaired two-tailed t-test was used to calculate the p-value. ** indicates $p < 0.01$. Right: n= 3; 10 to 15 animals were scored per replicate. "ns" = not significant; **** indicates $p < 0.0001$.

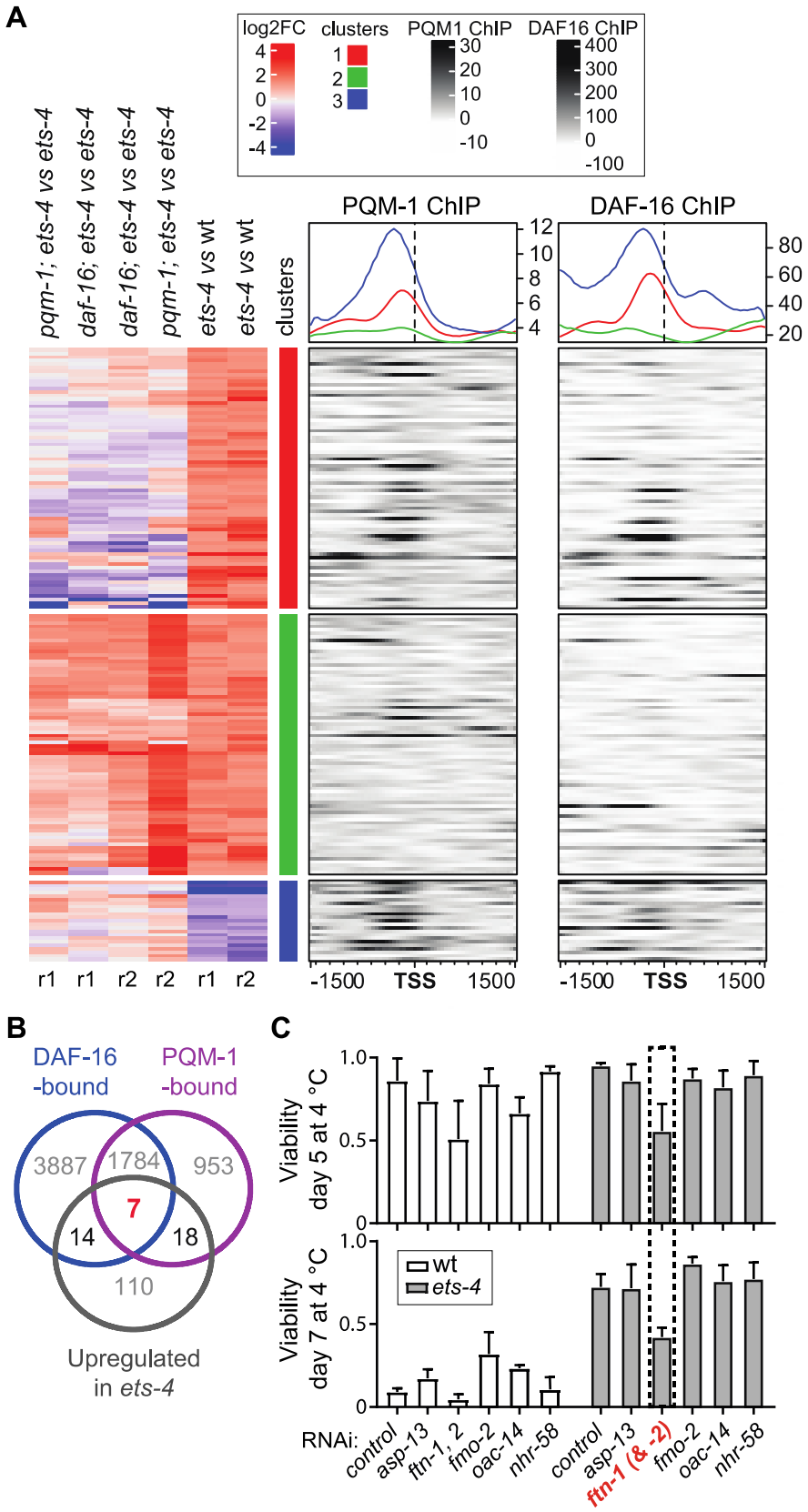
A
log2FC
4
2
0
-2
-4
clusters
1
2
3
PQM1 ChIP
30
20
10
0
-10
DAF16 ChIP
400
300
200
100
0
-100
pqm-1; ets-4 vs ets-4
daf-16; ets-4 vs ets-4
daf-16; ets-4 vs ets-4
pqm-1; ets-4 vs ets-4
ets-4 vs wt
ets-4 vs wt
clusters
PQM-1 ChIP
DAF-16 ChIP
12
10
8
6
4
80
60
40
20
r1
r1
r2
r2
r1
r2
-1500
TSS
1500
-1500
TSS
1500
B
DAF-16
-bound
PQM-1
-bound
3887
1784
953
7
14
18
110
Upregulated
in ets-4
C
Viability
day 5 at 4 °C
1.0
0.5
0
Viability
day 7 at 4 °C
1.0
0.5
0
wt
ets-4
RNAi:
control
asp-13
ftn-1, 2
fmo-2
oac-14
nhr-58
control
asp-13
ftn-1 (& -2)
fmo-2
oac-14
nhr-58

Figure 4. DAF-16 and PQM-1 co-regulate expression of some genes

A. Transcriptome analysis, by RNA-seq, performed on animals of the indicated genotypes, as described in details in the methods. Strains used: wt, *ets-4(rrr16)*, *daf-16(mu86); ets-4(rrr16),* and *pqm-1(ok485); ets-4(rrr16)*. The animals, treated according to 1B, were collected at day 1 at 4ºC. Left: Integrative heat map showing $\log_2$ fold changes in gene expression, between the indicated strains. "r1 and r2" indicate biological replicates. Each line represents one gene. Automated clustering showed three distinct clusters: cluster 1 (red) includes genes up-regulated in the *ets-4* animals (compared to wild type), and not changing or down-regulated in the double mutants (compared to *ets-4*). Cluster 2 (green) includes genes up-regulated across all samples. Cluster 3 (blue) includes genes that are down-regulated in the *ets-4* animals, and not changing or up-regulated in the double mutants. Right: Using the ChIP ENCODE data (Davis et al., 2018), we examined the binding of DAF-16 and PQM-1 around the transcription start sites (TSSs) of genes shown on the left. The line graphs above (colored according to the clusters) illustrate enrichments for DAF-16 or PQM-1 binding, within each cluster, around the TSS. Note that both DAF-16 and PQM-1 tend to bind the promoters of cluster 1 (red) and 3 (blue) genes, but not the cluster 2 (green) genes.

B. Diagram comparing relations between three sets of genes: Grey circle: genes upregulated more than 2-fold in *ets-4(rrr16)* mutants compared to wt (at day 1 at 4ºC), in the two replicates; Blue circle: all genes whose promoters are bound by DAF-16 (Tepper et al); Magenta: all genes whose promoters are bound by PQM-1 (Tepper et al). Note that seven genes were reproductively up-regulated in the absence of ETS-4, whose promoters are bound by both DAF-16 and PQM-1.

C. Five out of the seven genes (from B) were RNAi-depleted, from either wt or *ets-4(rrr16)* animals, and those animals were tested for cold resistance (according to 1B) at the indicated times. Note that only depleting *ftn-1* (and *ftn-2*, as RNAi is predicted to target both homologs) significantly reduced cold survival of *ets-4(rrr16)* animals (stippled box). Error bars represent SEM. n= 3; 200-350 animals were scored per time point.

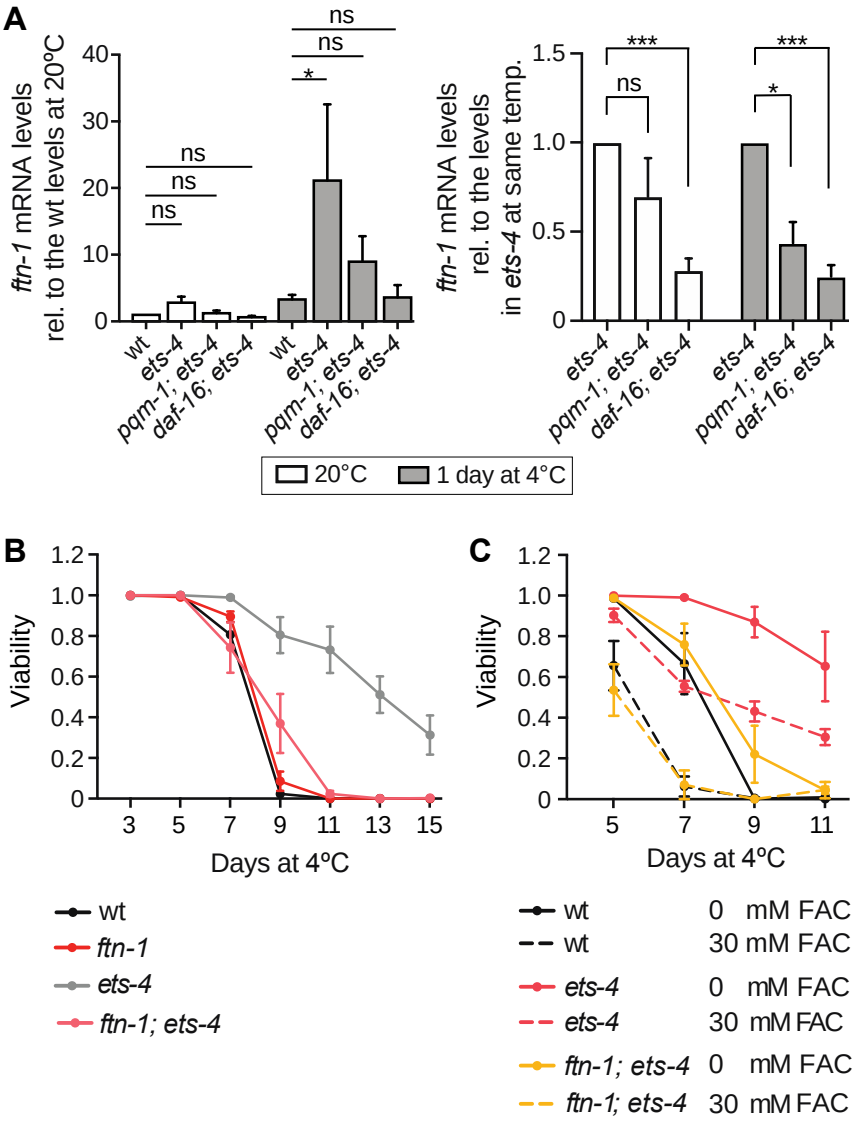

Figure 5. DAF-16 and PQM-1 promote cold survival by inducing *ftn-1*/ferritin

A. Left: Shown are *ftn-1* mRNA levels, measured by RT-qPCR, in animals of the indicated genotypes. Strains used: wt, *ets-4(rrr16)*, *pqm-1(ok485); ets-4(rrr16)*, and *daf-16(mu86); ets-4(rrr16).* The animals were sampled at 20°C, before cold adaptation, and after one day at 4°C, according to 1B. The mRNA levels were normalized to the levels of *act-1* (actin) mRNA. At each temperature, the values were then normalized to those from the wild type at 20°C. Right: same as A, except the *ftn-1* levels were normalized to the values from *ets-4(rrr16)* mutants within each temperature. n= 5; error bars represent SEM. P values were calculated using 2-

way ANOVA for multiple comparisons. “ns” = not significant; * indicates p > 0.05, and *** p > 0.001.

B. Viability of animals, of the indicated genotypes, subjected to cold as explained in 1B. Error bars represent SEM. n= 3; 250-400 animals were scored per time point. Note that combining the *ftn-1(ok3625)* mutation with *ets-4(rrr16)* reverted the enhanced cold survival of *ets-4* mutants to wild-type values, similar to the double *daf-16; ets-4* or *pqm-1; ets-4* mutants in 2B-C. Also, like *daf-16* and *pqm-1* single mutants in S2B, *ftn-1(ok3625)* single mutants survived cold as well as wt.

C. Viability of animals, of the genotypes as above, subjected to cold as explained in 1B, exposed to excess iron (in the form of ferric ammonium citrate, FAC). Error bars represent SEM. n= 3; 300–500 animals were scored per time point.

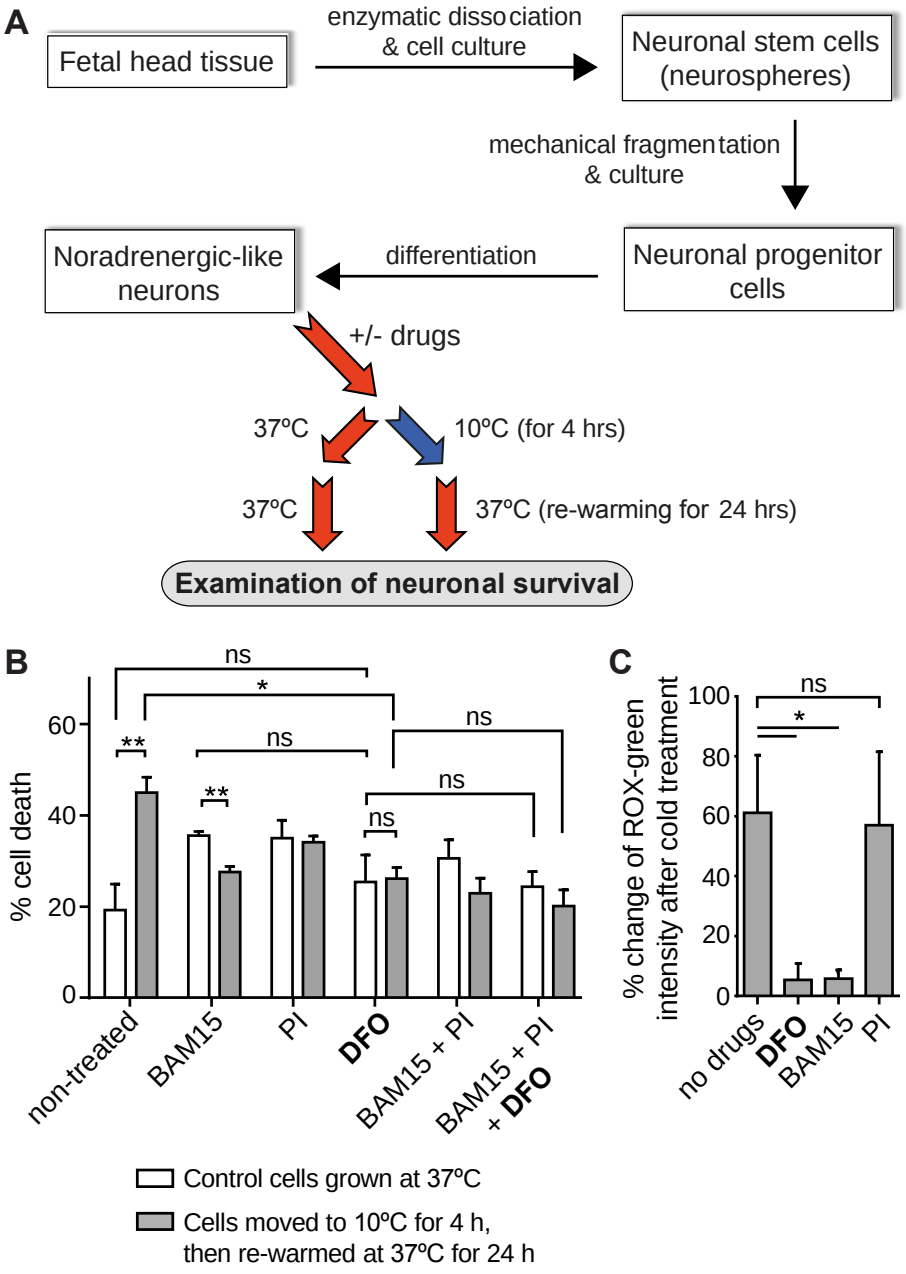

Figure 6. Sequestering free iron promotes cold survival of mammalian neurons

A. Experimental flow testing cold resistance of murine neurons; for a detailed description see the methods. Drugs (BM15, PI and/or DFO) were administered before moving cells to the cold.

B. Viability of murine neurons, subjected to cold and the indicated drugs, was examined by staining with propidium iodide (for details see the methods). **"**BAM15" is a mitochondrial uncoupling drug, "PI" a cocktail of protease inhibitors, and "DFO" deferoxamine, an iron chelator. Error bars represent SEM. n= 3 experiments; p values, between cold-treated and control (37ºC) samples, were calculated with Student's t test, while the ANOVA plus Tukey post hoc test was used to compare samples subjected to different drugs. * indicates $p < 0.05$; ** $p < 0.01$; and "ns" not significant. Note that, in contrast to non-treated cells incubated at 10 ºC, treating cells with DFO prevented cell death to a similar extent like the treatment with BAM15, PI, or the combination of drugs.

C. Comparing ROS levels, measured using CellROX-green sensor (see methods), in murine neurons subjected to cold (according to A) and the indicated drugs. n= 3 experiments; p values were calculated by ANOVA plus post hoc Tukey test. * indicates $p < 0.05$; and "ns" not significant. Drugs were administered immediately before moving cells to cold. Error bars indicate SEM.

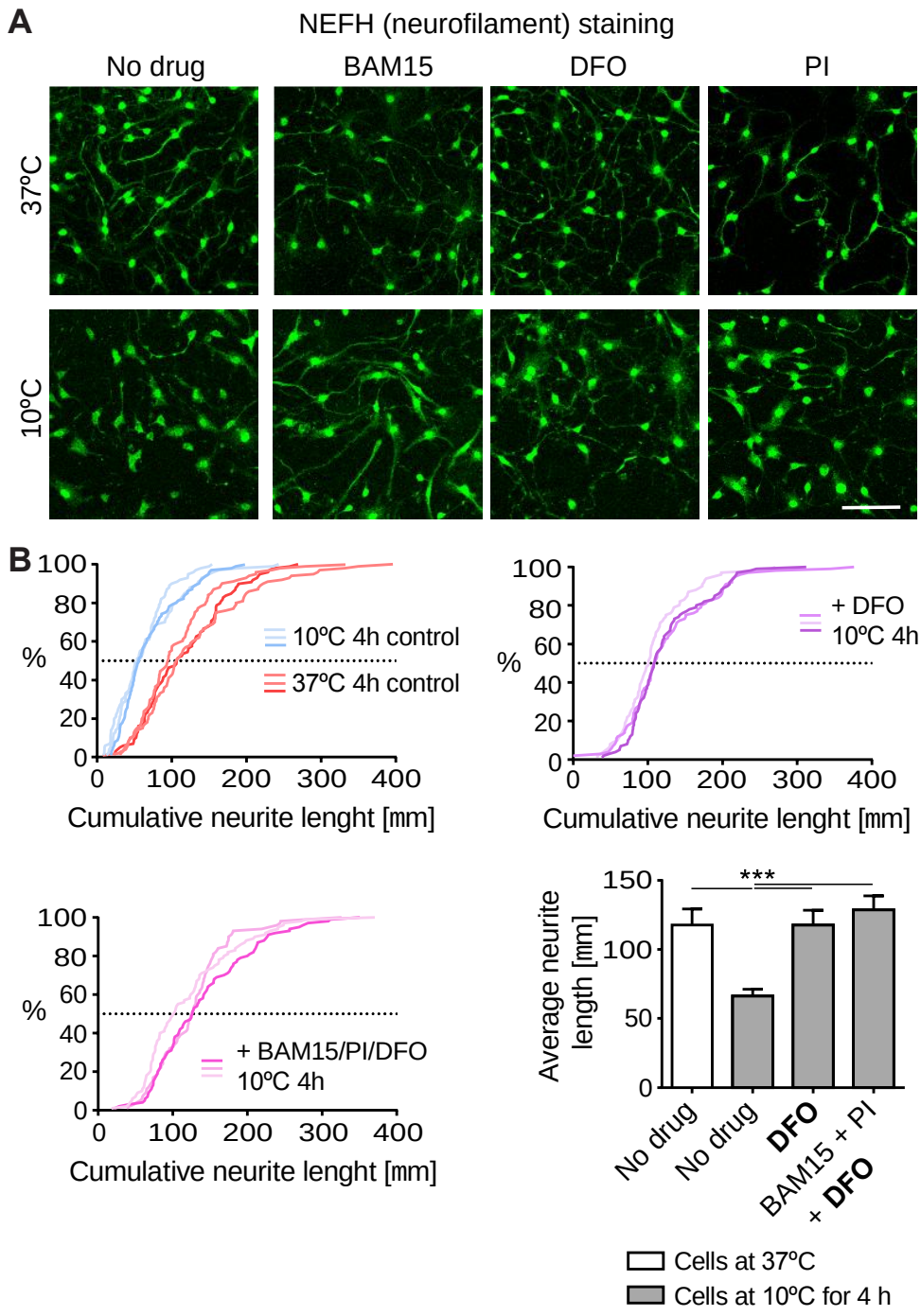
A
NEFH (neurofilament) staining
No drug
BAM15
DFO
PI
37ºC
10ºC
B
%
10ºC 4h control
37ºC 4h control
Cumulative neurite lenght [mm]
+ DFO
10ºC 4h
+ BAM15/PI/DFO
10ºC 4h
Average neurite length [mm]
***
No drug
No drug
DFO
BAM15 + PI + DFO
Cells at 37ºC
Cells at 10ºC for 4 h

Figure 7. Sequestering iron protects neurites from cold-induced fragmentation

A. Representative confocal images of murine neurons, subjected to cold (according to 6A) and the indicated drugs, and stained, by immunofluorescence, for NEFH to visualize neurites immediately after the cold treatment. Scale bar: 40 □m. Note that the neurites, which in control neurons degenerated upon cold exposure (the bottom left panel), were stabilized by adding DFO, similar to the protective effects of BAM15 or PI.

B. Quantifications of neurite lengths, visualized by NEFH labeling, corresponding to A. The cumulative plots (see methods) compared neurite lengths in cells treated as indicated. Each curve corresponds to one experimental replicate. The bar graph (bottom right) compares average neurite lengths. While cold treatment led to the shortening of neurites, treating cells with DFO alone stabilized the neurites equally well as when combined with BAM15 and PI. *** indicates $p < 0.001$.

METHODS

C. elegans handling and strains

Animals were grown at 20°C on standard NGM plates, fed with the OP50 *E. coli* bacteria (Brenner, 1974). Strains used in this study are listed in Table S1. The CRISPR tagged *daf-16 (syb707) I.* and *pqm-1(syb432) II.* strains were made by SunyBiotec. The C- terminal in-frame insertion of GFP-FLAG and mCHERRY-MYC, respectively, was confirmed by sequencing.

Cold adaptation protocol of *C. elegans* and scoring survival

Prior to cold adaptation, animals were grown at 20°C for two generations on OP50. They were then synchronized by bleaching, and L1 larvae were grown until day 1 of adulthood at 20°C. At day 1 of adulthood, they were cold adapted at 10°C for 2h and then shifted to 4°C. Animals were sampled at 48h intervals, and their survival was scored after 24h recovery at 20ºC (Fig. 1B). All further cold adaptation experiments were performed in this way, unless stated otherwise.

Treating *C. elegans* with Ferric Ammonium Citrate (FAC)

Animals were grown from L1 to day 1 of adulthood at 20°C on different concentrations of Ferric Ammonium Citrate (FAC), supplemented to agar in the plate. They were then cold-treated and scored for survival as above.

RNAi treatment of *C. elegans*

1mM IPTG was added to an overnight culture of RNAi bacteria. 300 □l of bacterial suspension was plated on 100 □l/ml of Carbenicillin and 1mM IPTG-containing agar plates. The L4440 (empty) vector was used as a negative RNAi control. Animals were placed on RNAi plates as L1 larvae, and then were grown to day 1 adulthood at 20°C, at which time point they were cold-adapted and scored as described above. The following RNAi clones were used in this study (brackets indicate the library): *ftn-1/ftn-2* (Ahringer); *fmo-2* (Vidal); *nhr-58* (Ahringer); *oac-14* (Ahringer), *asp-13* (Ahringer) and *ets-4* (Ahringer).

Poly-A mRNA sequencing

1000 day one adult animals were collected 24 hrs after cold adaptation protocol. All steps up to Trizol collection were performed at 4°C. Animals were washed 2 times in M9 buffer and snap frozen in Trizol. Samples were then lysed by freeze/thaw cycles, and RNA extraction

proceeded as described before (Arnold et al., 2014). Genomic DNA was removed using RNeasy Plus Mini Kit (Qiagen). Quality of RNA was monitored by Bioanalyzer RNA Nano chip (Agilent Technologies). Library was prepared using TruSeq Library Preparation Kit (Ilumina). Poly-A mRNA was sequenced using a Hiseq 50-cycle single-end reads protocol on a HiSeq 2500 device (Illumina). Raw RNA sequence data was deposited at GEO with accession No. GSE131870.

Genomic data analysis

FASTQC (Andrews, 2010) was used to check the quaility of the raw sequence data. The reads were mapped to C. elegans genome (Ensembl WBcel235) using STAR (Dobin et al., 2013), with default parameters except: outFilterMismatchNmax 3,outFilterMultimapNmax 1, alignIntronMax 15000, outFilterScoreMinOverLread 0.33, outFilterMatchNminOverLread 0.33. Count matrices were generated for the number of reads overlapping with the exons of protein coding genes using summarizeOverlaps from GenomicFeatures (Lawrence et al., 2013). Gene expression levels (exonic) from RNA-seq data were quantified as described previously (Hendriks et al., 2014). After normalization for library size, log2 expression levels were calculated after adding a pseudocount of 8 (y = log2[x + 8]). Genes with 2-fold changes in both replicates were considered significantly differentially expressed. The ChIP bigWig files for PQM-1 and DAF-16 was obtained from ENCODE project (Davis et al., 2018). EnrichedHeatmap (Gu et al., 2018) was used to generated the integrative heatmap.

RT-qPCR

Around 1000, day one-old adult *C. elegans* were collected at 20°C prior to adaptation or at one day at 4°C after adaptation, washed 2 times in M9 buffer at the respective temperature, and flash frozen in Trizol. RNA was isolated as above. 300 ng of RNA was used to prepare cDNA with the QuantiTect Reverse Transcription kit (Quiagen). cDNA was diluted 1:10 and 5 □l was used with the Light Cycler Syber Green master mix (Roche) and Ct values were calculated using Light Cycler 480 (Roche). Actin was used as a reference gene. Statistical analysis on all of the experiments was performed using the GraphPad/ Prism 8. Statistical method used to calculate P value is indicated in the figure legend. The following primers were used: *act-1* FW: CTATGTTCCAGCCATCCTTCTTGG, *act-1*RV: TGATCTTGATCTTCATGGTTGATGG; *ets-4* FW: CTGAGAACCCGAATCATCCA, *ets-4* RV: TCATTCATGTCTTGACTGCTCC; *ftn-1* FW:

CGGCCGTCAATAAACAGATTAACG, *ftn-1* RV: CACGCTCCTCATCCGATTGC; *daf-16* FW: AAAGAGCTCGTGGTGGGTTA, *daf-16* RV: TTCGAGTTGAGCTTTGTAGTCG; *pqm-1* FW: GTGCATCCACAGTAAACCTAATG, *pqm-1* RV: ATTGCAGGGTTCAGATGGAG; *ftn-2* FW: GAGCAGGTCAAATCTATCAACG, *ftn-2* RV: TCGAAGACGTACTCTCCAACTC.

Fluorescent imaging of *C. elegans* intestinal nuclei

Day one old *C. elegans* were anesthetized in 20 μM levamisol and placed on 2 % agar pads. DAF-16::GFP:::FLAG and PQM-1::mCHERRY::MYC were imaged on a spinning disc confocal microscope: Zeiss AxioImager equipped with a Yokogawa CSU-W1 scan-head, 2 PCO Edge cameras, a Plan-Apochromat 40x/1.3 oil objective and two 488nm and 561nm laser lines. Laser intensities and exposure times were kept constant for all samples, camera binning was set to 2. Mean fluorescence intensity in intestinal cell nuclei (three per worm) was quantified manually with FIJI/ImageJ (Schindelin et al., 2012). The mean fluorescence intensities of each nucleus were averaged and represent one data point for each animal. 10-15 animals were scored per genotype and biological replicate, in total around 40 animals per condition. Statistical analysis was performed using the GraphPad/ Prism 8. Two tailed, unpaired, t-test was performed to calculate the P value between conditions.

Oil red O staining, imaging and image analysis

Oil red O staining was performed as published (O'Rourke et al., 2009). In brief, 0.5 g of Oil Red O powder was mixed in 100 ml Isopropanol for 24h, protected from direct light. This solution was diluted in water to 60 %, stirred O/N, and sterile-filtered using a 0.22 m pore filter. Between 200-300 day one-old animals were collected with 1 ml of M9 buffer, and were washed once with M9. They were fixed in 75 % isopropanol for 15 min with gentle inversions every 3-4 minutes. 1 ml of filtered 60 % ORO was added to the animals after removal of isopropanol. Staining was performed for 6h on a shaker with maximum speed, covered with aluminum foil. Stained animals were placed on 2 % agar pads and imaged. Imaging and image analysis were performed as described before (Habacher et al., 2016). Briefly, animals were imaged using a wide field microscope Z1 (Carl Zeiss) using a 10x objective and a color camera AxioCam MRc (Carl Zeiss). RGB images were first corrected for shading in Zen Blue software (Carl Zeiss). Afterwards, images were analyzed using Fiji/ImageJ software suite (Schindelin et al., 2012), stitched with the Grid/Collection stitching plug-in (Schindelin et al., 2012), and

corrected for white balance. After conversion from RGB to HSB color space, red pixels were selected by color thresholding. A binary mask was created with the Saturation channel and applied to the thresholded image. After conversion to 32-bit, zero pixel values were replaced by NaN. The mean intensity of all remaining pixels was used as a representation of the amount of red staining in the animals (Fiji/ImageJ macro available upon request). 10-15 animals were imaged per genotype and biological replicate. 2 tailed t-test was used to asses significance with Graph Pad/Prism 8.

Suspension culture of mouse neuronal stem cells (NSC) using the neuronal cell sphere

Entire heads of fetal mouse (C57BL/6; gestation day between E9-11) were isolated and the tissue was fragmented into pieces followed by incubation in Trypsin-EDTA (0.05 %) (Thermo Fisher Scientific, Waltham, USA) for 15-min at 37°C. The tissue was subsequently transferred to DMEM/10 % FCS and triturated by pipetting up and down into single-cell suspension. The cell suspension was transferred on adherent, uncoated tissue culture plates. After 3-hour incubation in 5 % CO2 at 37°C, the residual non neuronal cells readily attached to the bottom of the plate and the floating neuronal stem cells were collected. The neuronal cells were transferred on to low-adhesive 6-well plates coated with Poly-HEMA (Poly 2-hydroxyethyl methacrylate; Sigma-Aldrich, St. Louis, USA) using DMEM medium (Thermo Fisher Scientific), supplemented with F-12 (Thermo Fisher Scientific), B-27 (Thermo Fisher Scientific), 100 ng/ml basic fibroblast growth factor (FGF-2, ORF Genetis, Kopavogur, Iceland), 100 ng/ml epidermal growth factor (EGF, ORF Genetis) and 5 µg/ml heparin (Sigma-Aldrich). After 1 day in culture (5 % CO_2/5 % O_2) the neuronal cells formed neuronal spheres which were further cultured and passaged weekly by chopping technique using the tissue chopper (Mahabadi et al., 2015).

Differentiation of NSC to noradrenergic neurons

Neuronal spheres were differentiated towards noradrenergic neurons using available protocols (Mahabadi et al., 2015). The spheres were dissociated by chopping into small cell aggregates and plated onto glass coverslips coated with 0.05 mg/mL poly-D-lysine (Thermo Fisher Scientific) and 3.3 µg/mL laminin (Sigma-Aldrich). Cells were incubated for 5 days in Neurobasal Medium, supplemented with B-27 serum-free supplement, penicillin/streptomycin (all Thermo Fisher Scientific) and neurotrophic factors: 50 ng/mL

BDNF, 30 ng/mL GDNF (Peprotech, London, UK), according to a modified protocol described elsewhere (Mahabadi et al., 2015).

Detection of NSC and mature neuronal markers

Neuronal stem cell and noradrenergic neuronal cell identity was confirmed by PCR-based detection of neuronal stem cell (NSC) gene marker such as *Sox2*, *Gbx2*, *Cd-81*, *Cdh1*, *S100b*, *Dach1*, *Pax6*, *Olig1 and* neural differentiation markers: *Cspg4, DβH, Darpp32, Nestin (NES)*. Moreover the neuronal spheres were immunostained for neuronal stem cell markers: Nestin (1: 500; DSHB, Iowa, USA), Foxg-1 (1:100; Abcam, Cambridge, UK), Emx1 (1: 100; Millipore, Burlington, USA) and Emx2 (1:100; Abgent, San Diego, USA) and differentiated neurons for Th (1:100; Abcam), S100b (1:100; Abcam), DβH (1:500; Abcam), Darpp32 (1:50; Abcam).

Hypothermia treatment of noradrenergic-like neurons

Hypothermia experimental paradigm for differentiated neurons was established by using two independent humidified airtight cell culture incubators. One water-jacketed type incubator was additionally equipped with cooler unit (10°C) and the other incubator was set to 37°C and both contained atmosphere control which was set to 5 % CO_2/5 % O_2. In accordance with the hypothermia setup differentiated neuronal cultures were placed in 10°C-incubator for 4 hours and finally returned to the 37°C-incubator for additional 24 hours of re-warming, if not stated otherwise. Such cooling/re-warming paradigm demonstrated statistically relevant rise of cell death after as early as 4-hour cooling time, which was used in assays evaluating the neuroprotective effects of compounds in cold. For discovering neuroprotective properties of compounds in cold, neuronal culture medium was replaced with a Neurobasal medium without neurotrophic factors supplemented with 100 μM deferoxamine (DFO concentration determined based on dose curve at 10°C) (Sigma-Aldrich), 100 nM BAM15 (Tocris, Bristol, UK), 1:500 dilution of protease inhibitor cocktail III PI (Sigma-Aldrich). All compounds were provided as a single or as a combined treatment.

Propidium iodide staining

After 4 hour cooling at 10°C, and additional 24 hours of re-warming at 37°C, neurons cultured on glass coverslips were incubated in the presence of 10 μg/mL propidium iodide (PI) (Cayman Chemical, Ann Arbor, USA) diluted in phosphate buffered saline (PBS), and co-stained with 1 μg/mL Hoechst 33342 (Life Technologies) for 25 min at 37°C. Cells were then

fixed in ice-cold 4 % buffered formaldehyde for 15 min, washed twice in PBS and placed in histology mounting medium (Sigma-Aldrich) on a glass slide. Prepared material was imaged using fluorescence microscope (Leica DMI 4000B, Germany) and LAS X SP8 software. Counting of total cells (blue nuclei) and necrotic cells (red-PI positive and round) was performed on 2-3 images from 3 coverslips as replicates. Collected data were statistically analyzed using Prism software (version 6.01 for Windows, La Jolla, CA).

CellROX-green staining of ROS production

To demonstrate whether cold-stabilizing drugs inhibit intracellular ROS levels neurosphere-derived neurons were incubated with the cell-permeable dye, CellROX Green Reagent (Life Technologies, Carlsbad, USA) in a final concentration of 5 μM, according to the procedure described elsewhere (Ou et al., 2018). The green fluorescence was emitted after binding the dye to DNA only upon its oxidation. In brief, murine neuronal cells were differentiated as above described in a 24-well plates on glass coverslips. Control cells (group 1) were maintained only at 37°C (non-cold control). Other cells (group 2) were exposed for 4 hrs to 10°C, in the presence or absence of following drugs: 100 μM DFO, 100 nM BAM15 and 1:500 dilution of protease inhibitor cocktail (PI). Subsequently, after 5 min re-warming at room temperature on the bench, ROS accumulation in neurons was assessed for both groups by staining with fluorogenic Cell-ROX green reagent in the dark for 30 min in 37°C. Additionally, before cooling procedure, reference neurons (for time 0) were labelled to detect fluorescent signal in initial precooling cultures. Z-stack well-focused confocal images at 0.55 μm intervals in the z-axis of 4 culture areas per each treatment and condition were collected for both groups. Maximal intensity projections of the Z stack images were produced for data analysis. Microscopy images were taken using a Leica TCS SP5 confocal microscope and LAS X SP8 software. The change in ROS production at 10°C incubated cells vs cells maintained only in 37°C was calculated using a following formula: $(F_2 - F_1)/F_0$ x 100%. The CellROX-green fluorescence of non-cold control cells (F_1; mean intensity) was subtracted from CellROX-fluorescence at the end of cold treatment (F_2; mean intensity). While F_0 stands for the initial mean CellROX-green fluorescent intensity of culture areas before 10 degree cooling.

Neurite tracing

Cultured neurons with or without DFO and BAM15/PI/DFO treatment were fixed with 4% paraformaldehyde, permeabilized and washed with 0.1% Triton X-100 in phosphate buffered

saline and stained by antibody against NEFH. NEFH+ neurite paths were traced with the 'Simple Neurite Tracer' plugin (Longair et al., 2011), ImageJ, using Z-stacked confocal images of neuronal culture (maximal intensity projection of 7 image z-stacks at 0.55 μm intervals in the z-axis). Given the data a cumulative frequency plots of neurite lengths for each experimental group were built using GraphPad Prism version 6.01 for Windows, GraphPad Software, La Jolla California USA.

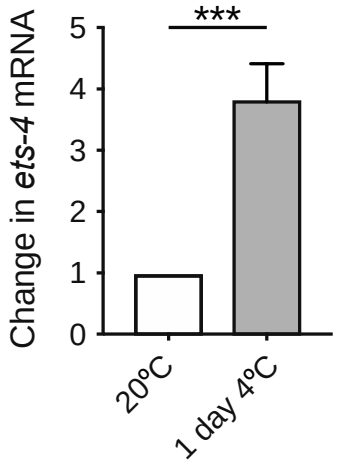

Figure S1. Evaluating *ets-4* mRNA levels in the cold

The levels of *ets-4* mRNA, normalized to actin mRNA, were measured (by RT-qPCR) in one day-old adult wild-type animals at 20°C, and after one day at 4°C, without rewarming. P value was calculated using un-paired student t-test (n= 3). Error bars represent SEM. ***; $p < 0.001$).

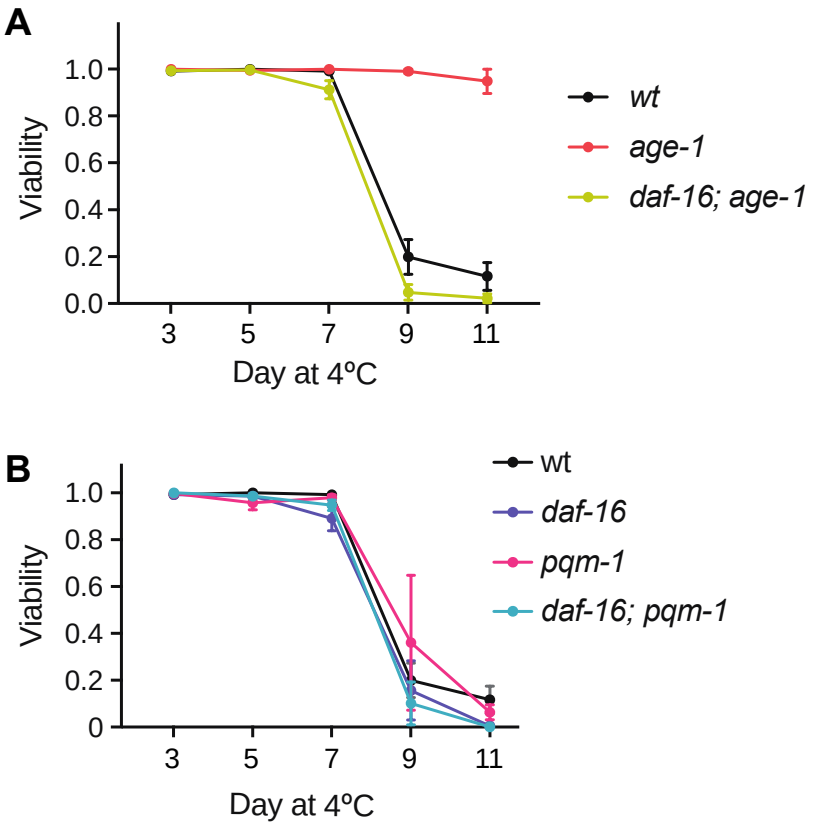

Figure S2. Examining cold survival of mutants affecting insulin signaling

A. Wild-type (wt), *age-1(hx546)*, and *daf-16(mu86); age-1(hx546)* animals were cold adapted as described in Fig. 1B. The *age-1* mutants recovered significantly better than wt, while there was no difference between the double *daf-16; age-1* mutant and wt (n= 3; 200-300 animals were scored per time point). Error bars represent SEM.

B. Wt, *daf-16(mu86)*, *pqm-1(ok485)*, and the double *daf-16(mu86); pqm-1(ok485)* mutants, were cold adapted (n= 3; 200-300 animals were scored per time point). There was no statistical difference between any of the tested animals. Error bars represent SEM. Statistical analysis for both panels can be found in Supplemental Table S2.

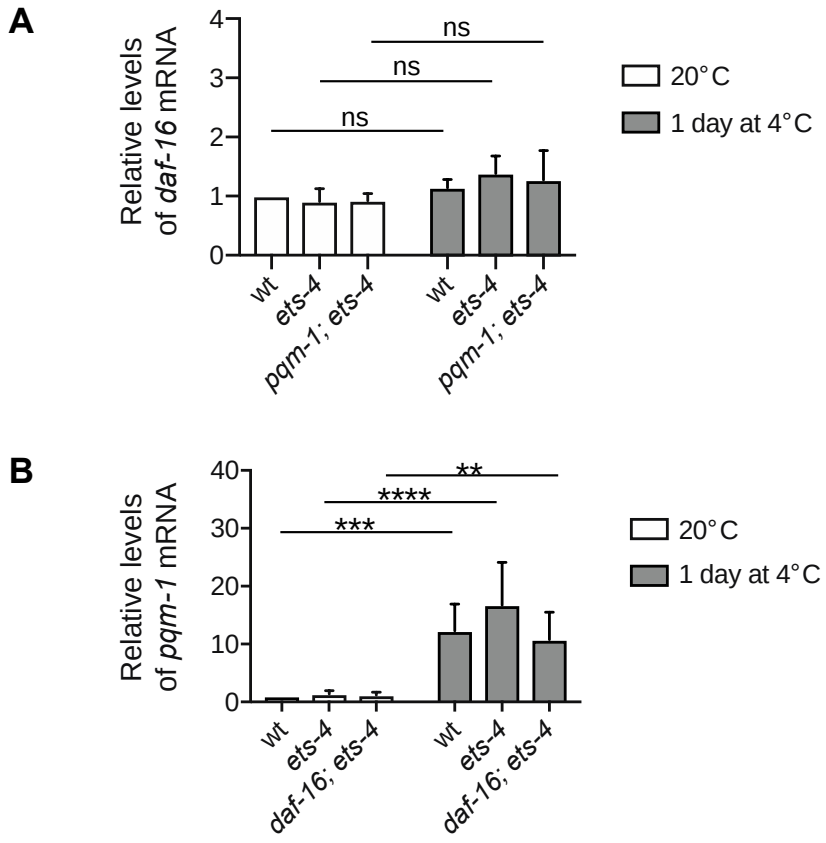

Figure S3. Evaluating levels of *daf-16* and *pqm-1* mRNAs in the cold

A. Animals were collected at 20°C, before adaptation, and after 1 day at 4°C, as described in Fig. 1B. The levels of *daf-16* mRNA, measured by RT-qPCR, were normalized to actin mRNA, and are shown relative to the *daf-16* mRNA level in wt at 20ºC. Wt and *ets-4(rrr16)* mutants were collected at 20°C, and after one day at 4°C (n= 5). P values were calculated using 2-way ANOVA. Error bars represent SEM. ns = not significant.

B. Relative *pqm-1* mRNA levels were measured as in A. Wild-type, *ets-4(rrr16)*, and *daf-16(mu86); ets-4(rrr16)* animals were collected at 20°C, and after one day at 4°C (n= 5). P values were calculated using 2-way ANOVA. Error bars represent SEM. ** $p > 0.01$; *** $p > 0.001$; **** $p > 0.0001$.

Gene name	Biological function	Suppression of cold survival upon RNAi
asp-13	Predicted aspartic-type endopeptidase activity	No
cpt-4	Carnitine Palmitoyl Transferase - predicted to have transferase activity, transferring acyl groups	NT*
fmo-2	Flavin containing monooxygenase 5	No
ftn-1	Ferritin - cellular iron homeostasis	Yes
nhr-58	Nuclear Hormone Receptor - predicted to have DNA-binding activity transcription factor activity	No
oac-14	Predicted to have transferase activity, transferring acyl groups other than amino-acyl groups	No
pals-37	Protein containing ALS2cr12	NT*

*NT - Not tested

Figure S4. Candidates potentially promoting the cold survival of *ets-4* animals

Candidate genes corresponding to the 7 genes in Fig. 4B, with indicated biological functions. Only *ftn-1* RNAi diminished the enhanced cold survival of *ets-4(rrr16)* mutants.

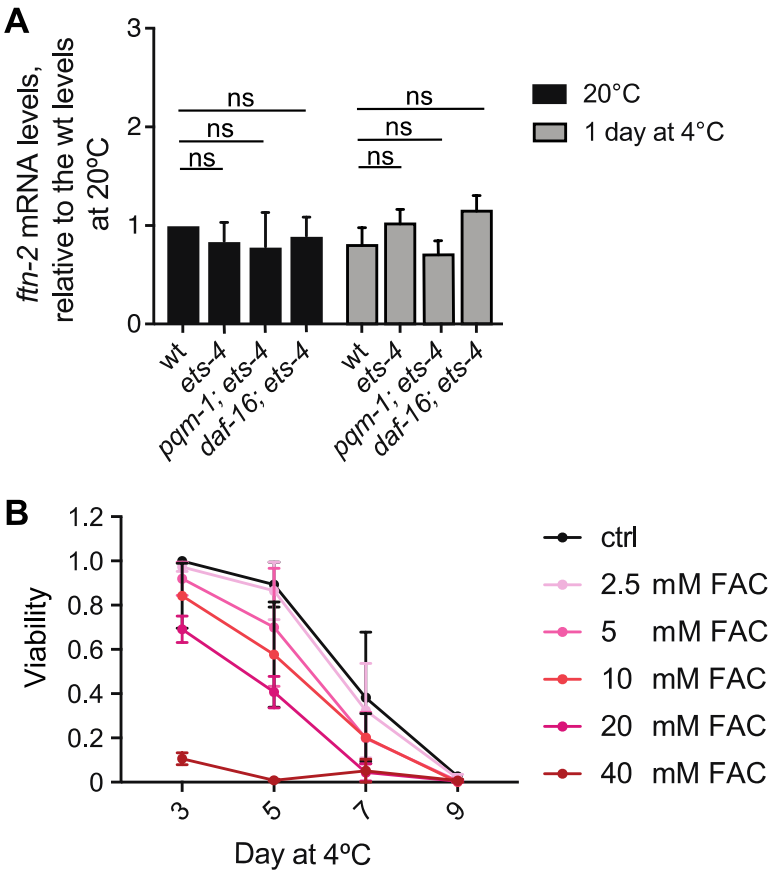

Figure S5. Interrogating the impact of iron deregulation on cold survival

A. Animals were collected at 20°C, prior to adaptation, and after one day at 4°C, without rewarming, as described in Fig. 1B, the genotypes are as in Fig. 5A. The levels of *ftn-2* mRNA, measured by RT-qPCR, were normalized to actin mRNA, and are shown relative to the *ftn-2* mRNA level in wt at 20ºC. Wt and *ets-4* animals were collected at 20°C and after one day at 4°C (n= 3). P values were calculated using 2- way ANOVA. Error bars represent SEM. ns = not significant.

B. Wt animals were exposed to the indicated concentrations of ferric ammonium citrate (FAC), provided in agarose plates. Animals were grown on FAC-supplemented plates from the L1 larval stage to day one adulthood, prior to cold adaptation as described in Fig. 1B. (n= 3; 200-300 animals were scored per condition). Error bars represent SEM.

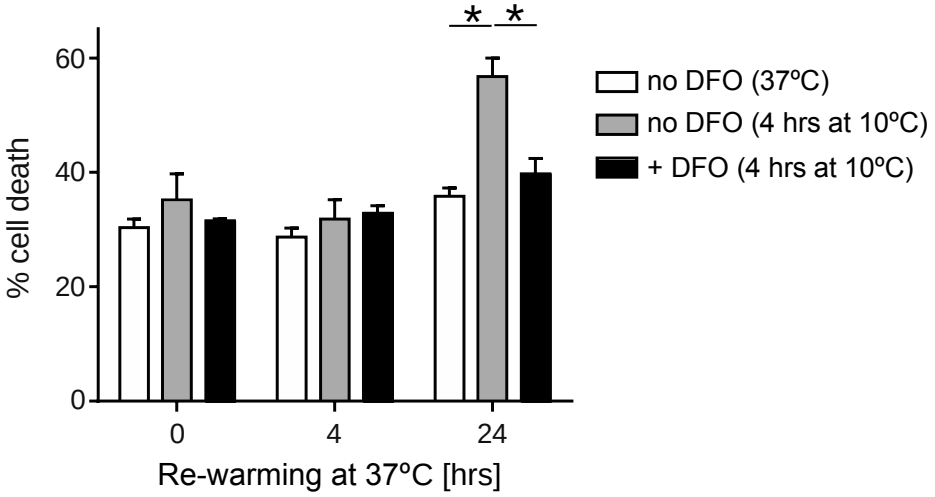

Figure S6. Cold-treatment induces neuronal death during rewarming.

Viability of murine neurons, subjected to cold +/- DFO, was examined during rewarming at 37ºC, by staining with propidium iodide (for details see the methods). Error bars represent SEM. n= 3 experiments; p values were calculated with Student's t test; * $p < 0.05$. Note that, in this procedure, neurons died during re-warming, which was prevented by the treatment with DFO.

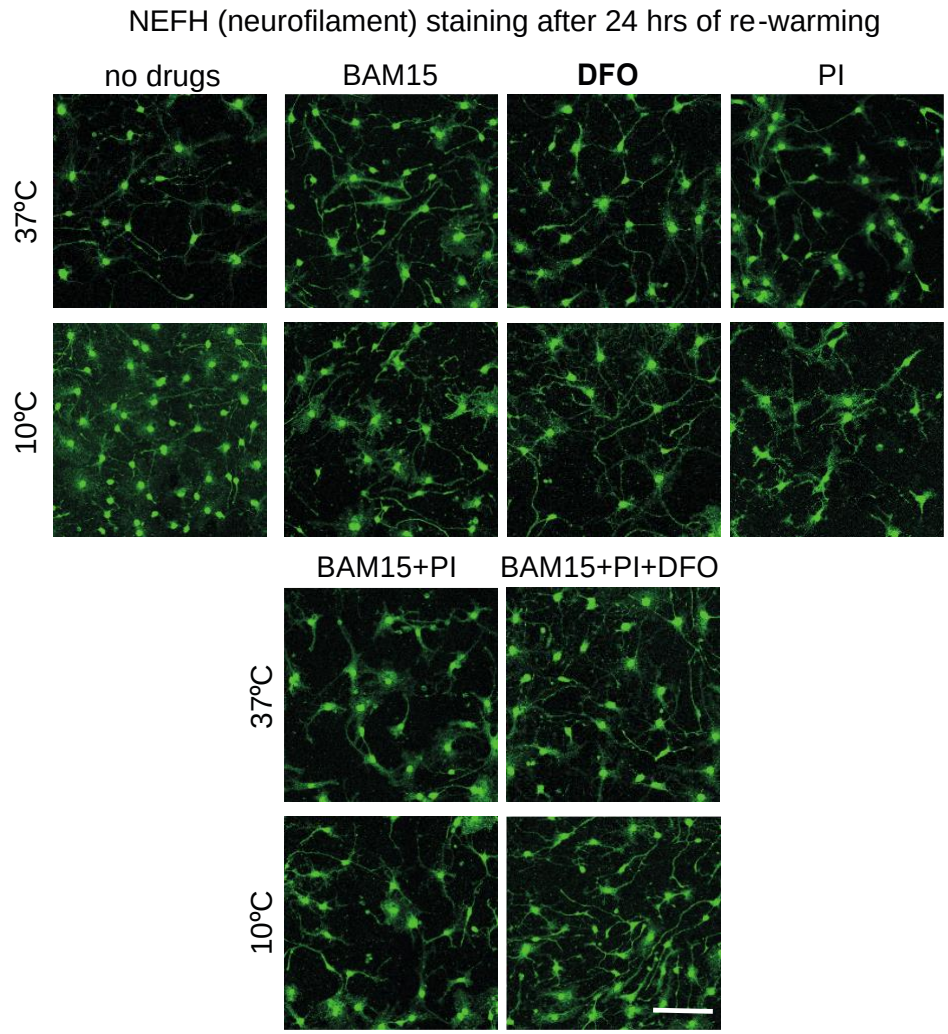

Figure S7. Sequestering iron has a long-lasting protective effect on neural integrity

Representative confocal images of murine neurons, subjected to cold (according to 6A) and the indicated drugs, and stained, by immunofluorescence, for NEFH to visualize neurites after 24 h rewarming at 37ºC. Scale bar: 40 □m. As in 7A, the neurites, which in control neurons degenerate upon cold exposure (the bottom left panel), were stabilized by adding DFO, similar to the protective effects of BAM15, PI, or the combinations of drugs. Note that, in contrast to 7A, here the cells were examined only after one day of re-warming. The neurites appeared well-preserved, arguing that the protective effects of drugs are long-lasting.

Table S1. The *C. elegans* strains used in this work

Genotype	**CGC**/RAF
wt	
age-1(hx546) II.; ets-4(rrr16) X.	2169
age-1(hx546) II.	**TJ1052**
daf-16(mu86) I.; age-1(hx546) II.	2150
daf-16(syb707) I.	5010
daf-16(mu86) I.	**CF1038**
ets-4(rrr16) X.	1758
daf-16(mu86) I.; ets-4(rrr16) X.	2107
pqm-1(ok485) II.; ets-4(rrr16) X.	2106
ftn-1(ok3625) V.	**RB2603**
pqm-1(ok485) II.	**RB711**
daf-16(mu86) I.; pqm-1(ok485) II.	2105
pqm-1(ok485) II.; ets-4(rrr16) X.	2033
pqm-1(syb432) II.	2156
pqm-1(syb432) II.; ets-4(rrr16) X.	2157
rege-1(rrr13) I.	5018
rege-1(rrr13) I.; ets-4(rrr16) X.	1759
daf-16(syb707) I.; ets-4(rrr16) X.	5054
daf-16(mu86) I.; pqm-1(ok485) II.; ets-4(rrr16) X.	5062
ftn-1(ok3625) V.; ets-4(rrr16) X.	5063

"CGC" indicates strain numbers available from the Caenorhabditis Genetics Center

"RAF" indicates strain numbers in the Ciosk lab collection

REFERENCES

1. Ackerman, D., and Gems, D. (2012). Insulin/IGF-1 and hypoxia signaling act in concert to regulate iron homeostasis in Caenorhabditis elegans. PLoS Genet *8*, e1002498.
2. Anderson, C.P., and Leibold, E.A. (2014). Mechanisms of iron metabolism in Caenorhabditis elegans. Front Pharmacol *5*.
3. Andrews, M.T. (2019). Molecular interactions underpinning the phenotype of hibernation in mammals. J Exp Biol *222*.
4. Andrews, S. (2010). FASTQC. A quality control tool for high throughput sequence data.
5. Arnold, A., Rahman, M.M., Lee, M.C., Muehlhaeusser, S., Katic, I., Gaidatzis, D., Hess, D., Scheckel, C., Wright, J.E., Stetak, A., et al. (2014). Functional characterization of C-elegans Y-box-binding proteins reveals tissue-specific functions and a critical role in the formation of polysomes. Nucleic Acids Res *42*, 13353-13369.
6. Ayyadevara, S., Alla, R., Thaden, J.J., and Reis, R.J.S. (2008). Remarkable longevity and stress resistance of nematode PI3K-null mutants. Aging Cell *7*, 13-22.
7. Balaban, R.S., Nemoto, S., and Finkel, T. (2005). Mitochondria, oxidants, and aging. Cell *120*, 483-495.
8. Biggar, K.K., Wu, C.W., Tessier, S.N., Zhang, J., Pifferi, F., Perret, M., and Storey, K.B. (2015). Modulation of Gene Expression in Key Survival Pathways During Daily Torpor in the Gray Mouse Lemur, Microcebus murinus. Genomics Proteomics Bioinformatics *13*, 111-118.
9. Blanco, M.B., Dausmann, K.H., Faherty, S.L., and Yoder, A.D. (2018). Tropical heterothermy is "cool": The expression of daily torpor and hibernation in primates. Evol Anthropol *27*, 147-161.
10. Brenner, S. (1974). The genetics of Caenorhabditis elegans. Genetics *77*, 71-94.
11. Cerri, M. (2017). The Central Control of Energy Expenditure: Exploiting Torpor for Medical Applications. Annu Rev Physiol *79*, 167-186.
12. Conti, B., Sanchez-Alavez, M., Winsky-Sommerer, R., Morale, M.C., Lucero, J., Brownell, S., Fabre, V., Huitron-Resendiz, S., Henriksen, S., Zorrilla, E.P., et al. (2006). Transgenic mice with a reduced core body temperature have an increased life span. Science *314*, 825-828.
13. Davis, C.A., Hitz, B.C., Sloan, C.A., Chan, E.T., Davidson, J.M., Gabdank, I., Hilton, J.A., Jain, K., Baymuradov, U.K., Narayanan, A.K., et al. (2018). The Encyclopedia of DNA elements (ENCODE): data portal update. Nucleic Acids Res *46*, D794-D801.
14. Dixon, S.J., and Stockwell, B.R. (2014). The role of iron and reactive oxygen species in cell death. Nat Chem Biol *10*, 9-17.
15. Dobin, A., Davis, C.A., Schlesinger, F., Drenkow, J., Zaleski, C., Jha, S., Batut, P., Chaisson, M., and Gingeras, T.R. (2013). STAR: ultrafast universal RNA-seq aligner. Bioinformatics *29*, 15-21.
16. Faherty, S.L., Villanueva-Canas, J.L., Blanco, M.B., Alba, M.M., and Yoder, A.D. (2018). Transcriptomics in the wild: Hibernation physiology in free-ranging dwarf lemurs. Mol Ecol *27*, 709-722.
17. Fielenbach, N., and Antebi, A. (2008). C-elegans dauer formation and the molecular basis of plasticity. Gene Dev *22*, 2149-2165.
18. Frezal, L., and Felix, M.A. (2015). C. elegans outside the Petri dish. Elife *4*.
19. Geiser, F. (2013). Hibernation. Curr Biol *23*, R188-193.
20. Gourley, B.L., Parker, S.B., Jones, B.J., Zumbrennen, K.B., and Leibold, E.A. (2003). Cytosolic aconitase and ferritin are regulated by iron in Caenorhabditis elegans. J Biol Chem *278*, 3227-3234.

21. Gu, Z.G., Eils, R., Schlesner, M., and Ishaque, N. (2018). EnrichedHeatmap: an R/Bioconductor package for comprehensive visualization of genomic signal associations. Bmc Genomics *19*.
22. Habacher, C., and Ciosk, R. (2017). ZC3H12A/MCPIP1/Regnase-1-related endonucleases: An evolutionary perspective on molecular mechanisms and biological functions. Bioessays *39*.
23. Habacher, C., Guo, Y., Venz, R., Kumari, P., Neagu, A., Gaidatzis, D., Harvald, E.B., Faergeman, N.J., Gut, H., and Ciosk, R. (2016). Ribonuclease-Mediated Control of Body Fat. Dev Cell *39*, 359-369.
24. Hendriks, G.J., Gaidatzis, D., Aeschimann, F., and Grosshans, H. (2014). Extensive Oscillatory Gene Expression during C. elegans Larval Development. Mol Cell *53*, 380-392.
25. Huang, H., and Salahudeen, A.K. (2002). Cold induces catalytic iron release of cytochrome P-450 origin: a critical step in cold storage-induced renal injury. Am J Transplant *2*, 631-639.
26. James, S.A., Roberts, B.R., Hare, D.J., de Jonge, M.D., Birchall, I.E., Jenkins, N.L., Cherny, R.A., Bush, A.I., and McColl, G. (2015). Direct in vivo imaging of ferrous iron dyshomeostasis in ageing Caenorhabditis elegans. Chem Sci *6*, 2952-2962.
27. Kell, D.B. (2009). Iron behaving badly: inappropriate iron chelation as a major contributor to the aetiology of vascular and other progressive inflammatory and degenerative diseases. BMC Med Genomics *2*, 2.
28. Kim, Y.I., Cho, J.H., Yoo, O.J., and Ahnn, J. (2004). Transcriptional regulation and life-span modulation of cytosolic aconitase and ferritin genes in C-elegans. J Mol Biol *342*, 421-433.
29. Klass, M.R. (1977). Aging in the nematode Caenorhabditis elegans: major biological and environmental factors influencing life span. Mech Ageing Dev *6*, 413-429.
30. Kops, G.J., Dansen, T.B., Polderman, P.E., Saarloos, I., Wirtz, K.W., Coffer, P.J., Huang, T.T., Bos, J.L., Medema, R.H., and Burgering, B.M. (2002). Forkhead transcription factor FOXO3a protects quiescent cells from oxidative stress. Nature *419*, 316-321.
31. Kutcher, M.E., Forsythe, R.M., and Tisherman, S.A. (2016). Emergency preservation and resuscitation for cardiac arrest from trauma. Int J Surg *33*, 209-212.
32. Lawrence, M., Huber, W., Pages, H., Aboyoun, P., Carlson, M., Gentleman, R., Morgan, M.T., and Carey, V.J. (2013). Software for Computing and Annotating Genomic Ranges. Plos Comput Biol *9*.
33. Loeb, J., and Northrop, J.H. (1916). Is There a Temperature Coefficient for the Duration of Life? Proc Natl Acad Sci U S A *2*, 456-457.
34. Longair, M.H., Baker, D.A., and Armstrong, J.D. (2011). Simple Neurite Tracer: open source software for reconstruction, visualization and analysis of neuronal processes. Bioinformatics *27*, 2453-2454.
35. Mahabadi, V.P., Movahedin, M., Semnanian, S., Mirnajafi-zadeh, J., and Faizi, M. (2015). In Vitro Differentiation of Neural Stem Cells into Noradrenergic-Like Cells. Int J Mol Cell Med *4*, 22-31.
36. Martins, R., Lithgow, G.J., and Link, W. (2016). Long live FOXO: unraveling the role of FOXO proteins in aging and longevity. Aging Cell *15*, 196-207.
37. Melvin, R.G., and Andrews, M.T. (2009). Torpor induction in mammals: recent discoveries fueling new ideas. Trends Endocrinol Metab *20*, 490-498.
38. Muckenthaler, M.U., Rivella, S., Hentze, M.W., and Galy, B. (2017). A Red Carpet for Iron Metabolism. Cell *168*, 344-361.
39. Murphy, C.T., and Hu, P.J. (2013). Insulin/insulin-like growth factor signaling in C. elegans. WormBook, 1-43.

40. Murphy, C.T., McCarroll, S.A., Bargmann, C.I., Fraser, A., Kamath, R.S., Ahringer, J., Li, H., and Kenyon, C. (2003). Genes that act downstream of DAF-16 to influence the lifespan of Caenorhabditis elegans. Nature *424*, 277-284.
41. Murray, P., Hayward, S.A., Govan, G.G., Gracey, A.Y., and Cossins, A.R. (2007). An explicit test of the phospholipid saturation hypothesis of acquired cold tolerance in Caenorhabditis elegans. Proc Natl Acad Sci U S A *104*, 5489-5494.
42. Nemoto, S., and Finkel, T. (2002). Redox regulation of forkhead proteins through a p66shc-dependent signaling pathway. Science *295*, 2450-2452.
43. Nordeen, C.A., and Martin, S.L. (2019). Engineering Human Stasis for Long-Duration Spaceflight. Physiology (Bethesda) *34*, 101-111.
44. O'Rourke, E.J., Conery, A.L., and Moy, T.I. (2009). Whole-animal high-throughput screens: the C. elegans model. Methods Mol Biol *486*, 57-75.
45. Ohta, A., Ujisawa, T., Sonoda, S., and Kuhara, A. (2014). Light and pheromone-sensing neurons regulates cold habituation through insulin signalling in Caenorhabditis elegans. Nat Commun *5*.
46. Ou, J.X., Ball, J.M., Luan, Y.Z., Zhao, T.T., Miyagishima, K.J., Xu, Y.F., Zhou, H.Z., Chen, J.G., Merriman, D.K., Xie, Z., et al. (2018). iPSCs from a Hibernator Provide a Platform for Studying Cold Adaptation and Its Potential Medical Applications. Cell *173*, 851-+.
47. Padilla, P.A., and Ladage, M.L. (2012). Suspended animation, diapause and quiescence: arresting the cell cycle in C. elegans. Cell Cycle *11*, 1672-1679.
48. Rauen, U., Kerkweg, U., Weisheit, D., Petrat, F., Sustmann, R., and de Groot, H. (2003). Cold-induced apoptosis of hepatocytes: Mitochondrial permeability transition triggered by nonmitochondrial chelatable iron. Free Radical Bio Med *35*, 1664-1678.
49. Savory, F.R., Sait, S.M., and Hope, I.A. (2011). DAF-16 and Delta(9) Desaturase Genes Promote Cold Tolerance in Long-Lived Caenorhabditis elegans age-1 Mutants. Plos One *6*.
50. Schindelin, J., Arganda-Carreras, I., Frise, E., Kaynig, V., Longair, M., Pietzsch, T., Preibisch, S., Rueden, C., Saalfeld, S., Schmid, B., et al. (2012). Fiji: an open-source platform for biological-image analysis. Nat Methods *9*, 676-682.
51. Senchuk, M.M., Dues, D.J., Scheer, C.E., Johnson, B.K., Madaj, Z.B., Bowman, M.J., Winn, M.E., and Van Reamsdonk, J.M. (2018). Activation of DAF-16/FOX0 by reactive oxygen species contributes to longevity in long-lived mitochondrial mutants in Caenorhabditis elegans. Plos Genetics *14*.
52. Tawe, W.N., Eschbach, M.L., Walter, R.D., and Henkle-Duhrsen, K. (1998). Identification of stress-responsive genes in Caenorhabditis elegans using RT-PCR differential display. Nucleic Acids Res *26*, 1621-1627.
53. Tepper, R.G., Ashraf, J., Kaletsky, R., Kleemann, G., Murphy, C.T., and Bussemaker, H.J. (2013). PQM-1 complements DAF-16 as a key transcriptional regulator of DAF-2-mediated development and longevity. Cell *154*, 676-690.
54. Theil, E.C. (2013). Ferritin: The Protein Nanocage and Iron Biomineral in Health and in Disease. Inorg Chem *52*, 12223-12233.
55. Thyagarajan, B., Blaszczak, A.G., Chandler, K.J., Watts, J.L., Johnson, W.E., and Graves, B.J. (2010). ETS-4 is a transcriptional regulator of life span in Caenorhabditis elegans. PLoS Genet *6*, e1001125.
56. Valentini, S., Cabreiro, F., Ackerman, D., Alam, M.M., Kunze, M.B.A., Kay, C.W.M., and Gems, D. (2012). Manipulation of in vivo iron levels can alter resistance to oxidative stress without affecting ageing in the nematode C. elegans. Mechanisms of Ageing and Development *133*, 282-290.

57. Wu, C.W., and Storey, K.B. (2014). FoxO3a-mediated activation of stress responsive genes during early torpor in a mammalian hibernator. Mol Cell Biochem *390*, 185-195.
58. Wu, C.W., and Storey, K.B. (2016). Life in the cold: links between mammalian hibernation and longevity. Biomol Concepts *7*, 41-52.
59. Xiao, R., Zhang, B., Dong, Y.M., Gong, J.K., Xu, T., Liu, J.F., and Xu, X.Z.S. (2013). A Genetic Program Promotes C. elegans Longevity at Cold Temperatures via a Thermosensitive TRP Channel. Cell *152*, 806-817.
60. Yenari, M.A., and Han, H.S. (2012). Neuroprotective mechanisms of hypothermia in brain ischaemia. Nat Rev Neurosci *13*, 267-278.

CHAPTER 3: ANNEX - PRELIMINARY RESULTS

INTRODUCTION

The effects of temperature change on fatty acid composition in cellular membranes is described as homeoviscous adaptation of phospholipid membranes, a term coined back in 1974 (Sinensky, 1974), where fatty acids change their saturation levels according to environmental temperature in order to remain fluid. The fatty acid unsaturation pathway is comprised of specific phospholipids, starting with saturated fats and corresponding fatty acid desaturases that introduce a double bond in the acyl chain, creating a kink that allows greater fluidity of the membrane. It was shown that *fat-5, -6* and *-7* fatty acid desaturases are required to synthetize monounsaturated fatty acids (MUFA) in *C. elegans*. Depletion of these synthetases leads to accumulation of saturated fatty acids that becomes lethal when exposed to cold (Brock et al., 2006; Savory et al., 2011; Taubert et al., 2006). These mutants also lack all *de novo* synthesized polyunsaturated fatty acids (PUFAs), which stimulate growth, reproduction and neurotransmission and serve as precursors for signaling molecules (Kahn-Kirby et al., 2004; Vasquez et al., 2014). In mammalian systems it was found that PUFAs do not all reside in the same subcellular compartment and have specific functions depending on the membranes in which they are located (van Meer et al., 2008). Unfortunately, due to technical constraints, measurements in *C. elegans*, reflect the total fatty acid content of the animal rather than localized subpopulations.

How fat content influences cold survival of *C. elegans* was explicitly examined by Murray et al. (Murray et al., 2007). They found that there is an increase of phospholipid unsaturation upon acclimation to mild cold at 10°C for several days, which correlated with better survival at 0°C than for worms transferred directly from 25°C to 0°C. Enzymes facilitating fatty acid unsaturation are required to survive both the transition from 10°C to 0°C and 25°C to 0°C. Further, they found animals that undergo cold acclimation at 10°C, change their lipid profile, and upon recovery they preserve that cold-specific lipid signature. They tested whether the lipid profile they acquired at 10°C would help them survive direct exposure to 0°C from 25°C. Interestingly, animals behaved as if they never experienced

acclimation at 10°C, which means that the fatty acid composition they acquired during cold acclimation was not sufficient to ensure survival upon transfer from 25°C directly to 0°C. Thus, the exact role played by changes in fatty acid composition in cold adaptation remains unclear. These findings suggest there may be alternative pathways that influence survival in the cold independent of bulk fat storage in the animal.

Here we have taken two approaches to understand the role of fat in cold response. First, we used a recently described regulator of fat metabolism in *C. elegans*, REGE-1 (Habacher et al., 2016; Watts and Ristow, 2017), which degrades *ets-4* mRNA to regulate ETS-4 transcriptional output. Some of the ETS-4 targets encode enzymes in the lipid catabolic pathway, leading to a fat loss phenotype in *rege-1* mutant animals. Consistently, *rege-1* animals die in cold prematurely (Habacher et al., 2016). In contrast, it is known that *daf-2/InsR* mutant exhibits higher fat content (Kimura et al., 1997). Why this is, remains unclear, especially since the downstream target of DAF-2 is DAF-16/FOXO, which is activated upon DAF-2 depletion, and should upregulate genes involved in lipid catabolism as well as fatty acid unsaturation, promoting unsaturated fatty acid accumulation (Watts and Ristow, 2017). Mutants of the *age-1/PI3K*, a kinase downstream of DAF-2, are able to survive cold exposure for longer periods of time than wild type animals (Savory et al., 2011). We asked if in our hands both *daf-2* and *age-1* mutants survive cold exposure longer and if an additional mutation of *rege-1* would suppress their fat levels and affect their cold survival. In parallel, we performed a forward genetic screen for mutations in the *rege-1* mutant background that would extend its survival but not rescue its fat depletion phenotype. In this way we hoped to uncouple the role of bulk fat content and cold survival.

RESULTS

REGE-1 contributes to the cold survival of *daf-2* and *age-1* animals

REGE-1 was identified in a cold sensitivity screen as an essential factor for cold survival (Habacher et al., 2016). Knowing that ETS-4 functions in parallel to the insulin signaling pathway in cold (Chapter 2), and that both *daf-2* and *age-1* are remain viable longer in the cold, we tested whether additional mutation in *rege-1* could compromise their extended

survival. We observed that *rege-1;daf-2*double mutant animals have severely delayed development, reaching adulthood almost 48h after the wild-type. We then tested their recovery upon cold exposure as described in chapter 2. We observed that loss of *rege-1* compromised the extended survival of *daf-2,* but this survival was still dramatically better than the wild type (Figure 1A). Similarly, we observed the same suppress of cold survival in *rege-1;age-1* double mutants which, however, remained more robust than wild type animals (Figure 1B). This observation confirms the essential role of REGE-1 in cold survival, even in long-lived genetic backgrounds.

Since in *rege-1* mutants ETS-4 is overexpressed, we asked if the levels of ETS-4 in the double *rege-1; age-1* mutant background are changed and if these animals are able to survive cold better than the wild type due to changes in the level of ETS-4. To examine the impact of ETS-4 levels, we used MosSCI technology to express ETS-4::GFP from its endogenous promoter and 3'UTR from a known Mos1 transposon site on chromosome II (MosSCI)(Zeiser et al., 2011). We crossed this strain into the *ets-4(rrr16)* background to preserve only one copy of *ets-4* and then in addition to *rege-1(rrr13)* background to be able to examine the *rege-1* phenotypes (Habacher et al., 2016). This strain was then crossed to *age-1(hx546)*. However, we did not observe a loss of GFP signal between in the *age-1* mutant background compared to the *rege-1* mutants (Figure 1C). Since the levels do not decrease, we can hypothesize that either ETS-4 functions upstream of insulin signaling, or in parallel, but in that case its function would likely be altered.

rege-1 is required for increased fat content in reduced insulin signaling mutant animals

Knowing that *rege-1* promotes normal fat content, we examined whether *rege-1* was necessary for the high fat content in the *daf-2* and *age-1* mutant animals. We estimated total fat content in day one adult animals with Oil Red O (ORO) dye that stains lipid droplets. Interestingly, we observed a complete loss of fat content in the double *rege-1;daf-2* mutant animals compared to the high fat *daf-2* mutants and wild type, almost to the level of *rege-1* (Figure 2A). We did not observe a significant increase in the fat levels in *age-1* mutants like in *daf-2* mutants relative to wild-type animals, but again *rege-1* deletion caused a loss of fat (Figure 2B).

This data overall suggest that the total fat content is not a sole contributor to cold survival since we did not observe a correlation between fat content and cold survival. When looking at the double *rege-1;daf-2* and *rege-1;age-1*, they both have less fat than wild-type but survive better in the cold. This is in contrast to the general belief that animals with more fat will be able to survive cold exposure better (Liu et al., 2017). It is possible that in the *rege-1*;*daf-2* and *rege-1*;*age-1* mutant background, DAF-16 will transcribe genes that will contribute to cold survival, but are not directly involved in fat storage. Additionally, we still do not know the fat composition of the double mutant animals, so we cannot say if specific fatty acids contribute to the phenotype or not.

Leukotriene A4 hydrolase homologue mutant is able to rescue *rege-1(rrr13)* cold sensitivity without altering fat levels

To explore the possibility of finding novel mechanisms of enhanced survival in cold independent of fat content, we performed genome wide mutagenesis to identify cold suppressors in *rege-1(rrr13)*; *ets-4(rr16)*; ETS-4::GFP background, where animals have reduced fat levels, characteristically pale appearance, and exhibit cold sensitive phenotype (Habacher et al., 2016). In this background we can as well trace ETS-4 expression levels and directly observe if the levels change upon mutation of a candidate gene. We mutagenized animals with EMS and screened over 50 000 haploid genomes. F2 animals were synchronized by hypochlorite treatment and left to grow until day one of adulthood. They were then adapted to the cold for 2h at 10°C and shifted to 4°C, as described in Chapter 2. They were scored for survival at day 5 when most of the *rege-1* animals are dead. We selected for analysis only surviving animals that were pale, indicative of fat storage defects characteristic of *rege-1* mutants (Figure 3A). However, we encountered several technical challenges in isolating strains of interest. First, unexpectedly, there were many animals surviving the cold at day 5. Second, our outcross strategy relied on the population-based estimation of the homozygous phenotype, and, in combination with weaker alleles, this assumption may have led to errors in identifying homozygotes. Nonetheless, we recovered one confident mutant that demonstrated robust survival. To sequence the mutation, we tested the bulk sequencing method which relies on a single backcross to the unmutagenized parental strain, and isolation of 50 independent homozygous F2 lines (Zuryn and Jarriault, 2013). They were then

expanded and pooled, their genomic DNA was extracted, and their genomes were sequenced for identify candidate mutations.

Our candidate strain that was pale yet survived the cold (Figure 3 B,C) had a mutation in the ZC416.6 transcript that is a gene *ltah-1.2.* The mutation was C – T transition, changing a conserved serine on position 90 to phenylalanine outside of the catalytic domain. LTAH-1.2 is a homologue of human leukotriene L4 hydrolase and is a class II DAF-16 target, meaning that it is normally downregulated in the *daf-2* background (Tepper et al., 2013). Upon RNAi depletion it was shown to elevate fat content and inhibit dipeptide transport in the cell in the wild type animals through inhibition of *pept-1* levels, another class II gene (Benner et al., 2011; Tepper et al., 2013).

In mammals, leukotriene A4 hydrolase/aminopeptidase (LTA4H) functions to catalyze the final step in leukotriene B4 biosynthesis while it also functions as a M1 aminopeptidase (Rudberg et al., 2002). In *C. elegans* there are two LTA4H homologs, *ltah-1.1* and *ltah-1.2*. Previous, it was shown that *ltah-1.1* lacked detectable leukotriene hydrolase activity *in vitro* (Baset et al., 1998). However, no one has closely looked into leukotrienes in *C. elegans* and if they exist it unclear. Leukotrienes are derivatives of arachidonic acid and function as mediators of innate immune response (Peters-Golden et al., 2005). Future studies may reveal the exact role of *ltah-1.2* in both physiological conditions and in cold adaptation in a wild-type background. Nevertheless, we identified a mutation that rescues *rege-1* cold sensitivity independently of gross fat content. Further, this screen provides insight for future screens to uncover more pathways that complement cold survival.

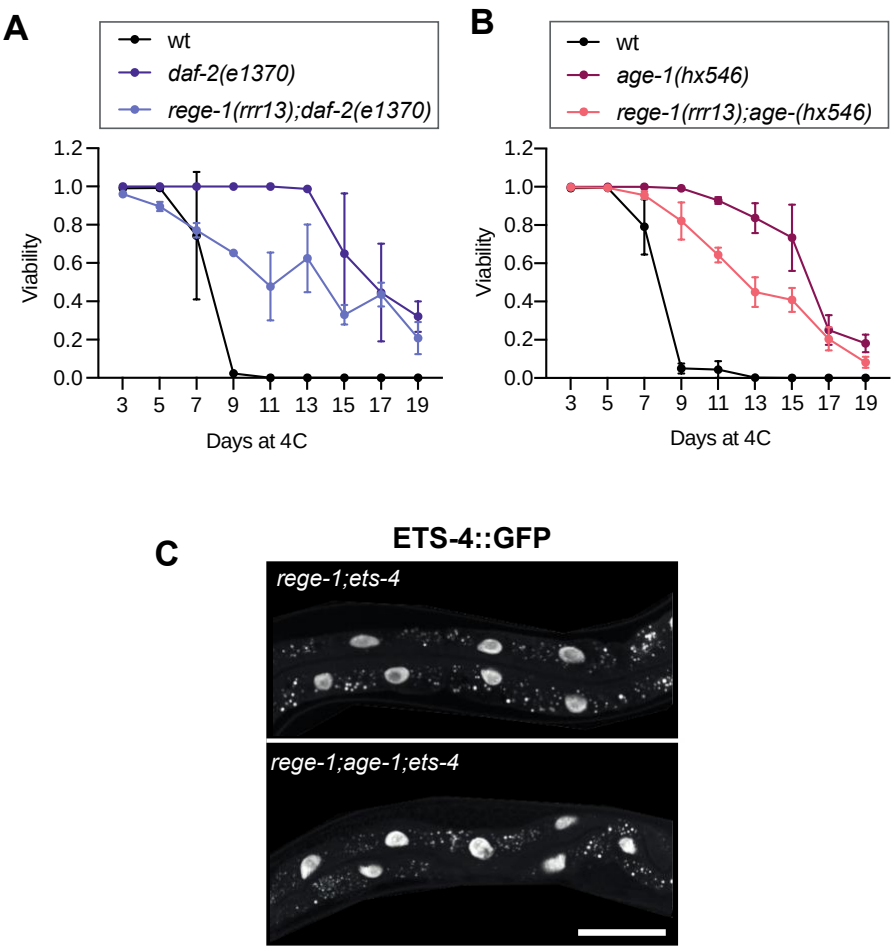

Figure 1. REGE-1 contributes to the cold survival of *daf-2* and *age-1* animals.

A. Day one adult animals of the following genotypes: wild-type, *daf-2(e1370)* and *rege-1(rrr13);daf-2(e1370)* were cold adapted as described before and scored for survival. Error bars represent standard deviation (SD) (n= 2, around 200 animals were scored per timepoint)

B. As in A just animals of the following genotypes: wild-type, *age-1(hx546)* and *rege-1(rrr13);age-1(hx546).* Error bars represent S.E.M. (n= 3, around 300 animals were scored per time point).

C. Day one adult animals at 20°C carrying ETS-4::GFP and *rege-1(rrr13);ets-4(rrr16)* or *rege-1(rrr13);age-1(hx546);ets-4(rrr16)* mutations were imaged using spinning disc confocal microscope.(n= 3, Scale bar = 50μm).

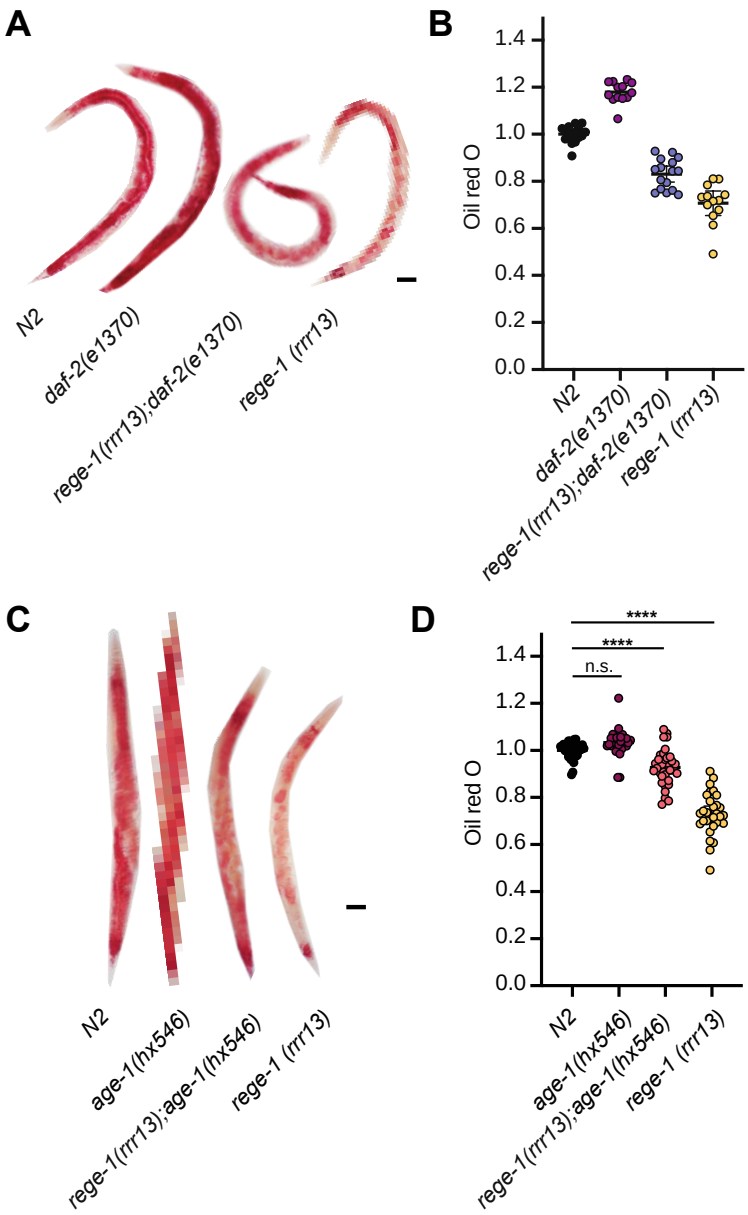

Figure 2. REGE-1 depletion is able to diminish the fat content of both *daf-2* and *age-1* animals.

A. Oil red O (ORO) staining of day one adult animals at 20°C of the following phenotype: wild-type, *daf-2(e1370)* and *rege-1(rrr13);daf-2(e1370).* Scale bar = 50µm.

B. Quantification of the ORO staining for the same animals as (A) normalized to the wild-type. Around 10 – 15 animals were measured per genotype in one biological replicate.

C. ORO staining as in (A) just for the following genotypes: wild-type, *age-1(hx546)* and *rege-1(rrr13);age-1(hx546).*Scale bar = 50µm

D. ORO quantifications normalized to the mean intensity of the wild-type. At least 20 animals were scored per genotype in three biological replicates. Each circle represents one animal. P value was calculated using a one-way ANOVA for multiple comparisons. (n.s.=not significant, **** p > 0.001)

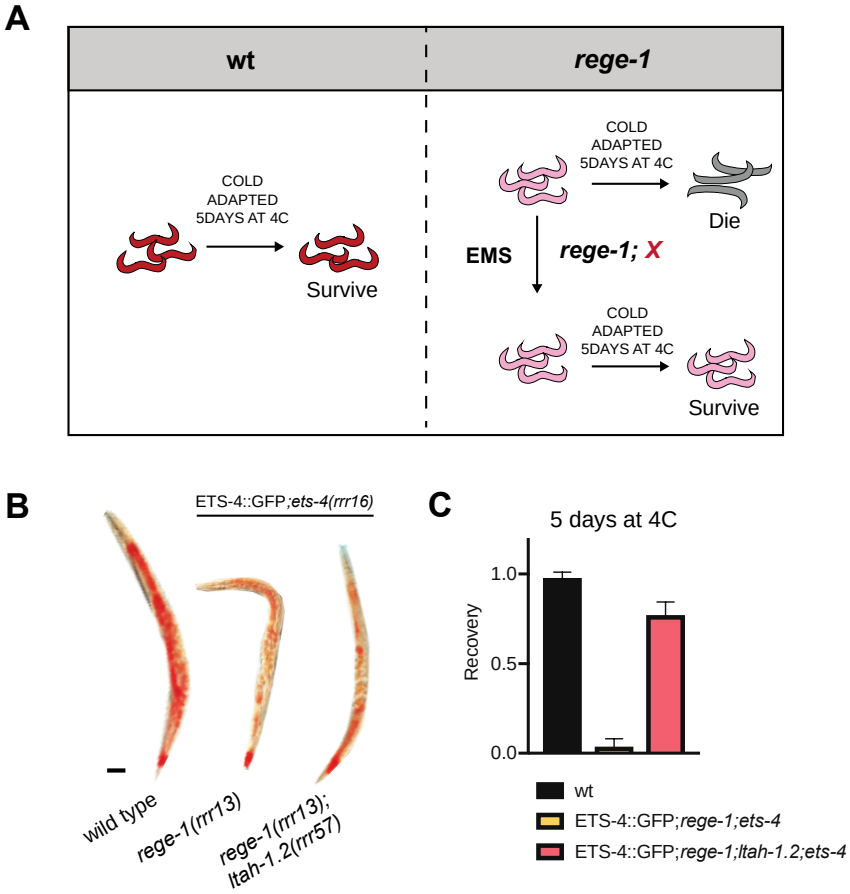

Figure 3. Leukotriene A4 hydrolase homologue mutant is able to rescue *rege-1(rrr13)* cold sensitivity without altering fat levels.

A. Schematic representation of the EMS mutagenesis screen. While wild-type animals survive cold adaptation and 5 days at 4°C, *rege-1* mutant animals do not. In the screen we hope to

identify a mutant that will be able to rescue *rege-1* cold sensitivity without changing its fat content.

B. ORO staining of day one adult animals at 20°C od wild type, ETS-4::GFP;*rege-1(rrr13);ets-4(rrr16)* and ETS-4::GFP;*rege-1(rrr13); ltah-1.2(rrr57); ets-4(rrr16)*. Scale bar =50μm.

C. Cold survival day one old adult animals cold adapted as previously described. Animals were scored for recovery after 5 days at 4°C. Data represents 2 biological replicates, around 100 animals were scored per genotype. Error bars represent SD

ADDITIONAL MATHERIALS AND METHODS

Strains and *C. elegans* culture

For these experiments we used wild type Bristol strain N2 and following other strains: *rege-1 (rrr13)*, *daf-2 (e1370), rege-1(rrr13); daf-2(e1370), age-1(hx546)*, *rege-1(rrr13); age-1(hx546)*, rrrSi400[Pets-4::ets-4-GFP::ets-4 3'UTR, unc-119];*rege-1(rrr13);ets-4(rrr16)*, rrrSi400[Pets-4::ets-4-GFP::ets-4 3'UTR, unc-119];*rege-1(rrr13);ets-4(rrr16);age-1(hx546),* rrrSi400[Pets-4::ets-4-GFP::ets-4 3'UTR, unc-119]; *rege-1(rrr13); ets-4(rrr16); ltah-1.2(rrr57).*

EMS mutagenesis and mutant identification

Animals were staged using hypochlorite solution and were grown until L4 larval stage, the animals were washed and diluted in M9 to about 4ml. 20ul of EMS (Sigma #M0880) was added and incubated for 3 hours while rotating. Animals were then washed 2x in M9 and transferred to 3 plates with OP50. The following day the adult animals (P0) were again synchronized by bleaching and F1 were placed on 3 new separate plates. After synchronization of F2 in the same way, animals were grown to day one adulthood and cold adapted as described before. F2 were screened for the desired phenotype at 5 days post adaptation. To identify the desired mutation, bulk sequencing approach was used (Zuryn and Jarriault, 2013). In brief, homozygous mutants were backcrossed once to the strain used for mutagenesis. From that cross, around 50 individual homozygous animals were singled out. Once the animals grew for a generation on the plate, they were all collected together and DNA was isolated using a Purgene DNA extraction kit from Quiagen. The genomic DNA was sequenced using Hiseq 2500 - 50 Cycle Single-end reads (NEB Ultra).

CHAPTER 4: DISCUSSION AND FUTURE PERSPECTIVES

Cold induced torpor and aging share signaling pathways

A link between temperature and aging has been observed in animals: that is, cold exposure enhances lifespan while higher temperatures can shorten it (Wu and Storey, 2016). This phenomenon is observed not only in *C. elegans* but also in mice and *Drosophila* (Conti et al., 2006; Klass, 1977; Miquel et al., 1976). Even in male humans, lower core body temperature is a biomarker for longer lifespan (Roth et al., 2002). Our lab has previously demonstrated that *C. elegans* enters a hibernation-like state after cold adaptation, where the total lifespan does not change, but is effectively extended for the time the animal spent "hibernating" in the cold (Habacher et al., 2016). Cold adaptation protocol comprises of a continuous growth of the animal at 20°C until they become adults, then placing them at 10°C for 2h, allowing them to adapt to cold. When placing them at 4°C for up to for 6 days, we observe a 100% survival rate and up to 13 days survival in the case of *daf-2* mutant animals.

Although exposure to cold extends lifespan in many species, there is a difference in how animals adapt to cold temperatures, if they adapt at all (Flouris and Piantoni, 2015). For example, hibernating animals will deliberately enter in a hypometabolic state and actively maintain lower body temperature, while animals that do not have systems that regulate their core body temperature must either avoid exposure to temperature extremes or adjust to them by insulation. Some common features are seen between these two groups of animals, such as a general repression of mRNA translation in cold temperatures and upregulation of the oxidative stress response. Both of these features are also relevant for lifespan extension (Wu and Storey, 2016). In *C. elegans* cold adaptation, we observe similar features. The animals do not move or eat within the time spent at 4°C and they progressively lose their body fat stores (Habacher et al., 2016). Conversely, we do see a great number of genes differentially expressed upon cold adaptation compared to 20°C and we have seen that cold adaptation can upregulate genes involved in oxidative stress response (Appendix A). For this reason, we propose that cold adaptation, similarly to hibernation, leads to oxidative damage. Although we see genes upregulated, it is not clear if the mRNAs are translated. Loss of polyribosomes on the translating mRNA is a common feature of cold stress response (Hofmann et al., 2012;

Knight et al., 2000) and it could mean that only some genes will eventually be translated and be active at 4°C.

Here, we show two transcription factors, namely DAF-16/FOXO and PQM-1/GATA to be stabilized in the intestinal nuclei upon cold adaptation. Interestingly, PQM-1 is absent in the animals at 20°C and shows a very strong upregulation upon cold adaptation, progressively increasing with the time spent at 4°C. Both *daf-16* and *pqm-1* are not required for survival in the cold. We could see that both of them are repressed by another transcription factor ETS-4/SPDEF. We have shown that inhibition of ETS-4, similar to inhibition of the insulin signaling pathway, is able to extend survival in cold adapted *C. elegans*. Both ETS-4 and insulin signaling act in parallel to inhibit lifespan extension and cold survival by inhibition of the FOXO transcription factor DAF-16 (Thyagarajan et al., 2010). Upon cold adaptation, we observe that besides DAF-16, ETS-4 represses PQM-1 factor that functions together with DAF-16 to promote cold survival during cold adaptation. We also observed, for the first time, that both DAF-16 and PQM-1 are present in the intestinal nuclei at the same time, which is in contrast to previous suggestion that their localization in the nucleus is mutually exclusively (Tepper et al., 2013). Additionally, we used an endogenously tagged CRIPSR lines for both DAF-16 and PQM-1 where we have fused the fluorophore to the C-terminus, covering all the possible isoforms. This allowed us to have a better look on the behavior of the endogenous gene locus but also of the endogenous protein levels.

By performing expression analysis in *ets-4* mutant animals after cold adaptation, we could see that ETS-4 acts as a transcriptional repressor, since around 150 genes were upregulated upon ets-4 deletion, while only around 20 were downregulated. This goes in line with previous assumptions that ETS-4 acts as a transcriptional repressor (Thyagarajan et al., 2010). We could also observe that some of these changes of gene expression, depend on both *daf-16* and *pqm-1.* We could see that around 20 genes upregulated in *ets-4* background have a DAF-16 binding site in their promoter, while 25 have a PQM-1 site. Since the binding data comes from ENCODE dataset (Davis et al., 2018), we do not know if these sites would be bound at 4°C, as well, we do not know if upon ETS-4 de-repression, we would be able to identify more genes bound by either DAF-16 or PQM-1. Interestingly, we found 7 genes to contain both of the binding sites and we identified one gene, *ftn-1,* that is upregulated upon

ets-4 deletion as it depends on both *daf-16* and *pqm-1*, and contains the binding site of both DAF-16 and PQM-1.

PQM-1 has emerged as an important regulator of lifespan in many known pathways that extend lifespan, such as dietary restriction (*eat-2*), mitochondrial dysfunction (*clk-1, isp-1, nuo-6*), gonad ablation (*glp-1*) and inhibition of insulin signaling (*daf-2*) (Senchuk et al., 2018; Shpigel et al., 2019; Tepper et al., 2013). This nonselective role of PQM-1 suggests that it promotes the expression of genes that are universally important for lifespan regulation. Similarly, DAF-16 is also required for lifespan extension upon insulin signaling inhibition, and mitochondrial dysfunction (Senchuk et al., 2018). We note that PQM-1 and DAF-16 are both upregulated upon oxidative stress (Senchuk et al., 2018; Tawe et al., 1998).

While cold adaptation upregulates oxidative stress response genes, we hypothesize that both DAF-16 and PQM-1 might be upregulated by the oxidative damage potentially created by cold adaptation. Furthermore, we have identified a regulatory axis that is able to enhance cold survival by upregulating a natural iron chelator, ferritin, which in turn decreases iron-generated ROS, by chelating iron.

Ferritin in cold adaptation

Ferritin is a conserved protein that binds large amount of free iron, sequestering it from the cytoplasm in an inactive form (Theil, 2013). Iron is found as a co-factor in many molecules like heme and enzymes such as dioxygenases and lipoxygenases, that transfer molecular oxygen to their substrates (Philpott et al., 2017; Solomon et al., 2003). It participates in iron-sulfur clusters in many proteins involved in the mitochondrial respiratory chain, facilitating redox reactions (Rouault, 2015). Certain DNA repair enzymes and ribonucleotide reductase that will form deoxyribonucleotides form ribonucleotides, use iron as an indispensable co-factor for their function. Catalytic subunit of DNA polymerases also binds to an iron-sulfur cluster that is essential for the formation of the stable complex. Over 95% of the intracellular iron is associated with proteins while the free iron makes up 3-5% (Eid et al., 2017). Increase in the percentage of the free iron can lead to ferroptosis, or an iron induced apoptosis. Free iron, is toxic as it can generate ROS by means of the Fenton reaction

and increase oxidative damage in cells leading to apoptosis (Joppe et al., 2019; Winterbourn, 1995).

C. elegans contains two ferritin genes, *ftn-1* and *ftn-2*. Our data suggest that iron excess is detrimental for cold survival while iron chelation provides a mild protection and is able to prolog survival upon cold adaptation. We hypothesize that iron is sequestered by ferritin FTN-1, and *ftn-1* itself is upregulated by DAF-16 and PQM-1. Thus, in this way, DAF-16 and PQM-1 can promote survival. *ftn-1,* and not *ftn-2,* was found upregulated in a DAF-16 dependent manner in several mutant backgrounds, including those inducing mitochondrial dysfunction and extending lifespan, as well as in *daf-2* mutants that themselves are longer lived (Ackerman and Gems, 2012; Senchuk et al., 2018). This is presumably because ferritin is needed to cope with oxidative stress; its overexpression has been shown to help protect against ROS-induced protein damage (Valentini et al., 2012). FTN-2 is a main iron storing ferritin in *C. elegans* and upon deletion, it will decrease lifespan and will not be able to store iron, nor will it be able to survive additional iron load supplemented externally. This suggest that proper iron storage is required for normal lifespan in *C. elegans*. However, *ftn-2,* is not upregulated by DAF-16 and is not upregulated upon oxidative stress in mitochondrial mutants, as well as upon cold adaptation, while *ftn-1* is (James et al., 2015; Senchuk et al., 2018). We hypothesize that *ftn-1* is a stress responsive ferritin that will be upregulated when there are already higher levels of ROS. Since *ftn-1* is lowly expressed at 20°C it is not surprising that *ftn-1* is not required for a normal lifespan and *ftn-1* overexpression is not sufficient to extend lifespan in wild-type background (Valentini et al., 2012). Indeed, it would be interesting to test the role of *ftn-1* in long-lived or sensitized genetic backgrounds to further strengthen the idea of FTN-1 being able to battle ROS upon oxidative stress in these mutant backgrounds. In the case of cold adaptation, we could observe that in *ets-4* mutant background, where *ftn-1* levels are high, we have a protective effect against iron overload, promoting survival in the cold, that depends on *ftn-1*.

There are a few studies linking cold exposure and iron homeostasis in humans as well (Agarwal, 2007). People with iron deficiency are less able to maintain their body temperature in a cold water bath compared to the control group. Additionally, in the context of organ preservation and transplantation, iron was released upon cold exposure, creating damage and inducing apoptosis, while iron chelation provided protection and prevented apoptosis in

cells (Huang and Salahudeen, 2002; Pizanis et al., 2011; Rauen et al., 2000). This provides exciting evidence for a conserved role of iron sequestration in a protective response to cold. It also suggests that there are molecular pathways that could be augmented to balance iron levels during hypothermia induction in humans, leading potentially to therapeutic application.

Fat accumulation does not correlate with *C. elegans* cold survival

In this work we have tackled the question whether there can be extended cold survival that is independent of fat content. *C. elegans* has been used to study fat metabolism since many fat metabolic enzymes are conserved (Watts and Ristow, 2017). Fatty acids are essential components of all membranes and also serve as energy storage molecules esterified to glycerol, forming triglycerides (TAGs). Worms derive most of their fatty acids from food, but certain mono and polyunsaturated fats are synthetized *de novo* (Watts and Browse, 2002). We know that the animals that experience very low temperatures gradually lose their fat stores when exposed to cold temperatures (Habacher et al., 2016; Liu et al., 2017). These animals likely remain metabolically active, although metabolism was not explicitly measured; from observation we know that worms do not move nor feed while in cold (Habacher et al., 2016). It was previously shown that fatty acid desaturases, enzymes essential for monounsaturated fatty acid formation, are upregulated in cold in both *C. elegans* and mice and are required for cold survival in *C. elegans* (Murray et al., 2007; Savory et al., 2011) (Marcher et al., 2015). However, the lipid profile acquired at 0°C is not sufficient to extend cold survival on its own. Therefore, we hypothesize that a specific type of unsaturated fatty acid over the total body fat content, or pathways completely independent of total body fat might play a role in the survival after cold adaptation.

To address the correlation between the total fat content and survival, we used *rege-1* mutant animals that have significantly less body fat compared to the wild type (Habacher et al., 2016). This is because high levels of ETS-4 in *rege-1* mutant background will transcribe lipid catabolic genes and reduce the total body fat (Habacher et al., 2016). We then looked if *rege-1* would be able to lower the fat content of the long lived and cold-surviving *daf-2* and *age-1* worms. We observed significant fat loss upon *rege-1* deletion in the long lived mutants compared to the wild-type, probably due to ETS-4 being stabilized in the gut nuclei.

Interestingly, *rege-1;daf-2* and *rege-1;age-1* double mutants survive significantly better than wild-type animals when recovering from cold adaptation, irrespective of the lowered body fat content. This data suggests that the bulk fat content is not an absolute determinant of extended cold survival. It also suggests that insulin signaling likely acts in parallel to ETS-4.

Given this data, we see that *rege-1* does not die because of fat loss but because of something else, that can be rescued by additional mutation of *daf-2* or *age-1*. We can imagine that the prolonged survival upon cold adaptation in the both *rege-1;daf-2* and *rege-1;age-1* depends on either *daf-16*, *pqm-1* or even *ftn-1*. For this we would need to establish an epistatic relationship between these genes and see if they would work in the same manner as they work in *ets-4* background. If not, we would need to perform a genome wide expression profiling to identify changes in gene expression in these mutants, hopefully getting more insight in the processes they are regulating.

Additionally, since monounsaturated fatty acids play an important role for cold survival, we can ask if in *rege-1;daf-2* and *rege-1;age-1* we have an upregulation of specific types of polyunsaturated fatty acids that are directly derived from monounsaturated fats, that would provide protection at 4°C. Prostaglandins and thromboxanes are fatty-acid derived immunogenic molecules (Malmsten, 1986). They are produced from a polyunsaturated fatty acid, arachidonic acid, through a cyclooxygenase reaction and have been found to promote smooth muscle contraction (Ruan et al., 2011). We can speculate that this feature might be important in in general entry in the hypometabolic state. Interestingly, our transcriptome analysis in animals exposed to cold showed that genes associated with arachidonic acid metabolism as well as prostaglandin and thromboxane synthesis, are upregulated (Appendix B). Whether this upregulation is required for cold survival and weather such polyunsaturated fatty acid derivative could enhance survival in *rege-1;daf-2* and *rege-1;age-1,* remains unclear but suggests it is important to better understand the role of lipid signaling molecules in cold adaptation. Taken together, these findings suggest that besides specific fatty acids, there might be other fat-independent mechanisms that could play an important role in cold survival. One such mechanism may be the regulation of free iron levels, as described in Chapter 2.

Leukotriene A4 hydrolase homolog depletion extends cold survival of *rege-1* animals regardless of fat content.

To identify suppressors of *rege-1* cold survival that are independent of fat content we performed a forward mutagenesis screen. We looked at day 5 at 4°C after cold adaptation and picked animals that were alive upon recovery. Unexpectedly, the initial screen revealed too many potential candidate strains. Re-screening for homozygous mutants after outcross was too laborious for the large number of candidates.

Despite these technical issues that impeded a global analysis, we identified one mutation in the leukotriene A4 hydrolase (LTA4H) homolog, *ltah-1.2*, that rescues cold survival in *rege-1* mutants (Benner et al., 2011). LTA4H is a bifunctional enzyme in mammals, acting as both a hydrolase and an aminopeptidase (Rudberg et al., 2002). Its hydrolase domain converts leukotriene A4 to B4 in the lipoxygenase pathway. Leukotrienes are lipid derivatives that form from one PUFA, arachidonic acid, and participate in the immune response (Peters-Golden et al., 2005). *C. elegans* has two LTA4H homologs: *ltah-1.1* and *ltah-1.2*. Characterization of *ltah-1.1* showed it was unable convert LTA4 to LTB4 and therefore it was proposed that it acts as an aminopeptidase (Baset et al., 1998). The aminopeptidase function of LTA4H is associated with cleavage of the proline-glycine-proline tripeptide (PGP) that induces chemotaxis of neutrophils to the infection (Paige et al., 2014) Interestingly, inhibition of leukotriene B4 synthesis, was shown to be protective against oxidative damage and subsequent apoptosis in brain and retinal cells (Subramanian et al., 2016; Ye et al., 2018). *ltah-1.2* is DAF-16/FOXO class II gene, downregulated upon repression of the insulin signaling pathway (Tepper et al., 2013). We suggest that one of the reasons of *daf-2* and *age-1* animals are surviving better after cold adaptation, may be the DAF-16/FOXO dependent downregulation of *ltah-1.2*. This we could address by crossing the *ltah-1.2* to either *daf-2* or *age-1* mutant animals and inspect for epistatic relationship. Interestingly, lipoxygenase pathway requires iron as a co-factor and there is a possibility that iron sequestration could also inhibit production of lipid signaling molecules such as leukotrienes and additionally enhance survival upon cold adaptation.

Future perspectives

Taken together, the data produced during my doctoral studies provide new insights into the metabolic pathways underlying the organismal response to chronic cold exposure. These pathways hold potential for artificially stimulating cold survival. Since all of the components of the pathway are conserved, it is tempting to think of that the protective effects of ETS-4/SPDEF inhibition might be applicable in mammalian systems, as we could already see the protective effects of iron chelation in mammalian neurons.

However, there remains a deficit in our understanding concerning the role of ETS-4/SPDEF in cold survival. We still do not know if ETS-4 inhibits DAF-16 and PQM-1 directly, or it competes for DNA binding sites to inhibit transcription of protective genes. We also do not know which mammalian counterpart performs functions analogous to PQM-1. It is known that ETS transcription factors acquire repressive features if they become SUMOylated (Leight et al., 2015). Likewise, in hibernating animals, upon torpor, there will be a strong increase in SUMO conjugated proteins (Lee et al., 2007). We would need to further see if that is the case in *C. elegans* and if it will increase ETS-4 repressive features and if in that case ETS-4 would increase repression on the DAF-16 and PQM-1 target genes or it would repress directly DAF-16 and PQM-1.

Downstream of ETS-4/SPDEF, DAF-16/FOXO, and PQM-1/GATA transcription factors, iron chelation may attenuate the immune response to provide protection in cold. Iron stabilizes thermogenesis and is an important co-factor in enzymes such as cyclooxygenases and lipoxygenases that produce lipid signaling molecules from polyunsaturated fatty acid (Malmsten, 1986). Both iron chelation and inhibition of arachidonic acid derivatives are already feasible in humans (Eid et al., 2017; Lien et al., 2018). These findings suggest these interventions could be used to enhance existing therapies which are based on lowering body temperature. In fact, both upregulation of the oxidative stress response genes and downregulation of pro-inflammatory lipid derivatives are features of naturally occurring hibernators (Wu et al., 2015; Giroud et al., 2018). Even though *ftn-1* was found as the main effector of DAF-16 and PQM-1 in cold protection, we still haven't explored genes that are specifically regulated by either DAF-16 or PQM-1 in *ets-4* mutant background. Additionally, there are still genes that are differentially expressed in *ets-4* background whose expression

does not depend on either *daf-16* or *pqm-1*. Looking further into these changing genes might uncover additional pathways through which *ets-4* inhibition prolongs survival upon cold adaptation.

Finally, my work shows that *C. elegans* is a powerful tool to study cold adaptation, since iron metabolism and synthesis of PUFA mediators are conserved pathways. However, it remains to be tested how many of the pathway intermediates exist and function identically in worms and mammals. Using genetic tools available in *C. elegan*s, we may identify additional regulators of cold response. Testing these in human and rodent tissues may allow us to incorporate our current and potential future discoveries into therapies that can induce a "hibernation" phenotype that promotes survival, in human tissues.

LIST OF ABBREVIATIONS

AAK	AMP-Activated Kinase
AMPK	AMP-activated protein kinase
Aop	anterior open
ASJ	amphid neurons
ATP	adenosine triphosphate
BAT	brown adipose tissue
cAMP	cyclic adenosine monophosphate
CEH	*C. elegans* Homeobox
cGMP	cyclic guanosine monophosphate
ChIP	chromatin immunoprecipitation
CRISPR/Cas9	Clustered Regularly Interspaced Short Palindromic Repeats/ CRISPR associated 9
CST	Caenorhabditis STE20-like kinase
CW	cold warming
DAE	DAF-16 associated element
DAF	abnormal DAuer Formation
DBE	DAF-16 binding element
DF	Deferoxamine
DIE	iron dependent element
DMT1	divalent metal transporter 1
eEF2	Eukaryotic Translation Elongation Factor 2
eIF2a	Eukaryotic translation initiation factor 2A
ELT	Erythroid-Like Transcription factor family
ETS	E twenty six
EV	empty vector
FAC	Ferric Ammonium Citrate
FBXL5	F-box and leucine rich repeat protein 5
FEV	Fifth Ewing Variant
FFA	free fatty acid
FOXO	Forkhead box class O
FPN	ferroportin
FTH	ferritin heavy subunit
FTL	ferritin light subunit
FTN	ferritin
GFP	green fluorescent protein
GLUT4	glucose transporter 4
HIF	hypoxia inducible factor
HLH	helix-loop-helix
HO	heme oxygenase

HRE	hypoxia responsive element
HSF	heat shock factor
HSL	hormone sensitive lipase
HSP	heat shock protein
I/R	ischemia/re-perfusion
IGF-1R	Insulin-like growth factor 1 receptor
IIS	Insulin/insulin-like growth factor (IGF)-1 signaling
INS	insulin
IRE	iron responsive element
IRP	iron responsive RNA binding protein
JUNK	c-Jun N-terminal kinase
LIN	abnormal cell LINeage
LTA4H	leukotriene A4 hydrolase
MAPK	Mitogen-activated protein kinases
MATH	meprin-associated Traf homology
MCPIP	Monocyte chemotactic protein-induced protein
MFRN	mitoferrin
MUFA	monounsaturated fatty acids
NAD	Nicotinamide adenine dinucleotide
NGM	nematode growth media
NRF	nuclear respiratory factor
ORO	Oil red O
PABP	poly-A binding protein
PDK	Pyruvate dehydrogenase kinase isoenzyme 4
PDK	Pyruvate dehydrogenase kinase
PGP	proline-glycine-proline tripeptide
PI3K	Phosphoinositide 3-kinase
PIP2	Phosphatidylinositol 4,5-bisphosphate
PIP3	Phosphatidylinositol (3,4,5)-trisphosphate
PKA	protein kinase A
PKC	protein kinase C
PNT	pointed
Pol II	RNA polymerase two
PQM	ParaQuat (Methylviologen) responsive
PTEN	Phosphatase and tensin homolog
PTL	pancreatic triacylglycerol lipase
PTM	posttranscriptional modifications
PUFA	polyunsaturated fatty acids
REGE	regnase
RLE	Regulation of Longevity by E3 ubiquitin ligase
RNA	ribonucleic acid

ROI	region of interest
ROS	reactive oxygen species
RT qPCR	real time quantitative polymerase chain reaction
SAM	sterile alpha motif
SGK	Serum- and Glucocorticoid- inducible Kinase
SIRT	sirtuin
SKN	SKiNhead
SMK	SMEK - Dictyostelium Suppressor of MEK null
SOD	superoxide dismutase
SPDEF	SAM Pointed Domain Containing ETS Transcription Factor
SUMO	Small ubiquitin-related modifier
SWI/SNF	SWItch/Sucrose Non-Fermentable
T2DM	type 2 diabetes mellitus
TAG	triglycerides
Tf	transferrin
TFR1	transferrin receptor
TG	triglycerides
TIA	T-cell intracellular antigen
TIAR	TIA -related
TRPA	transient receptor potential cation channel subfamily A member
TTM	targeted temperature management
UTR	untranslated region
UV	ultra violet
VEGF	vascular endothelial growth factor
WAT	white adipose tissue

ACKNOWLEDGMENTS

Throughout the time of my PhD there have been a great amount of people that have influenced the progression and the general atmosphere. First, I would like to thank Rafal Ciosk, for giving me the opportunity to work on this interesting and challenging project, and allowed me to explore the topic from many different angles. I would like to thank Susan Gasser for the support during my final year of the PhD, providing mentorship and guidance for both scientific progression and career development. Essential part was as well my thesis committee members Dominique Glauser, and later Collin Ewald, who provided critical input and gave valuable insight for the project. Additionally, I extend my gratitude to the amazing facilities at FMI, specifically FAIM members, Laurent, Steve and Jan, who helped with many imaging challenges. Elida Keller, for the administrative support and constant encouragement thorough the years.

I would also like to thank all of the Ciosk lab members that were essential part of my PhD experience. Jorge and Cris from whom I learned ins and outs of *C. elegans*, Anca, Conny, Chrissi, Silvi and Pooja who were absolute support in and out of the lab. Andi, Yanwu, Ricky and Janosch who contributed to the fun atmosphere in the lab.

Additionally, I would like to thank Susan Gasser group members, who were amazingly welcoming and supportive in the past year. Colin, Stephen and Jan who ensured a great office atmosphere and a wealth of knowledge I could gain from. Verena, Anais, Jennifer, Daphne, Anna and the rest of the group who were very supportive from the very beginning. I was also lucky to be able to share the lab with two close friends, Shany and Michi and observe their growth in the start-up.

I would like to thank Daniela and Migle for being my dance partners and amazing friends.

Finally, I would like to thank my family for being there for me whenever I needed encouragement and unconditional love. Specifically, Milos who was a rock-solid support and the voice of reason when I was not. And our dog Niko for cuddles.

REFERENCES

1. Ackerman, D., and Gems, D. (2012). Insulin/IGF-1 and hypoxia signaling act in concert to regulate iron homeostasis in Caenorhabditis elegans. PLoS genetics *8*, e1002498.
2. Agarwal, R. (2007). Nonhematological benefits of iron. Am J Nephrol *27*, 565-571.
3. Anderson, C.P., and Leibold, E.A. (2014). Mechanisms of iron metabolism in Caenorhabditis elegans. Frontiers in pharmacology *5*, 113.
4. Andrews, M.T. (2004). Genes controlling the metabolic switch in hibernating mammals. Biochem Soc Trans *32*, 1021-1024.
5. Arnold, W., Ruf, T., Frey-Roos, F., and Bruns, U. (2011). Diet-independent remodeling of cellular membranes precedes seasonally changing body temperature in a hibernator. PloS one *6*, e18641.
6. Bansal, A., Kwon, E.S., Conte, D., Jr., Liu, H., Gilchrist, M.J., MacNeil, L.T., and Tissenbaum, H.A. (2014). Transcriptional regulation of Caenorhabditis elegans FOXO/DAF-16 modulates lifespan. Longev Healthspan *3*, 5.
7. Barisic, D., Stadler, M.B., Iurlaro, M., and Schubeler, D. (2019). Mammalian ISWI and SWI/SNF selectively mediate binding of distinct transcription factors. Nature.
8. Barnes, B.M. (1989). Freeze avoidance in a mammal: body temperatures below 0 degree C in an Arctic hibernator. Science *244*, 1593-1595.
9. Baset, H.A., Ford-Hutchinson, A.W., and O'Neill, G.P. (1998). Molecular cloning and functional expression of a Caenorhabditis elegans aminopeptidase structurally related to mammalian leukotriene A4 hydrolases. J Biol Chem *273*, 27978-27987.
10. Beitel, G.J., Tuck, S., Greenwald, I., and Horvitz, H.R. (1995). The Caenorhabditis elegans gene lin-1 encodes an ETS-domain protein and defines a branch of the vulval induction pathway. Genes & development *9*, 3149-3162.
11. Benedetti, G.M., and Silverstein, F.S. (2018). Targeted Temperature Management in Pediatric Neurocritical Care. Pediatr Neurol *88*, 12-24.
12. Benner, J., Daniel, H., and Spanier, B. (2011). A glutathione peroxidase, intracellular peptidases and the TOR complexes regulate peptide transporter PEPT-1 in C. elegans. PloS one *6*, e25624.
13. Berdichevsky, A., Viswanathan, M., Horvitz, H.R., and Guarente, L. (2006). C. elegans SIR-2.1 interacts with 14-3-3 proteins to activate DAF-16 and extend life span. Cell *125*, 1165-1177.
14. Bernard, S.A., Gray, T.W., Buist, M.D., Jones, B.M., Silvester, W., Gutteridge, G., and Smith, K. (2002). Treatment of comatose survivors of out-of-hospital cardiac arrest with induced hypothermia. N Engl J Med *346*, 557-563.
15. Blackwell, T.K., Steinbaugh, M.J., Hourihan, J.M., Ewald, C.Y., and Isik, M. (2015). SKN-1/Nrf, stress responses, and aging in Caenorhabditis elegans. Free radical biology & medicine *88*, 290-301.
16. Brock, T.J., Browse, J., and Watts, J.L. (2006). Genetic regulation of unsaturated fatty acid composition in C. elegans. PLoS genetics *2*, e108.
17. Calabuig-Navarro, V., Yamauchi, J., Lee, S., Zhang, T., Liu, Y.Z., Sadlek, K., Coudriet, G.M., Piganelli, J.D., Jiang, C.L., Miller, R., et al. (2015). Forkhead Box O6 (FoxO6) Depletion Attenuates Hepatic Gluconeogenesis and Protects against Fat-induced Glucose Disorder in Mice. J Biol Chem *290*, 15581-15594.

18. Carey, H.V., Andrews, M.T., and Martin, S.L. (2003). Mammalian hibernation: cellular and molecular responses to depressed metabolism and low temperature. Physiol Rev *83*, 1153-1181.
19. Chen, A.T., Guo, C., Itani, O.A., Budaitis, B.G., Williams, T.W., Hopkins, C.E., McEachin, R.C., Pande, M., Grant, A.R., Yoshina, S., et al. (2015). Longevity Genes Revealed by Integrative Analysis of Isoform-Specific daf-16/FoxO Mutants of Caenorhabditis elegans. Genetics *201*, 613-629.
20. Chiabrando, D., Fiorito, V., Marro, S., Silengo, L., Altruda, F., and Tolosano, E. (2013). Cell-specific regulation of Ferroportin transcription following experimentally-induced acute anemia in mice. Blood Cells Mol Dis *50*, 25-30.
21. Choi, H.A., Ko, S.B., Presciutti, M., Fernandez, L., Carpenter, A.M., Lesch, C., Gilmore, E., Malhotra, R., Mayer, S.A., Lee, K., et al. (2011). Prevention of shivering during therapeutic temperature modulation: the Columbia anti-shivering protocol. Neurocrit Care *14*, 389-394.
22. Chollangi, S., Thompson, J.W., Ruiz, J.C., Gardner, K.H., and Bruick, R.K. (2012). Hemerythrin-like domain within F-box and leucine-rich repeat protein 5 (FBXL5) communicates cellular iron and oxygen availability by distinct mechanisms. J Biol Chem *287*, 23710-23717.
23. Conti, B., Sanchez-Alavez, M., Winsky-Sommerer, R., Morale, M.C., Lucero, J., Brownell, S., Fabre, V., Huitron-Resendiz, S., Henriksen, S., Zorrilla, E.P., et al. (2006). Transgenic mice with a reduced core body temperature have an increased life span. Science *314*, 825-828.
24. Craig, M.P., and Sumanas, S. (2016). ETS transcription factors in embryonic vascular development. Angiogenesis *19*, 275-285.
25. Dark, J. (2005). Annual lipid cycles in hibernators: integration of physiology and behavior. Annu Rev Nutr *25*, 469-497.
26. Davis, C.A., Hitz, B.C., Sloan, C.A., Chan, E.T., Davidson, J.M., Gabdank, I., Hilton, J.A., Jain, K., Baymuradov, U.K., Narayanan, A.K., et al. (2018). The Encyclopedia of DNA elements (ENCODE): data portal update. Nucleic Acids Res *46*, D794-D801.
27. De Val, S., Chi, N.C., Meadows, S.M., Minovitsky, S., Anderson, J.P., Harris, I.S., Ehlers, M.L., Agarwal, P., Visel, A., Xu, S.M., et al. (2008). Combinatorial regulation of endothelial gene expression by ets and forkhead transcription factors. Cell *135*, 1053-1064.
28. Dorman, J.B., Albinder, B., Shroyer, T., and Kenyon, C. (1995). The age-1 and daf-2 genes function in a common pathway to control the lifespan of Caenorhabditis elegans. Genetics *141*, 1399-1406.
29. Dowen, R.H. (2019). CEH-60/PBX and UNC-62/MEIS Coordinate a Metabolic Switch that Supports Reproduction in C. elegans. Developmental cell.
30. Dowen, R.H., Breen, P.C., Tullius, T., Conery, A.L., and Ruvkun, G. (2016). A microRNA program in the C. elegans hypodermis couples to intestinal mTORC2/PQM-1 signaling to modulate fat transport. Genes & development *30*, 1515-1528.
31. Duncan, O.F., Granat, L., Ranganathan, R., Singh, V.K., Mazaud, D., Fanto, M., Chambers, D., Ballard, C.G., and Bateman, J.M. (2018). Ras-ERK-ETS inhibition alleviates neuronal mitochondrial dysfunction by reprogramming mitochondrial retrograde signaling. PLoS genetics *14*, e1007567.
32. Eddy, S.F., and Storey, K.B. (2003). Differential expression of Akt, PPARgamma, and PGC-1 during hibernation in bats. Biochem Cell Biol *81*, 269-274.

33. Eid, R., Arab, N.T., and Greenwood, M.T. (2017). Iron mediated toxicity and programmed cell death: A review and a re-examination of existing paradigms. Biochim Biophys Acta Mol Cell Res *1864*, 399-430.
34. Erecinska, M., Thoresen, M., and Silver, I.A. (2003). Effects of hypothermia on energy metabolism in Mammalian central nervous system. J Cereb Blood Flow Metab *23*, 513-530.
35. Ewald, C.Y., Landis, J.N., Porter Abate, J., Murphy, C.T., and Blackwell, T.K. (2015). Dauer-independent insulin/IGF-1-signalling implicates collagen remodelling in longevity. Nature *519*, 97-101.
36. Ferreira, C., Santambrogio, P., Martin, M.E., Andrieu, V., Feldmann, G., Henin, D., and Beaumont, C. (2001). H ferritin knockout mice: a model of hyperferritinemia in the absence of iron overload. Blood *98*, 525-532.
37. Flouris, A.D., and Piantoni, C. (2015). Links between thermoregulation and aging in endotherms and ectotherms. Temperature (Austin) *2*, 73-85.
38. Frerichs, K.U., Smith, C.B., Brenner, M., DeGracia, D.J., Krause, G.S., Marrone, L., Dever, T.E., and Hallenbeck, J.M. (1998). Suppression of protein synthesis in brain during hibernation involves inhibition of protein initiation and elongation. Proceedings of the National Academy of Sciences of the United States of America *95*, 14511-14516.
39. Frezal, L., and Felix, M.A. (2015). C. elegans outside the Petri dish. eLife *4*.
40. Fukushige, T., Hawkins, M.G., and McGhee, J.D. (1998). The GATA-factor elt-2 is essential for formation of the Caenorhabditis elegans intestine. Dev Biol *198*, 286-302.
41. Giannakou, M.E., Goss, M., Junger, M.A., Hafen, E., Leevers, S.J., and Partridge, L. (2004). Long-lived Drosophila with overexpressed dFOXO in adult fat body. Science *305*, 361.
42. Giroud, S., Evans, A.L., Chery, I., Bertile, F., Tascher, G., Bertrand-Michel, J., Gauquelin-Koch, G., Arnemo, J.M., Swenson, J.E., Lefai, E., et al. (2018). Seasonal changes in eicosanoid metabolism in the brown bear. Naturwissenschaften *105*, 58.
43. Gourley, B.L., Parker, S.B., Jones, B.J., Zumbrennen, K.B., and Leibold, E.A. (2003). Cytosolic aconitase and ferritin are regulated by iron in Caenorhabditis elegans. J Biol Chem *278*, 3227-3234.
44. Grabek, K.R., Diniz Behn, C., Barsh, G.S., Hesselberth, J.R., and Martin, S.L. (2015a). Enhanced stability and polyadenylation of select mRNAs support rapid thermogenesis in the brown fat of a hibernator. eLife *4*.
45. Grabek, K.R., Martin, S.L., and Hindle, A.G. (2015b). Proteomics approaches shed new light on hibernation physiology. Journal of comparative physiology. B, Biochemical, systemic, and environmental physiology *185*, 607-627.
46. Gregorieff, A., Stange, D.E., Kujala, P., Begthel, H., van den Born, M., Korving, J., Peters, P.J., and Clevers, H. (2009). The ets-domain transcription factor Spdef promotes maturation of goblet and paneth cells in the intestinal epithelium. Gastroenterology *137*, 1333-1345 e1331-1333.
47. Gu, X., Wei, Z.Z., Espinera, A., Lee, J.H., Ji, X., Wei, L., Dix, T.A., and Yu, S.P. (2015). Pharmacologically induced hypothermia attenuates traumatic brain injury in neonatal rats. Experimental neurology *267*, 135-142.
48. Guevara-Aguirre, J., and Rosenbloom, A.L. (2015). Obesity, diabetes and cancer: insight into the relationship from a cohort with growth hormone receptor deficiency. Diabetologia *58*, 37-42.
49. Guillermin, M.L., Castelletto, M.L., and Hallem, E.A. (2011). Differentiation of carbon dioxide-sensing neurons in Caenorhabditis elegans requires the ETS-5 transcription factor. Genetics *189*, 1327-1339.

50. Habacher, C., Guo, Y., Venz, R., Kumari, P., Neagu, A., Gaidatzis, D., Harvald, E.B., Faergeman, N.J., Gut, H., and Ciosk, R. (2016). Ribonuclease-Mediated Control of Body Fat. Developmental cell *39*, 359-369.
51. Hamdi, A., Roshan, T.M., Kahawita, T.M., Mason, A.B., Sheftel, A.D., and Ponka, P. (2016). Erythroid cell mitochondria receive endosomal iron by a "kiss-and-run" mechanism. Biochimica et biophysica acta *1863*, 2859-2867.
52. Heimbucher, T., Liu, Z., Bossard, C., McCloskey, R., Carrano, A.C., Riedel, C.G., Tanasa, B., Klammt, C., Fonslow, B.R., Riera, C.E., et al. (2015). The Deubiquitylase MATH-33 Controls DAF-16 Stability and Function in Metabolism and Longevity. Cell metabolism *22*, 151-163.
53. Henderson, S.T., and Johnson, T.E. (2001). daf-16 integrates developmental and environmental inputs to mediate aging in the nematode Caenorhabditis elegans. Current biology : CB *11*, 1975-1980.
54. Herinckx, G., Hussain, N., Opperdoes, F.R., Storey, K.B., Rider, M.H., and Vertommen, D. (2017). Changes in the phosphoproteome of brown adipose tissue during hibernation in the ground squirrel, Ictidomys tridecemlineatus. Physiol Genomics *49*, 462-472.
55. Hertweck, M., Gobel, C., and Baumeister, R. (2004). C. elegans SGK-1 is the critical component in the Akt/PKB kinase complex to control stress response and life span. Developmental cell *6*, 577-588.
56. Hindle, A.G., and Martin, S.L. (2014). Intrinsic circannual regulation of brown adipose tissue form and function in tune with hibernation. Am J Physiol Endocrinol Metab *306*, E284-299.
57. Hofmann, S., Cherkasova, V., Bankhead, P., Bukau, B., and Stoecklin, G. (2012). Translation suppression promotes stress granule formation and cell survival in response to cold shock. Molecular biology of the cell *23*, 3786-3800.
58. Hollenhorst, P.C., Jones, D.A., and Graves, B.J. (2004). Expression profiles frame the promoter specificity dilemma of the ETS family of transcription factors. Nucleic Acids Res *32*, 5693-5702.
59. Honda, Y., and Honda, S. (1999). The daf-2 gene network for longevity regulates oxidative stress resistance and Mn-superoxide dismutase gene expression in Caenorhabditis elegans. FASEB J *13*, 1385-1393.
60. Hsu, A.L., Murphy, C.T., and Kenyon, C. (2003). Regulation of aging and age-related disease by DAF-16 and heat-shock factor. Science *300*, 1142-1145.
61. Hu, Y.O., Wang, Y., Ye, B.P., and Wang, D.Y. (2008). Phenotypic and behavioral defects induced by iron exposure can be transferred to progeny in Caenorhabditis elegans. Biomed Environ Sci *21*, 467-473.
62. Huang, H., and Salahudeen, A.K. (2002). Cold induces catalytic iron release of cytochrome P-450 origin: a critical step in cold storage-induced renal injury. Am J Transplant *2*, 631-639.
63. Jacobs, D., Beitel, G.J., Clark, S.G., Horvitz, H.R., and Kornfeld, K. (1998). Gain-of-function mutations in the Caenorhabditis elegans lin-1 ETS gene identify a C-terminal regulatory domain phosphorylated by ERK MAP kinase. Genetics *149*, 1809-1822.
64. Jaffrey, S.R., Haile, D.J., Klausner, R.D., and Harford, J.B. (1993). The interaction between the iron-responsive element binding protein and its cognate RNA is highly dependent upon both RNA sequence and structure. Nucleic Acids Res *21*, 4627-4631.
65. James, S.A., Roberts, B.R., Hare, D.J., de Jonge, M.D., Birchall, I.E., Jenkins, N.L., Cherny, R.A., Bush, A.I., and McColl, G. (2015). Direct in vivo imaging of ferrous iron dyshomeostasis in ageing Caenorhabditis elegans. Chem Sci *6*, 2952-2962.

66. Jiang, W., Wei, Y., Long, Y., Owen, A., Wang, B., Wu, X., Luo, S., Dang, Y., and Ma, D.K. (2018). A genetic program mediates cold-warming response and promotes stress-induced phenoptosis in C. elegans. eLife *7*.
67. Joppe, K., Roser, A.E., Maass, F., and Lingor, P. (2019). The Contribution of Iron to Protein Aggregation Disorders in the Central Nervous System. Front Neurosci *13*, 15.
68. Juozaityte, V., Pladevall-Morera, D., Podolska, A., Norgaard, S., Neumann, B., and Pocock, R. (2017). The ETS-5 transcription factor regulates activity states in Caenorhabditis elegans by controlling satiety. Proceedings of the National Academy of Sciences of the United States of America *114*, E1651-E1658.
69. Kahn-Kirby, A.H., Dantzker, J.L., Apicella, A.J., Schafer, W.R., Browse, J., Bargmann, C.I., and Watts, J.L. (2004). Specific polyunsaturated fatty acids drive TRPV-dependent sensory signaling in vivo. Cell *119*, 889-900.
70. Kappeler, L., De Magalhaes Filho, C., Dupont, J., Leneuve, P., Cervera, P., Perin, L., Loudes, C., Blaise, A., Klein, R., Epelbaum, J., et al. (2008). Brain IGF-1 receptors control mammalian growth and lifespan through a neuroendocrine mechanism. PLoS biology *6*, e254.
71. Kenyon, C., Chang, J., Gensch, E., Rudner, A., and Tabtiang, R. (1993). A C. elegans mutant that lives twice as long as wild type. Nature *366*, 461-464.
72. Kenyon, C., and Murphy, C.T. (2006). Enrichment of regulatory motifs upstream of predicted DAF-16 targets. Nature genetics *38*, 397-398; author reply 398.
73. Kenyon, C.J. (2010). The genetics of ageing. Nature *464*, 504-512.
74. Kim, S., and Ponka, P. (1999). Control of transferrin receptor expression via nitric oxide-mediated modulation of iron-regulatory protein 2. J Biol Chem *274*, 33035-33042.
75. Kim, Y.I., Cho, J.H., Yoo, O.J., and Ahnn, J. (2004). Transcriptional regulation and life-span modulation of cytosolic aconitase and ferritin genes in C.elegans. J Mol Biol *342*, 421-433.
76. Kimura, K.D., Tissenbaum, H.A., Liu, Y., and Ruvkun, G. (1997). daf-2, an insulin receptor-like gene that regulates longevity and diapause in Caenorhabditis elegans. Science *277*, 942-946.
77. Klang, I.M., Schilling, B., Sorensen, D.J., Sahu, A.K., Kapahi, P., Andersen, J.K., Swoboda, P., Killilea, D.W., Gibson, B.W., and Lithgow, G.J. (2014). Iron promotes protein insolubility and aging in C. elegans. Aging (Albany NY) *6*, 975-991.
78. Klass, M.R. (1977). Aging in the nematode Caenorhabditis elegans: major biological and environmental factors influencing life span. Mechanisms of ageing and development *6*, 413-429.
79. Knight, J.E., Narus, E.N., Martin, S.L., Jacobson, A., Barnes, B.M., and Boyer, B.B. (2000). mRNA stability and polysome loss in hibernating Arctic ground squirrels (Spermophilus parryii). Molecular and cellular biology *20*, 6374-6379.
80. Kops, G.J., Dansen, T.B., Polderman, P.E., Saarloos, I., Wirtz, K.W., Coffer, P.J., Huang, T.T., Bos, J.L., Medema, R.H., and Burgering, B.M. (2002). Forkhead transcription factor FOXO3a protects quiescent cells from oxidative stress. Nature *419*, 316-321.
81. Korfhagen, T.R., Kitzmiller, J., Chen, G., Sridharan, A., Haitchi, H.M., Hegde, R.S., Divanovic, S., Karp, C.L., and Whitsett, J.A. (2012). SAM-pointed domain ETS factor mediates epithelial cell-intrinsic innate immune signaling during airway mucous metaplasia. Proceedings of the National Academy of Sciences of the United States of America *109*, 16630-16635.
82. Kwon, E.S., Narasimhan, S.D., Yen, K., and Tissenbaum, H.A. (2010). A new DAF-16 isoform regulates longevity. Nature *466*, 498-502.

83. Landis, J.N., and Murphy, C.T. (2010). Integration of diverse inputs in the regulation of Caenorhabditis elegans DAF-16/FOXO. Dev Dyn *239*, 1405-1412.
84. Lawson, D.M., Artymiuk, P.J., Yewdall, S.J., Smith, J.M., Livingstone, J.C., Treffry, A., Luzzago, A., Levi, S., Arosio, P., Cesareni, G., et al. (1991). Solving the structure of human H ferritin by genetically engineering intermolecular crystal contacts. Nature *349*, 541-544.
85. Lee, D., An, S.W.A., Jung, Y., Yamaoka, Y., Ryu, Y., Goh, G.Y.S., Beigi, A., Ma, D., Ha, C.M., Taubert, S., et al. (2018).
86. Lee, M., Choi, I., and Park, K. (2002). Activation of stress signaling molecules in bat brain during arousal from hibernation. J Neurochem *82*, 867-873.
87. Lee, S., and Dong, H.H. (2017). FoxO integration of insulin signaling with glucose and lipid metabolism. J Endocrinol *233*, R67-R79.
88. Lee, Y.J., Miyake, S., Wakita, H., McMullen, D.C., Azuma, Y., Auh, S., and Hallenbeck, J.M. (2007). Protein SUMOylation is massively increased in hibernation torpor and is critical for the cytoprotection provided by ischemic preconditioning and hypothermia in SHSY5Y cells. J Cereb Blood Flow Metab *27*, 950-962.
89. Leight, E.R., Glossip, D., and Kornfeld, K. (2005). Sumoylation of LIN-1 promotes transcriptional repression and inhibition of vulval cell fates. Development *132*, 1047-1056.
90. Leight, E.R., Murphy, J.T., Fantz, D.A., Pepin, D., Schneider, D.L., Ratliff, T.M., Mohammad, D.H., Herman, M.A., and Kornfeld, K. (2015). Conversion of the LIN-1 ETS protein of Caenorhabditis elegans from a SUMOylated transcriptional repressor to a phosphorylated transcriptional activator. Genetics *199*, 761-775.
91. Leprince, D., Gegonne, A., Coll, J., de Taisne, C., Schneeberger, A., Lagrou, C., and Stehelin, D. (1983). A putative second cell-derived oncogene of the avian leukaemia retrovirus E26. Nature *306*, 395-397.
92. Leto, D., and Saltiel, A.R. (2012). Regulation of glucose transport by insulin: traffic control of GLUT4. Nat Rev Mol Cell Biol *13*, 383-396.
93. Li, C., Hisamoto, N., and Matsumoto, K. (2015). Axon Regeneration Is Regulated by Ets-C/EBP Transcription Complexes Generated by Activation of the cAMP/Ca2+ Signaling Pathways. PLoS genetics *11*, e1005603.
94. Li, Y.H., and Zhang, G.G. (2016). Towards understanding the lifespan extension by reduced insulin signaling: bioinformatics analysis of DAF-16/FOXO direct targets in Caenorhabditis elegans. Oncotarget *7*, 19185-19192.
95. Lien, E.L., Richard, C., and Hoffman, D.R. (2018). DHA and ARA addition to infant formula: Current status and future research directions. Prostaglandins Leukot Essent Fatty Acids *128*, 26-40.
96. Lin, K., Hsin, H., Libina, N., and Kenyon, C. (2001). Regulation of the Caenorhabditis elegans longevity protein DAF-16 by insulin/IGF-1 and germline signaling. Nature genetics *28*, 139-145.
97. Lin, X.X., Sen, I., Janssens, G.E., Zhou, X., Fonslow, B.R., Edgar, D., Stroustrup, N., Swoboda, P., Yates, J.R., 3rd, Ruvkun, G., et al. (2018). DAF-16/FOXO and HLH-30/TFEB function as combinatorial transcription factors to promote stress resistance and longevity. Nature communications *9*, 4400.
98. Liu, F., Xiao, Y., Ji, X.-L., Zhang, K.-Q., and Zou, C.-G. (2017). The cAMP-PKA pathway-mediated fat mobilization is required for cold tolerance in C. elegans. Scientific reports *7*.

99. Luk, I.Y., Reehorst, C.M., and Mariadason, J.M. (2018). ELF3, ELF5, EHF and SPDEF Transcription Factors in Tissue Homeostasis and Cancer. Molecules *23*.
100. Macara, I.G., Hoy, T.G., and Harrison, P.M. (1972). The formation of ferritin from apoferritin. Kinetics and mechanism of iron uptake. Biochem J *126*, 151-162.
101. Mackereth, C.D., Scharpf, M., Gentile, L.N., MacIntosh, S.E., Slupsky, C.M., and McIntosh, L.P. (2004). Diversity in structure and function of the Ets family PNT domains. J Mol Biol *342*, 1249-1264.
102. Madden, L.K., Hill, M., May, T.L., Human, T., Guanci, M.M., Jacobi, J., Moreda, M.V., and Badjatia, N. (2017). The Implementation of Targeted Temperature Management: An Evidence-Based Guideline from the Neurocritical Care Society. Neurocrit Care *27*, 468-487.
103. Majima, H.J., Oberley, T.D., Furukawa, K., Mattson, M.P., Yen, H.C., Szweda, L.I., and St Clair, D.K. (1998). Prevention of mitochondrial injury by manganese superoxide dismutase reveals a primary mechanism for alkaline-induced cell death. J Biol Chem *273*, 8217-8224.
104. Malmsten, C.L. (1986). Prostaglandins, thromboxanes, and leukotrienes in inflammation. Am J Med *80*, 11-17.
105. Marcher, A.B., Loft, A., Nielsen, R., Vihervaara, T., Madsen, J.G., Sysi-Aho, M., Ekroos, K., and Mandrup, S. (2015). RNA-Seq and Mass-Spectrometry-Based Lipidomics Reveal Extensive Changes of Glycerolipid Pathways in Brown Adipose Tissue in Response to Cold. Cell reports *13*, 2000-2013.
106. Marziali, G., Perrotti, E., Ilari, R., Lulli, V., Coccia, E.M., Moret, R., Kuhn, L.C., Testa, U., and Battistini, A. (2002). Role of Ets-1 in transcriptional regulation of transferrin receptor and erythroid differentiation. Oncogene *21*, 7933-7944.
107. Mathew, R., Pal Bhadra, M., and Bhadra, U. (2017). Insulin/insulin-like growth factor-1 signalling (IIS) based regulation of lifespan across species. Biogerontology *18*, 35-53.
108. McGhee, J.D. (2007). The C. elegans intestine. WormBook, 1-36.
109. McGinniss, J., Marshall, P., and Honiden, S. (2015). Novel Uses of Targeted Temperature Management. Clin Chest Med *36*, 385-400.
110. Miquel, J., Lundgren, P.R., Bensch, K.G., and Atlan, H. (1976). Effects of temperature on the life span, vitality and fine structure of Drosophila melanogaster. Mechanisms of ageing and development *5*, 347-370.
111. Miyazaki, M., Shimozuru, M., and Tsubota, T. (2019). Skeletal muscles of hibernating black bears show minimal atrophy and phenotype shifting despite prolonged physical inactivity and starvation. PloS one *14*, e0215489.
112. Mizunuma, M., Neumann-Haefelin, E., Moroz, N., Li, Y., and Blackwell, T.K. (2014). mTORC2-SGK-1 acts in two environmentally responsive pathways with opposing effects on longevity. Aging Cell *13*, 869-878.
113. Montemiglio, L.C., Testi, C., Ceci, P., Falvo, E., Pitea, M., Savino, C., Arcovito, A., Peruzzi, G., Baiocco, P., Mancia, F., et al. (2019). Cryo-EM structure of the human ferritin-transferrin receptor 1 complex. Nature communications *10*, 1121.
114. Morin, P., Jr., Ni, Z., McMullen, D.C., and Storey, K.B. (2008). Expression of Nrf2 and its downstream gene targets in hibernating 13-lined ground squirrels, Spermophilus tridecemlineatus. Mol Cell Biochem *312*, 121-129.
115. Morin, P., Jr., and Storey, K.B. (2006). Evidence for a reduced transcriptional state during hibernation in ground squirrels. Cryobiology *53*, 310-318.
116. Muckenthaler, M.U., Rivella, S., Hentze, M.W., and Galy, B. (2017). A Red Carpet for Iron Metabolism. Cell *168*, 344-361.

117. Murphy, C.T. (2006). The search for DAF-16/FOXO transcriptional targets: approaches and discoveries. Exp Gerontol *41*, 910-921.
118. Murphy, C.T., and Hu, P.J. (2013). Insulin/insulin-like growth factor signaling in C. elegans. WormBook, 1-43.
119. Murray, P., Hayward, S.A., Govan, G.G., Gracey, A.Y., and Cossins, A.R. (2007). An explicit test of the phospholipid saturation hypothesis of acquired cold tolerance in Caenorhabditis elegans. Proceedings of the National Academy of Sciences of the United States of America *104*, 5489-5494.
120. Nakashima, K., Todd, M.M., and Warner, D.S. (1995). The relation between cerebral metabolic rate and ischemic depolarization. A comparison of the effects of hypothermia, pentobarbital, and isoflurane. Anesthesiology *82*, 1199-1208.
121. Ni, Z., and Storey, K.B. (2010). Heme oxygenase expression and Nrf2 signaling during hibernation in ground squirrels. Can J Physiol Pharmacol *88*, 379-387.
122. Noah, T.K., Kazanjian, A., Whitsett, J., and Shroyer, N.F. (2010). SAM pointed domain ETS factor (SPDEF) regulates terminal differentiation and maturation of intestinal goblet cells. Exp Cell Res *316*, 452-465.
123. Noah, T.K., Lo, Y.H., Price, A., Chen, G., King, E., Washington, M.K., Aronow, B.J., and Shroyer, N.F. (2013). SPDEF functions as a colorectal tumor suppressor by inhibiting beta-catenin activity. Gastroenterology *144*, 1012-1023 e1016.
124. O'Brien, D., Jones, L.M., Good, S., Miles, J., Vijayabaskar, M.S., Aston, R., Smith, C.E., Westhead, D.R., and van Oosten-Hawle, P. (2018). A PQM-1-Mediated Response Triggers Transcellular Chaperone Signaling and Regulates Organismal Proteostasis. Cell reports *23*, 3905-3919.
125. Ogg, S., and Ruvkun, G. (1998). The C. elegans PTEN homolog, DAF-18, acts in the insulin receptor-like metabolic signaling pathway. Molecular cell *2*, 887-893.
126. Oh, S.W., Mukhopadhyay, A., Svrzikapa, N., Jiang, F., Davis, R.J., and Tissenbaum, H.A. (2005). JNK regulates lifespan in Caenorhabditis elegans by modulating nuclear translocation of forkhead transcription factor/DAF-16. Proceedings of the National Academy of Sciences of the United States of America *102*, 4494-4499.
127. Ohgami, R.S., Campagna, D.R., Greer, E.L., Antiochos, B., McDonald, A., Chen, J., Sharp, J.J., Fujiwara, Y., Barker, J.E., and Fleming, M.D. (2005). Identification of a ferrireductase required for efficient transferrin-dependent iron uptake in erythroid cells. Nature genetics *37*, 1264-1269.
128. Ohta, A., Ujisawa, T., Sonoda, S., and Kuhara, A. (2014). Light and pheromone-sensing neurons regulates cold habituation through insulin signalling in Caenorhabditis elegans. Nature communications *5*, 4412.
129. Okahata, M., Ohta, A., Mizutani, H., Minakuchi, Y., Toyoda, A., and Kuhara, A. (2016). Natural variations of cold tolerance and temperature acclimation in Caenorhabditis elegans. Journal of comparative physiology. B, Biochemical, systemic, and environmental physiology *186*, 985-998.
130. Osborne, P.G., Gao, B., and Hashimoto, M. (2004). Determination in vivo of newly synthesized gene expression in hamsters during phases of the hibernation cycle. Jpn J Physiol *54*, 295-305.
131. Page, M.M., Peters, C.W., Staples, J.F., and Stuart, J.A. (2009). Intracellular antioxidant enzymes are not globally upregulated during hibernation in the major oxidative tissues of the 13-lined ground squirrel Spermophilus tridecemlineatus. Comp Biochem Physiol A Mol Integr Physiol *152*, 115-122.

132. Paige, M., Wang, K., Burdick, M., Park, S., Cha, J., Jeffery, E., Sherman, N., and Shim, Y.M. (2014). Role of leukotriene A4 hydrolase aminopeptidase in the pathogenesis of emphysema. J Immunol *192*, 5059-5068.
133. Pal, M., Koul, S., and Koul, H.K. (2013). The transcription factor sterile alpha motif (SAM) pointed domain-containing ETS transcription factor (SPDEF) is required for E-cadherin expression in prostate cancer cells. J Biol Chem *288*, 12222-12231.
134. Palmers, P.J., Hiltrop, N., Ameloot, K., Timmermans, P., Ferdinande, B., Sinnaeve, P., Nieuwendijk, R., and Malbrain, M.L. (2015). From therapeutic hypothermia towards targeted temperature management: a decade of evolution. Anaesthesiol Intensive Ther *47*, 156-161.
135. Perman, S.M., Goyal, M., Neumar, R.W., Topjian, A.A., and Gaieski, D.F. (2014). Clinical applications of targeted temperature management. Chest *145*, 386-393.
136. Peters-Golden, M., Canetti, C., Mancuso, P., and Coffey, M.J. (2005). Leukotrienes: underappreciated mediators of innate immune responses. J Immunol *174*, 589-594.
137. Philpott, C.C., Ryu, M.S., Frey, A., and Patel, S. (2017). Cytosolic iron chaperones: Proteins delivering iron cofactors in the cytosol of mammalian cells. J Biol Chem *292*, 12764-12771.
138. Pizanis, N., Gillner, S., Kamler, M., de Groot, H., Jakob, H., and Rauen, U. (2011). Cold-induced injury to lung epithelial cells can be inhibited by iron chelators - implications for lung preservation. European journal of cardio-thoracic surgery : official journal of the European Association for Cardio-thoracic Surgery *40*, 948-955.
139. Ponka, P., Beaumont, C., and Richardson, D.R. (1998). Function and regulation of transferrin and ferritin. Semin Hematol *35*, 35-54.
140. Rauen, U., Petrat, F., Li, T., and De Groot, H. (2000). Hypothermia injury/cold-induced apoptosis--evidence of an increase in chelatable iron causing oxidative injury in spite of low O2-/H2O2 formation. FASEB J *14*, 1953-1964.
141. Rigano, K.S., Gehring, J.L., Evans Hutzenbiler, B.D., Chen, A.V., Nelson, O.L., Vella, C.A., Robbins, C.T., and Jansen, H.T. (2017). Life in the fat lane: seasonal regulation of insulin sensitivity, food intake, and adipose biology in brown bears. Journal of comparative physiology. B, Biochemical, systemic, and environmental physiology *187*, 649-676.
142. Rizki, G., Iwata, T.N., Li, J., Riedel, C.G., Picard, C.L., Jan, M., Murphy, C.T., and Lee, S.S. (2011). The evolutionarily conserved longevity determinants HCF-1 and SIR-2.1/SIRT1 collaborate to regulate DAF-16/FOXO. PLoS genetics *7*, e1002235.
143. Robinson, J.D., and Powell, J.R. (2016). Long-term recovery from acute cold shock in Caenorhabditis elegans. BMC Cell Biol *17*, 2.
144. Romney, S.J., Newman, B.S., Thacker, C., and Leibold, E.A. (2011). HIF-1 regulates iron homeostasis in Caenorhabditis elegans by activation and inhibition of genes involved in iron uptake and storage. PLoS genetics *7*, e1002394.
145. Romney, S.J., Thacker, C., and Leibold, E.A. (2008). An iron enhancer element in the FTN-1 gene directs iron-dependent expression in Caenorhabditis elegans intestine. J Biol Chem *283*, 716-725.
146. Roth, G.S., Lane, M.A., Ingram, D.K., Mattison, J.A., Elahi, D., Tobin, J.D., Muller, D., and Metter, E.J. (2002). Biomarkers of caloric restriction may predict longevity in humans. Science *297*, 811.
147. Rouault, T.A. (2015). Mammalian iron-sulphur proteins: novel insights into biogenesis and function. Nat Rev Mol Cell Biol *16*, 45-55.
148. Ruan, Y.C., Zhou, W., and Chan, H.C. (2011). Regulation of smooth muscle contraction by the epithelium: role of prostaglandins. Physiology *26*, 156-170.

149. Rudberg, P.C., Tholander, F., Thunnissen, M.M., Samuelsson, B., and Haeggstrom, J.Z. (2002). Leukotriene A4 hydrolase: selective abrogation of leukotriene B4 formation by mutation of aspartic acid 375. Proceedings of the National Academy of Sciences of the United States of America *99*, 4215-4220.
150. Ruf, T., and Geiser, F. (2015). Daily torpor and hibernation in birds and mammals. Biol Rev Camb Philos Soc *90*, 891-926.
151. Saigal, S., Sharma, J.P., Dhurwe, R., Kumar, S., and Gurjar, M. (2015). Targeted temperature management: Current evidence and practices in critical care. Indian J Crit Care Med *19*, 537-546.
152. Salahudeen, A.A., and Bruick, R.K. (2009). Maintaining Mammalian iron and oxygen homeostasis: sensors, regulation, and cross-talk. Ann N Y Acad Sci *1177*, 30-38.
153. Salahudeen, A.A., Thompson, J.W., Ruiz, J.C., Ma, H.W., Kinch, L.N., Li, Q., Grishin, N.V., and Bruick, R.K. (2009). An E3 ligase possessing an iron-responsive hemerythrin domain is a regulator of iron homeostasis. Science *326*, 722-726.
154. Samuelson, A.V., Carr, C.E., and Ruvkun, G. (2007). Gene activities that mediate increased life span of C. elegans insulin-like signaling mutants. Genes & development *21*, 2976-2994.
155. Savory, F.R., Sait, S.M., and Hope, I.A. (2011). DAF-16 and Delta9 desaturase genes promote cold tolerance in long-lived Caenorhabditis elegans age-1 mutants. PloS one *6*, e24550.
156. Schiavi, A., Maglioni, S., Palikaras, K., Shaik, A., Strappazzon, F., Brinkmann, V., Torgovnick, A., Castelein, N., De Henau, S., Braeckman, B.P., et al. (2015). Iron-Starvation-Induced Mitophagy Mediates Lifespan Extension upon Mitochondrial Stress in C. elegans. Current biology : CB *25*, 1810-1822.
157. Schmid, C., Schwarz, V., and Hutter, H. (2006). AST-1, a novel ETS-box transcription factor, controls axon guidance and pharynx development in C. elegans. Dev Biol *293*, 403-413.
158. Seidel, J.J., and Graves, B.J. (2002). An ERK2 docking site in the Pointed domain distinguishes a subset of ETS transcription factors. Genes & development *16*, 127-137.
159. Senchuk, M.M., Dues, D.J., Schaar, C.E., Johnson, B.K., Madaj, Z.B., Bowman, M.J., Winn, M.E., and Van Raamsdonk, J.M. (2018). Activation of DAF-16/FOXO by reactive oxygen species contributes to longevity in long-lived mitochondrial mutants in Caenorhabditis elegans. PLoS genetics *14*, e1007268.
160. Shao, Z.H., Sharp, W.W., Wojcik, K.R., Li, C.Q., Han, M., Chang, W.T., Ramachandran, S., Li, J., Hamann, K.J., and Vanden Hoek, T.L. (2010). Therapeutic hypothermia cardioprotection via Akt- and nitric oxide-mediated attenuation of mitochondrial oxidants. Am J Physiol Heart Circ Physiol *298*, H2164-2173.
161. Shibata, Y., Branicky, R., Landaverde, I.O., and Hekimi, S. (2003). Redox regulation of germline and vulval development in Caenorhabditis elegans. Science *302*, 1779-1782.
162. Shpigel, N., Shemesh, N., Kishner, M., and Ben-Zvi, A. (2019). Dietary restriction and gonadal signaling differentially regulate post-development quality control functions in Caenorhabditis elegans. Aging Cell *18*, e12891.
163. Sinensky, M. (1974). Homeoviscous adaptation--a homeostatic process that regulates the viscosity of membrane lipids in Escherichia coli. Proceedings of the National Academy of Sciences of the United States of America *71*, 522-525.
164. Slack, C., Alic, N., Foley, A., Cabecinha, M., Hoddinott, M.P., and Partridge, L. (2015). The Ras-Erk-ETS-Signaling Pathway Is a Drug Target for Longevity. Cell *162*, 72-83.

165. Solomon, E.I., Decker, A., and Lehnert, N. (2003). Non-heme iron enzymes: contrasts to heme catalysis. Proceedings of the National Academy of Sciences of the United States of America *100*, 3589-3594.
166. Storey, K.B. (2010). Out cold: biochemical regulation of mammalian hibernation - a mini-review. Gerontology *56*, 220-230.
167. Storey, K.B. (2015). Regulation of hypometabolism: insights into epigenetic controls. The Journal of experimental biology *218*, 150-159.
168. Storey, K.B., and Storey, J.M. (2004). Metabolic rate depression in animals: transcriptional and translational controls. Biol Rev Camb Philos Soc *79*, 207-233.
169. Storey, K.B., and Storey, J.M. (2007). Tribute to P. L. Lutz: putting life on 'pause'--molecular regulation of hypometabolism. The Journal of experimental biology *210*, 1700-1714.
170. Subramanian, P., Mendez, E.F., and Becerra, S.P. (2016). A Novel Inhibitor of 5-Lipoxygenase (5-LOX) Prevents Oxidative Stress-Induced Cell Death of Retinal Pigment Epithelium (RPE) Cells. Invest Ophthalmol Vis Sci *57*, 4581-4588.
171. Suh, Y., Atzmon, G., Cho, M.O., Hwang, D., Liu, B., Leahy, D.J., Barzilai, N., and Cohen, P. (2008). Functionally significant insulin-like growth factor I receptor mutations in centenarians. Proceedings of the National Academy of Sciences of the United States of America *105*, 3438-3442.
172. Sumanas, S., and Choi, K. (2016). ETS Transcription Factor ETV2/ER71/Etsrp in Hematopoietic and Vascular Development. Curr Top Dev Biol *118*, 77-111.
173. Sun, X., Chen, W.D., and Wang, Y.D. (2017). DAF-16/FOXO Transcription Factor in Aging and Longevity. Frontiers in pharmacology *8*, 548.
174. Suswam, E.A., Li, Y.Y., Mahtani, H., and King, P.H. (2005). Novel DNA-binding properties of the RNA-binding protein TIAR. Nucleic Acids Res *33*, 4507-4518.
175. Svensk, E., Stahlman, M., Andersson, C.H., Johansson, M., Boren, J., and Pilon, M. (2013). PAQR-2 regulates fatty acid desaturation during cold adaptation in C. elegans. PLoS genetics *9*, e1003801.
176. Taubert, S., Van Gilst, M.R., Hansen, M., and Yamamoto, K.R. (2006). A Mediator subunit, MDT-15, integrates regulation of fatty acid metabolism by NHR-49-dependent and -independent pathways in C. elegans. Genes & development *20*, 1137-1149.
177. Tawe, W.N., Eschbach, M.L., Walter, R.D., and Henkle-Duhrsen, K. (1998). Identification of stress-responsive genes in Caenorhabditis elegans using RT-PCR differential display. Nucleic Acids Res *26*, 1621-1627.
178. Tepper, R.G., Ashraf, J., Kaletsky, R., Kleemann, G., Murphy, C.T., and Bussemaker, H.J. (2013). PQM-1 complements DAF-16 as a key transcriptional regulator of DAF-2-mediated development and longevity. Cell *154*, 676-690.
179. Tessier, S.N., Audas, T.E., Wu, C.W., Lee, S., and Storey, K.B. (2014). The involvement of mRNA processing factors TIA-1, TIAR, and PABP-1 during mammalian hibernation. Cell Stress Chaperones *19*, 813-825.
180. Theil, E.C. (2000). Targeting mRNA to regulate iron and oxygen metabolism. Biochem Pharmacol *59*, 87-93.
181. Theil, E.C. (2013). Ferritin: the protein nanocage and iron biomineral in health and in disease. Inorg Chem *52*, 12223-12233.
182. Thompson, J.W., and Bruick, R.K. (2012). Protein degradation and iron homeostasis. Biochimica et biophysica acta *1823*, 1484-1490.
183. Thompson, J.W., Salahudeen, A.A., Chollangi, S., Ruiz, J.C., Brautigam, C.A., Makris, T.M., Lipscomb, J.D., Tomchick, D.R., and Bruick, R.K. (2012). Structural and molecular

characterization of iron-sensing hemerythrin-like domain within F-box and leucine-rich repeat protein 5 (FBXL5). J Biol Chem *287*, 7357-7365.
184. Thyagarajan, B., Blaszczak, A.G., Chandler, K.J., Watts, J.L., Johnson, W.E., and Graves, B.J. (2010). ETS-4 is a transcriptional regulator of life span in Caenorhabditis elegans. PLoS genetics *6*, e1001125.
185. Tullet, J.M., Araiz, C., Sanders, M.J., Au, C., Benedetto, A., Papatheodorou, I., Clark, E., Schmeisser, K., Jones, D., Schuster, E.F., et al. (2014). DAF-16/FoxO directly regulates an atypical AMP-activated protein kinase gamma isoform to mediate the effects of insulin/IGF-1 signaling on aging in Caenorhabditis elegans. PLoS genetics *10*, e1004109.
186. Tullet, J.M., Hertweck, M., An, J.H., Baker, J., Hwang, J.Y., Liu, S., Oliveira, R.P., Baumeister, R., and Blackwell, T.K. (2008). Direct inhibition of the longevity-promoting factor SKN-1 by insulin-like signaling in C. elegans. Cell *132*, 1025-1038.
187. Tupone, D., Madden, C.J., and Morrison, S.F. (2013). Central activation of the A1 adenosine receptor (A1AR) induces a hypothermic, torpor-like state in the rat. J Neurosci *33*, 14512-14525.
188. Valentini, S., Cabreiro, F., Ackerman, D., Alam, M.M., Kunze, M.B., Kay, C.W., and Gems, D. (2012). Manipulation of in vivo iron levels can alter resistance to oxidative stress without affecting ageing in the nematode C. elegans. Mechanisms of ageing and development *133*, 282-290.
189. van Breukelen, F., and Carey, V. (2002). Ubiquitin conjugate dynamics in the gut and liver of hibernating ground squirrels. Journal of comparative physiology. B, Biochemical, systemic, and environmental physiology *172*, 269-273.
190. van Breukelen, F., and Martin, S.L. (2015). The Hibernation Continuum: Physiological and Molecular Aspects of Metabolic Plasticity in Mammals. Physiology *30*, 273-281.
191. van Meer, G., Voelker, D.R., and Feigenson, G.W. (2008). Membrane lipids: where they are and how they behave. Nat Rev Mol Cell Biol *9*, 112-124.
192. Vasquez, V., Krieg, M., Lockhead, D., and Goodman, M.B. (2014). Phospholipids that contain polyunsaturated fatty acids enhance neuronal cell mechanics and touch sensation. Cell reports *6*, 70-80.
193. Vivekanand, P. (2018). Lessons from Drosophila Pointed, an ETS family transcription factor and key nuclear effector of the RTK signaling pathway. Genesis *56*, e23257.
194. Vucetic, M., Stancic, A., Otasevic, V., Jankovic, A., Korac, A., Markelic, M., Velickovic, K., Golic, I., Buzadzic, B., Storey, K.B., et al. (2013). The impact of cold acclimation and hibernation on antioxidant defenses in the ground squirrel (Spermophilus citellus): an update. Free radical biology & medicine *65*, 916-924.
195. Wang, H., Jiang, X., Wu, J., Zhang, L., Huang, J., Zhang, Y., Zou, X., and Liang, B. (2016). Iron Overload Coordinately Promotes Ferritin Expression and Fat Accumulation in Caenorhabditis elegans. Genetics *203*, 241-253.
196. Wang, Y., Zhou, Y., and Graves, D.T. (2014). FOXO transcription factors: their clinical significance and regulation. Biomed Res Int *2014*, 925350.
197. Watts, J.L., and Browse, J. (2002). Genetic dissection of polyunsaturated fatty acid synthesis in Caenorhabditis elegans. Proceedings of the National Academy of Sciences of the United States of America *99*, 5854-5859.
198. Watts, J.L., and Ristow, M. (2017). Lipid and Carbohydrate Metabolism in Caenorhabditis elegans. Genetics *207*, 413-446.
199. Webb, A.E., Kundaje, A., and Brunet, A. (2016). Characterization of the direct targets of FOXO transcription factors throughout evolution. Aging Cell *15*, 673-685.

200. Wei, G.H., Badis, G., Berger, M.F., Kivioja, T., Palin, K., Enge, M., Bonke, M., Jolma, A., Varjosalo, M., Gehrke, A.R., et al. (2010). Genome-wide analysis of ETS-family DNA-binding in vitro and in vivo. The EMBO journal *29*, 2147-2160.
201. Wei, Y., Zhang, J., Xu, S., Peng, X., Yan, X., Li, X., Wang, H., Chang, H., and Gao, Y. (2018). Controllable oxidative stress and tissue specificity in major tissues during the torpor-arousal cycle in hibernating Daurian ground squirrels. Open Biol *8*.
202. Westin, B., Miller, J.A., Jr., Nyberg, R., and Wedenberg, E. (1959). Neonatal asphyxia pallida treated with hypothermia alone or with hypothermia and transfusion of oxygenated blood. Surgery *45*, 868-879.
203. Winterbourn, C.C. (1995). Toxicity of iron and hydrogen peroxide: the Fenton reaction. Toxicol Lett *82-83*, 969-974.
204. Wolff, S., Ma, H., Burch, D., Maciel, G.A., Hunter, T., and Dillin, A. (2006). SMK-1, an essential regulator of DAF-16-mediated longevity. Cell *124*, 1039-1053.
205. Wu, C.W., Biggar, K.K., and Storey, K.B. (2013). Biochemical adaptations of mammalian hibernation: exploring squirrels as a perspective model for naturally induced reversible insulin resistance. Braz J Med Biol Res *46*, 1-13.
206. Wu, C.W., Biggar, K.K., Zhang, J., Tessier, S.N., Pifferi, F., Perret, M., and Storey, K.B. (2015). Induction of Antioxidant and Heat Shock Protein Responses During Torpor in the Gray Mouse Lemur, Microcebus murinus. Genomics Proteomics Bioinformatics *13*, 119-126.
207. Wu, C.W., and Storey, K.B. (2014). FoxO3a-mediated activation of stress responsive genes during early torpor in a mammalian hibernator. Mol Cell Biochem *390*, 185-195.
208. Wu, C.W., and Storey, K.B. (2016). Life in the cold: links between mammalian hibernation and longevity. Biomol Concepts *7*, 41-52.
209. Xiao, R., Zhang, B., Dong, Y., Gong, J., Xu, T., Liu, J., and Xu, X.Z. (2013). A genetic program promotes C. elegans longevity at cold temperatures via a thermosensitive TRP channel. Cell *152*, 806-817.
210. Yaribeygi, H., Farrokhi, F.R., Butler, A.E., and Sahebkar, A. (2019). Insulin resistance: Review of the underlying molecular mechanisms. J Cell Physiol *234*, 8152-8161.
211. Ye, L., Wu, J., Cohen, P., Kazak, L., Khandekar, M.J., Jedrychowski, M.P., Zeng, X., Gygi, S.P., and Spiegelman, B.M. (2013). Fat cells directly sense temperature to activate thermogenesis. Proceedings of the National Academy of Sciences of the United States of America *110*, 12480-12485.
212. Ye, Z.N., Wu, L.Y., Liu, J.P., Chen, Q., Zhang, X.S., Lu, Y., Zhou, M.L., Li, W., Zhang, Z.H., Xia, D.Y., et al. (2018). Inhibition of leukotriene B4 synthesis protects against early brain injury possibly via reducing the neutrophil-generated inflammatory response and oxidative stress after subarachnoid hemorrhage in rats. Behav Brain Res *339*, 19-27.
213. Yen, K., Patel, H.B., Lublin, A.L., and Mobbs, C.V. (2009). SOD isoforms play no role in lifespan in ad lib or dietary restricted conditions, but mutational inactivation of SOD-1 reduces life extension by cold. Mechanisms of ageing and development *130*, 173-178.
214. Yin, Q., Ge, H., Liao, C.C., Liu, D., Zhang, S., and Pan, Y.H. (2016). Antioxidant Defenses in the Brains of Bats during Hibernation. PloS one *11*, e0152135.
215. Yokobori, S., and Yokota, H. (2016). Targeted temperature management in traumatic brain injury. J Intensive Care *4*, 28.
216. Zatzman, M.L. (1984). Renal and cardiovascular effects of hibernation and hypothermia. Cryobiology *21*, 593-614.

217. Zeiser, E., Frokjaer-Jensen, C., Jorgensen, E., and Ahringer, J. (2011). MosSCI and gateway compatible plasmid toolkit for constitutive and inducible expression of transgenes in the C. elegans germline. PloS one *6*, e20082.
218. Zheng, S., Chiu, H., Boudreau, J., Papanicolaou, T., Bendena, W., and Chin-Sang, I. (2018). A functional study of all 40 Caenorhabditis elegans insulin-like peptides. J Biol Chem *293*, 16912-16922.
219. Zuryn, S., and Jarriault, S. (2013). Deep sequencing strategies for mapping and identifying mutations from genetic screens. Worm *2*, e25081.

APPENDIX

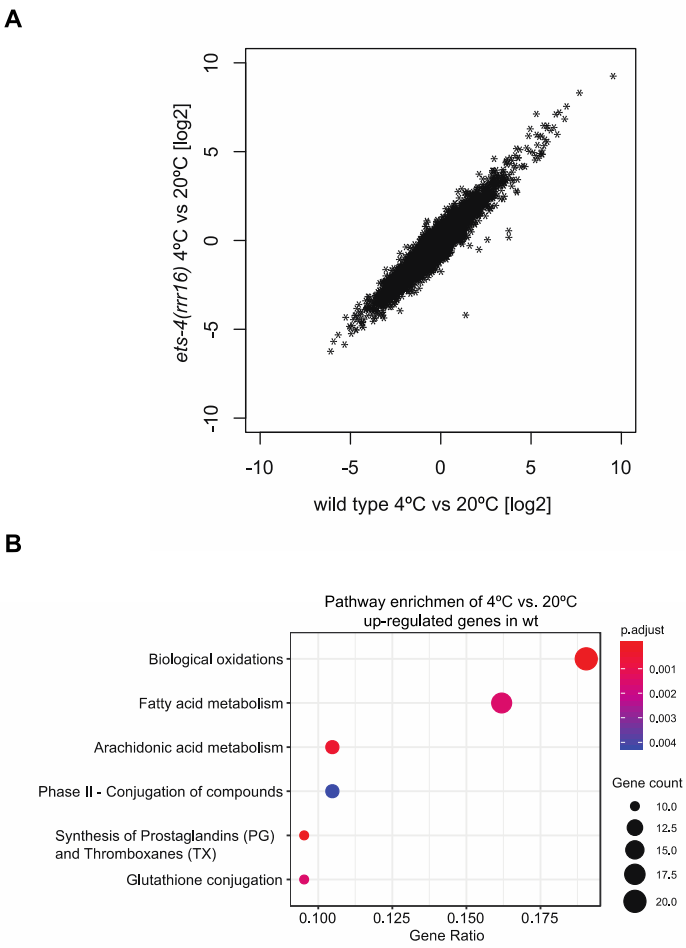

Appendix. Cold adaptation evokes a strong transcriptional response in both wt and *ets-4(rrr16).*

A. Poly-A mRNA sequencing was performed on wild-type, *ets-4* at 20°C and one day at 4°C adapted as described in Chapter 2. Correlation represents log2 fold change (log2) in either *ets-4* single mutant or wt at 20°C over 4°C. Each star represents one gene.

B. Bubble diagram shows significantly enriched pathways of up regulated genes in wild-type at day one 4°C compared to 20°C. The *p* values were adjusted by Benjamini-Hochberg procedure. Gene count indicates the number of genes in each category. Gene ratio indicates genes found to be upregulated in cold, divided by total number of genes submitted for the analysis.